STUDY ON OXYGENATED VOLATILE ORGANIC COMPOUNDS (OVOCS) FORMATION AND IMPACT IN HONG KONG: A COMBINED FIELD STUDY AND CHAMBER SIMULATION

TAN YAN

PhD

The Hong Kong Polytechnic University

2021

The Hong Kong Polytechnic University

Department of Civil and Environmental Engineering

Study on Oxygenated Volatile Organic Compounds (OVOCs) Formation and Impact in Hong Kong: A Combined Field Study and Chamber Simulation

TAN Yan

A thesis submitted in partial fulfilment of the requirements for the degree of Doctor of Philosophy

April 2021

CERTIFICATE OF ORIGINALITY

I hereby declare that this thesis is my own work and that, to the best of my knowledge and belief, it reproduces no material previously published or written, nor material that has been accepted for the award of any other degree or diploma, except where due acknowledgement has been made in the text.

_____ (Signed)

TAN Yan_____ (Name of student)

ABSTRACT

As an important constituent of volatile organic compounds (VOCs), oxygenated volatile organic compounds (OVOCs) participate directly in photochemical reactions due to their high reactivity. In addition to primary emission, OVOCs are generated as typical products of the oxidation of VOCs by hydroxyl radicals (OH), ozone (O_3), nitrate radicals (NO_3), and chlorine radicals (Cl) in the atmosphere. Furthermore, OVOCs are the precursors of O_3, peroxy acetyl nitrate (PAN), and secondary organic aerosols (SOA), and they play a non-negligible role in the atmosphere. A study that included a field campaign and laboratory experimentation was conducted to investigate the formation and impact of OVOCs in Hong Kong.

The field measurement study was carried out from August to October 2018 at a rural coastal site (Hok Tsui site) in Hong Kong. VOC and OVOC species were monitored continuously with proton transfer reaction quadrupole mass spectrometry (PTR-QMS), and the concentrations of OVOCs were found to be higher than those reported in previous studies in rural areas. Diurnal variations in the VOC concentrations were observed to be influenced by photochemical reactions. The amount of O_3 formation was estimated via the maximum incremental reactivity model, and the top five contributors were isoprene (13.46 μg/m^3), methyl ethyl ketone (12.74 μg/m^3), xylene (8.52 μg/m^3), acetaldehyde (8.22 μg/m^3), and acrolein (4.32 μg/m^3), which suggests that OVOCs

ABSTRACT

were the dominant species with the potential for O_3 formation. Five major VOC sources were identified with the positive matrix factorization method, including (1) biomass burning (63.7%), (2) ship-related emissions (13.5%), (3) secondary formation (9.2%), (4) industry-related and vehicle-related sources (8.1%), and (5) biogenic emissions (5.5%). The positive matrix factorization results showed that the Hok Tsui site was strongly influenced by both the urban plumes from the Guangdong–Hong Kong–Macao Greater Bay Area/Pearl River Delta region and by oceanic emissions.

Because the results of the field study indicated that OVOCs and isoprene were critical in Hong Kong, a new environmental chamber was constructed to better understand the relationship between the formation of OVOCs and isoprene. The chamber consists of a 6-m^3 Teflon film inside a stainless-steel enclosure with controllable temperature and relative humidity, and organic compounds with *m/z* values between 31 and 400 were identified by proton transfer reaction-time-of-flight-mass spectrometry (PTR-ToF-MS) and high-resolution time-of-flight-chemical ionization mass spectrometer (ToF-CIMS). The chamber can thus be used to investigate and simulate the gaseous chemical reactions and secondary aerosol formation after obtaining the characterization of performance and yields satisfactory results.

Furthermore, nocturnal oxidation of isoprene by OH radicals, O_3, and NO_3 radicals was investigated under various concentrations of NO_2. Methyl vinyl ketone plus

methacrolein and formaldehyde were the major OVOC products of isoprene oxidation detected by PTR-ToF-MS. It was interesting to note that $C_5H_{10}N_2O_8$ (isoprene dihydroxy dinitrates), a secondary generation product, was the most abundant compound among the highly oxygenated products detected by high-resolution ToF–CIMS. As indicated by the isoprene oxidation experiments, the oxidation processes driven by OH radicals, O_3, and NO_3 radicals, and the combined oxidation by $OH + NO_3$ radicals, existed concurrently in the reaction system, and the pathways were affected by the NO_2 concentration. In addition, as the NO_2 concentration increased from 1 ppb to 800 ppb, the yield of SOA grew 150-fold. The highly oxygenated compounds detected in this reaction system could explain more than 90% of SOA formation. In addition, the carbon balance in the oxidation of isoprene varied from 37.2% to 60.4% as the NO_2 concentration changed, indicating that other products that were not detected in this study still account for a large portion.

According to the results of this field campaign and laboratory experiments to evaluate the formation and impact of OVOCs based on the situation in Hong Kong, OVOCs were the dominant species and exerted a significant influence on O_3 formation. Meanwhile, the contribution of isoprene oxidation to the formation of OVOCs was examined and analyzed, and the pathways were found to be influenced by the NO_2 concentration.

PUBLICATIONS

Journal articles:

1. **Tan, Y.**, Han, S.W., Chen, Y., Zhang Z.Z., Li, H.W., Li, W.Q., Yuan, Q., Li, X.W., Wang, T., Lee, S.C.*, 2021. Characteristics and source apportionment of volatile organic compounds (VOCs) at a coastal site in Hong Kong. Science of The Total Environment, 777, 146241.

2. **Tan, Y.**, Liu, C., Ho, K.F., Ma, Q.X., Lee, S.C.*, 2021. Characterization of an indoor environmental chamber and identification of C_1–C_4 OVOCs during isoprene ozonolysis. Indoor and Built Environment, 30, 554-564.

3. **Tan, Y.**, Chen, Y., Wang, T., Wang, Z.*, Lee, S.C.* Chamber simulation of nocturnal isoprene oxidation. In preparation.

4. Lyu, X.P., Guo, H.*, Yao, D.W., Lu, H.X., Huo, Y.X., Xu, W., Kreisberg, N., Goldstein, A.H., Jayne, J., Worsnop, D., **Tan, Y.**, Lee, S.C., Wang, T., 2020. In Situ Measurements of Molecular Markers Facilitate Understanding of Dynamic Sources of Atmospheric Organic Aerosols. Environmental Science & Technology, 54, 11058-11069.

5. Zhang, Z.Z., Gao, Y., Yuan, Q., **Tan, Y.**, Li, H.W., Cui, L., Huang, Y., Cheng, Y.,

Xiu, G.L., Lai, S.C., Chow, J.C., Watson, J.G., Lee, S.C.*, 2020. Effects of indoor activities and outdoor penetration on PM$_{2.5}$ and associated organic/elemental carbon at residential homes in four Chinese cities during winter. Science of The Total Environment, 739, 139684.

6. Gong, H., Chu, W.*, Xu, K.H., Xia, X.J., Gong, H., **Tan, Y.**, Pu, S.Y.*, 2020. Efficient degradation, mineralization and toxicity reduction of sulfamethoxazole under photo-activation of peroxymonosulfate by ferrate (VI). Chemical Engineering Journal, 389, 124084.

7. Li, H.W., Wang, D.F., Cui, L., Gao, Y., Huo, J., Wang, X., Zhang, Z.Z., **Tan, Y.**, Huang, Y., Cao, J.J., Chow, J.C., Lee, S.C.*, Fu, Q.Y.*, 2019. Characteristics of atmospheric PM$_{2.5}$ composition during the implementation of stringent pollution control measures in shanghai for the 2016 G20 summit. Science of the total environment, 648, 1121-1129.

Patent:

1. **Tan, Y.**, Han, S.W., Lee, S.C.* A walk-in box-in-box environment-controllable chamber, Hong Kong Invention Patent Application, 32021031962.2.

CONFERENCE PRESENTATIONS

1. **Tan, Y.** (presenter), Lee, S.C.* Characterization of products in an environmental chamber for mixtures of isoprene/ozone and isoprene/ozone/nitrogen dioxide. 11th Asian Aerosol Conference (AAC), 27 – 30 May 2019, Hong Kong.

2. **Tan, Y.** (presenter), Lee, S.C.* C_1-C_4 OVOCs formation from reaction of isoprene and O_3. The AGU Jing (Joint International Network in Geoscience) Meeting, 17 – 20 October 2018, Xi'an.

3. **Tan, Y.** (presenter), Lee, S.C.* A chamber study of the isoprene ozonolysis reaction: development and formation of SOA. 23rd China Atmospheric Environment Science and Technology Conference, 8 – 9 December 2017, Beijing.

AWARDS

1. Outstanding Poster Presentation Award, The AGU Jing (Joint International Network in Geoscience) Meeting, 2018, Xi'an. **Tan, Y.**, Lee, S.C.* C_1-C_4 OVOCs formation from reaction of isoprene and O_3.

2. Best Oral Presentation Award, 23rd China Atmospheric Environment Science and Technology Conference, 2017, Beijing. **Tan, Y.**, Lee, S.C.* A chamber study of the isoprene ozonolysis reaction: development and formation of SOA.

ACKNOWLEDGEMENTS

I would like to express the deepest gratitude to my supervisor, Professor LEE Shun-cheng, who is an erudite, patient and kind scientist. I want to thank him for providing me the opportunity for PhD study, giving me all the necessary resources during my research period, encouraging me when I was in a tight corner, and mentoring for lifelong development. I must say that it is so lucky for me to have such a nice supervisor during my 4-year PhD journey.

I want to give my special thanks to other dedicated experts, including Professor HO Kin Fai, Professor WANG Tao and Dr. WANG Zhe, who provided me suggestions and strong assistance for my experiments. I would also like to thank the technicians of our laboratory, Mr. TAM W.F., Mr. POON Steven, and Mr. CHAN Jazz, for their technical support.

I must thank my friend for their guidance and support. Many thanks to Dr. CHEN Yi, who helped me on writing and reviewing papers and gave me a lot of suggestions. Thanks to Dr. GONG Han, Dr. LIU Chang, Dr. CUI Long and Dr. LI Haiwei for their kind assistance and great support. I would like to give my gratitude to all my group mates who helped me in completing my research.

Very special thanks to Mr. HAN Shuwen, who provided me continuous support from

academic work to daily life. I wish to extend sincere thanks to his company for such long time. Auld Lang Syne.

I want to take the time to thank my parents. Thank my mother, who always listen to me and encourage me. Thank my father, who always enlighten me and support me. I cannot finish my study without their selfless and devoted love.

I am grateful for the valuable comments from the examiners, Prof. WU Chang-yu, Prof. ZOU Shichun, and Dr. WANG Peng for the suggestions to improve the thesis.

TABLE OF CONTENTS

LIST OF FIGURES

LIST OF TABLES

LIST OF ABBREVIATIONS

AVOCs	Anthropogenic Volatile Organic Compounds
BVOCs	Biogenic Volatile Organic Compounds
Cl	Chlorine Radical
CO	Carbon Monoxide
GBA	The Guangdong–Hong Kong–Macao Greater Bay Area
GCU	Gas Calibration Unit
H_3O^+	Hydronium Ions
HO_2	Hydroperoxy Radicals
ToF-CIMS	Time-of-Flight Chemical Ionization Mass Spectrometer
HT	Hok Tsui
MACR	Methacrolein
MEK	Methyl Ethyl Ketone
MIR	Maximum Incremental Reactivity
MVK	Methyl Vinyl Ketone
NO	Nitrogen Monoxide
NO_2	Nitrogen Dioxide
NO_3	Nitrate Radicals
NO_X	Nitrogen Oxides
OFP	Ozone Formation Potential
OH	Hydroxyl Radicals
OVOCs	Oxygenated Volatile Organic Compounds
PFA	Poly(tetrafluoroethylene-co-perfluoropropyl vinyl ether)
PMF	Positive Matrix Factorization
PolyU	The Hong Kong Polytechnic University
ppb	Parts Per Billion
ppt	Parts Per Trillion

PRD	Pearl River Delta
PTR-QMS	Proton Transfer Reaction-Quadrupole Mass Spectrometry
PTR-TOF-MS	Proton Transfer Reaction-Time-of-Flight -Mass Spectrometry
RH	Relative Humidity
RO_2	Organic Peroxy Radicals
SMPS	Scanning Mobility Particle Sizer
SO_2	Sulphur Dioxide
SOA	Secondary Organic Aerosol
T	Temperature
TOPs	Terpenes Oxidation Products
VOCs	Volatile Organic Compounds

Chapter 1 Introduction

1.1 Background

Volatile organic compounds (VOCs) are typical air pollutants, and many are harmful to human health (Azuma et al., 2016) and even carcinogenic (Loh et al., 2007; Stolwijk, 1990). In addition to direct impact on human health, VOCs also exert significant influence on the atmospheric chemistry. In the troposphere, VOCs can react with ozone (O_3), hydroxyl radicals (OH), nitrate radicals (NO_3), and halogens such as chlorine radicals (Cl) to generate intermediates such as hydroperoxyl radicals (HO_2) and organic peroxyl radicals (RO_2), which leads to the recycling of nitrogen oxides (NO_X) and further influences photochemical processes (Claeys et al., 2004; Tham et al., 2016; Wang et al., 2016), especially the formation of O_3 (Sillman and He, 2002; Na et al., 2005; Zheng et al., 2009; Pusede and Cohen, 2012) and secondary organic aerosols (SOA) (Tsigaridis and Kanakidou, 2003; Lack et al., 2004; Lee et al., 2004; Yuan et al., 2013). In addition, VOCs are toxic substances (Wang and Milford, 2001; Guo et al., 2007; Yen and Horng, 2009; Huang et al., 2015; Sun et al., 2018) and the precursors of photochemical smog (Hansen and Palmgren, 1996; Pitten et al., 2000; Mølhave, 2003; Kang et al., 2004), so it is crucial to identify and understand their characteristics.

As an important component of VOCs, oxygenated volatile organic compounds (OVOCs), which are a category of VOCs that include oxygen-containing functional groups, have estimated emission rates of approximately 150 to 500 Tg C yr^{-1} (Singh et al., 2004). Typical OVOCs include aldehydes, ketones, alcohols, ethers, esters, and some low-carbon organic acids, and they play a considerable role in the atmosphere. They can participate directly in photochemical reactions due to their high chemical reactivity and further produce highly oxidizable air pollutants such as O_3 (Louie et al., 2013), peroxy acetyl nitrate (PAN) (Folkins and Chatfield, 2000), and SOA (Derwent et al., 2010).

As a crowded major city in the Guangdong–Hong Kong–Macao Greater Bay Area (GBA), Hong Kong has recently faced increasing concerns about air pollution linked to VOC emissions (Lee et al., 2002; So and Wang, 2004; Guo et al., 2007, 2006; Chan and Yao, 2008; Lau et al., 2010) and O_3 pollution (So and Wang, 2003; Wang et al., 2017). The complexity of Hong Kong's VOC sources has been cited in many studies (Lee et al., 2002; Guo et al., 2007; Lau et al., 2010; Cui et al., 2018; Chen et al., 2020). Most of these studies were conducted in urban microenvironments with offline techniques such as gas chromatography with mass spectrometry (GC-MS) detection, flame ionization detection (FID), and electron capture detection (ECD) and high-performance liquid chromatography (HPLC), and they focused on the alkanes, alkenes, and aromatics emitted from vehicles and industry. The research and database on

OVOCs is scant for Hong Kong and the GBA/Pearl River Delta (PRD) region. Little is known about the properties, formation, and source apportionment of OVOCs in Hong Kong. A comprehensive field study for both VOCs and OVOCs in Hong Kong and the GBA/PRD region is needed to identify their characteristics. In addition, OVOCs are difficult to detect with offline methods due to their short lifetime and high reactivity. Therefore, the latest online monitoring techniques should be implemented into field study. The Cape D'Aguilar Supersite Air-Quality Monitoring Station (known as the HT site) is located at Hok Tsui (HT) on the southeastern tip of Hong Kong Island. Comprehensive field measurements were conducted at the HT site to investigate the concentrations of VOCs and OVOCs using an online instrument, proton transfer reaction quadrupole mass spectrometry (PTR-QMS). The O_3 formation potential was used to identify the key contributors to O_3 generation at the HT site, and positive matrix factorization was used to analyze the emission sources of the individual VOCs and OVOCs.

The results of this field study show that Hong Kong is strongly influenced by urban plumes from the GBA/PRD and by oceanic emissions, and that OVOCs were the dominant species at the HT site with the potential for O_3 formation. In particular, the concentration of isoprene in Hong Kong was higher than those cited in other rural studies (Guo et al., 2006; Yuan et al., 2013; Zou et al., 2015; Li et al., 2019), and isoprene is also the major contributor to O_3 formation.

It is well known that isoprene can be oxidized by OH radicals, O_3, NO_3 radicals, and Cl radicals (Clark et al., 2016; Liu et al., 2016b; Santos et al., 2018) and that this leads to the formation of OVOCs, O_3, and SOA, which further affect air quality and the climate (Ng et al., 2008; Wennberg et al., 2018). Various studies have examined the oxidation of isoprene with OH radicals, O_3, and NO_3 radicals (Berndt and Böge, 1997; Stevens et al., 1999; Zhang et al., 2003; Ng et al., 2008; Peeters et al., 2009; Mutzel et al., 2015), with a focus on the products, mechanisms, and effect of isoprene oxidation with a single oxidant. Conversely, it has been reported that OH radicals can be generated in the oxidation process of isoprene by O_3 and NO_3 radicals (Atkinson et al., 1992; Kwan et al., 2012). In general, oxidants coexist in the atmosphere and participate in the oxidation of isoprene. Nevertheless, few studies have investigated the reaction in a comprehensive system and considered the synergy of associated oxidants in the oxidation process of isoprene, especially for highly oxygenated products.

Environmental chambers have been widely used in recent decades as a useful tool to investigate and infer chemical mechanisms and kinetics (McMurry and Grosjean, 1985; Lee et al., 2001a; Carter et al., 2005; Wang et al., 2014; Leskinen et al., 2015). To better understand isoprene oxidation and its contributions to highly oxygenated compounds, a 6-m^3 Teflon chamber was constructed, and a series of chamber experiments was conducted to investigate the nocturnal oxidation of isoprene in a complex system with three oxidants (OH radicals, O_3, and NO_3 radicals). In addition, state-of-the-art online

techniques were implemented to focus on both small molecules and highly oxygenated compounds, including proton transfer reaction-time-of-flight-mass spectrometry (PTR-ToF-MS) and high-resolution time-of-flight-chemical ionization mass spectrometer (ToF-CIMS). A full spectrum of products was identified, and the contributions of various oxidants to isoprene oxidation was estimated, and the effects of humidity on the oxidation process were investigated. Moreover, the contributions of the detected highly oxygenated compounds to SOA formation were calculated. Overall, these results are expected to provide updated observations of VOCs and OVOCs to the growing database for the mechanism of isoprene oxidation in the GBA/PRD based on the situation in Hong Kong.

1.2 Aims and objectives

Continuous field measurements were conducted at the HT site in Hong Kong from August to October 2018. This was the first use of online high-resolution PTR-QMS to monitor VOCs and OVOCs at a coastal site in Hong Kong. The observations and results from this field study were used as the basis for the construction of a chamber to investigate the related gaseous chemistry and secondary aerosol formation. Hence, the overall objective of this study was to advance our understanding of the formation and impact of OVOCs based on the situation in Hong Kong by addressing significant knowledge gaps.

The major objectives of this study are therefore as follows:

1) Measure the concentrations of VOCs and OVOCs at the HT site and compare them with those from other sites to identify the characteristics in Hong Kong;

2) Determine the contribution of VOCs to O_3 formation and identify the key species for O_3 generation at the HT site;

3) Identify and update the source profiles of VOCs and OVOCs in Hong Kong;

4) Develop and evaluate the performance of the new chamber system for investigation of gaseous chemistry and secondary aerosol formation;

5) Investigate the isoprene oxidation process in a comprehensive system with OH radicals, O_3 and NO_3 radicals;

6) Evaluate the contributions of various oxidants to isoprene oxidation under various concentrations of NO_2.

1.3 Outline of the dissertation

This thesis comprises eight chapters as follows:

Chapter 1 provides a brief background and presents the major research objectives of this study.

Chapter 2 presents a detailed literature review of VOCs and OVOCs, characteristic field measurements in Hong Kong and the GBA, the development of environmental chambers around the world, and related oxidation reactions of isoprene with various radicals in chamber simulations.

Chapter 3 describes the methods used in this study, including the sampling locations, the instrumentation used in both field study and chamber simulation, and the models used in this study.

Chapter 4 presents a comprehensive field study at a coastal rural site in Hong Kong, with a focus on photochemical reactivity and source apportionment of VOCs and OVOCs.

Chapter 5 introduces the development of a new indoor environmental chamber system at PolyU, including its design philosophy and characterization.

Chapter 6 describes the investigation of the nocturnal isoprene oxidation reaction in a complex system using the developed chamber system.

Chapter 7 summarizes the study's major findings and results.

Chapter 8 highlights the significance of this study and suggests topics for future research.

Chapter 2 Literature Review

2.1 Overview of VOCs

2.1.1 Description of VOCs

Volatile organic compounds (VOCs) are among the most important air pollutants. These organic compounds normally include fewer than 15 carbon atoms, and the mixing ratio in the atmospheric environment ranges from concentrations in parts per trillion by volume (pptv) to concentrations in parts per billion by volume (ppbv) (Kansal, 2009). The European Union explicitly defines VOCs as having boiling points lower than 250°C at a standard atmospheric pressure of 101.3 kPa.

VOCs are easily emitted into the atmosphere from urban, oceanic, and terrestrial activities because of their relatively low boiling points (Guenther, 1995). Urban sources include various emissions from cooking (Lee et al., 2001b; Mugica et al., 2001), vehicles (Lee et al., 2002; Lau and Chan, 2003), paints (Guo et al., 2004; Ho et al., 2004), combustion (Khalili et al., 1995; Srivastava et al., 2005), and even breathing (Phillips et al., 1999; Delfino et al., 2003). Oceanic emissions come mainly from seawater (Kot-Wasik et al., 2004) and phytoplankton (Kameyama et al., 2014). Emissions from vegetation (Sharkey et al., 1996; Sharkey and Yeh, 2001) and from invertebrates (Greene and Gordon, 2003) represent the main contributions from

terrestrial activities.

VOCs can be categorized into various groups including halogenated hydrocarbons, alcohols, aldehydes, aromatics, alkanes, ketones, alkenes, ethers, esters, paraffins, and sulfur-containing compounds (Kamal et al., 2016) based on their different functional groups. As an important type of VOCs, oxygenated volatile organic compounds (OVOCs) are VOCs with oxygen-containing functional groups, including aldehydes, ketones, alcohols, ethers, some low-carbon organic acids, and esters. OVOCs play a non-negligible role in the atmosphere due to their high chemical reactivity. According to their direct emission sources, VOCs can be divided into two types: biogenic volatile organic compounds (BVOCs) and anthropogenic VOCs. Vegetation is the dominant source of BVOCs (Warneck, 1999), accounting for 69% of the total VOC emissions (Middleton, 1995), whereas the remaining 31% come from anthropogenic sources such as industry, coatings, solvents, and vehicles (Garcia et al., 1992; Mugica et al., 1998; Barletta et al., 2005).

Many studies have reported that a number of VOC species are harmful to human health (Azuma et al., 2016) and even carcinogenic (Stolwijk, 1990; Loh et al., 2007). VOCs can be directly inhaled into the human respiratory system and exert an acute influence on the liver, kidneys, brain, and central nervous system, and even cancer has been seen in severe cases (Schiffman, 1998; Pitten et al., 2000; Wolfe and Patz, 2002; Tam and

Neumann, 2004).

2.1.2 VOC oxidation in the atmosphere

In addition to the physical deposition process, VOCs can participate in the chemical processes of photolysis, reacting with ozone (O_3), hydroxyl radicals (OH), nitrate radicals (NO_3), and halogens such as chlorine radicals (Cl) (Middleton, 1995; Fantechi et al., 1998). In the troposphere, reaction with OH radicals is the dominant process of tropospheric loss for a large number of VOCs during the daytime, whereas reaction with NO_3 radicals is the major contributor at nighttime (Monks, 2005). In addition, VOCs can be oxidized by O_3 and by Cl radicals in marine and coastal areas (Fantechi et al., 1998).

The atmosphere contains two major sources that generate OH radicals; either the photolysis of O_3 forms excited oxygen and then reacts with water vapor (equations 2.1 and 2.2) (Atkinson, 1997a),

$$O_3 + hv \rightarrow O_2 + O(^1D), \lambda \leq 335\,nm \quad 2.1$$

$$O(^1D) + H_2O \rightarrow 2\,OH \quad 2.2$$
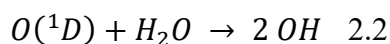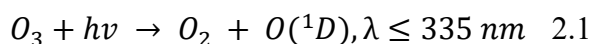
or HO_2 reacts directly with NO when the NO concentration is low (equation 2.3).

$$HO_2 + NO \rightarrow NO_2 + OH \quad 2.3$$

Moreover, in some polluted areas, OH radicals can also be generated from the photolysis of nitrous acid (HONO), hydrogen peroxide (H_2O_2), formaldehyde (HCHO), and other carbonyls in the presence of NO (Atkinson, 2000).

NO_3 radicals can be produced by the following reactions (equations 2.4 and 2.5) in the atmosphere (Atkinson, 1997a):

$$NO + O_3 \rightarrow NO_2 + O_2 \quad 2.4$$

$$NO_2 + O_3 \rightarrow NO_3 + O_2 \quad 2.5$$

NO_3 radicals undergo photolysis and rapid reaction with NO leading to the low concentration at daytime, and they have a lifetime in the region of 5 s for overhead sun and clear sky conditions (Monks, 2005). However, at night, NO_3 radicals can accumulate, and the ground-level concentration can increase to approximately 1×10^{10} molecule cm^{-3} (Platt and Heintz, 1994). Similar to the reaction of OH radicals, NO_3 reacts with isoprene via addition to a carbon–carbon double (C=C) bonds.

O_3 is generated from the photolysis of NO_2 (equations 2.6 and 2.7), which was first reported by Blacet (1952).

$$NO_2 + hv \rightarrow NO + O(^3D), \lambda \leq 420\ nm \quad 2.6$$

$$O(^3D) + O_2 + Air \rightarrow O_3 + Air \quad 2.7$$
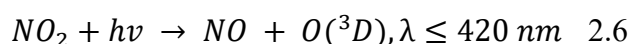
In addition, the degradation of VOCs will generate intermediates such as organic peroxyl radicals (RO_2) and hydroperoxyl radicals (HO_2). These intermediates can react with NO and form O_3 via photolysis (Atkinson, 2000). Although the photolysis of NO_2 during the daytime is the major contributor to O_3 formation, O_3 participates in this chemical reaction during both the day and night due to its long lifetime and residuals at night. The reaction rates between O_3 and alkanes, saturated hydrocarbons, and aromatic hydrocarbons are quite slow (Atkinson and Arey, 2003), so the dominant reaction involving O_3 in the atmosphere is with the C=C bonds contained in VOCs. First, O_3 adds to the C=C bond to form the primary ozonide (POZ), and these energy-rich POZs then rapidly decompose into two parts, carbonyl and Criegee intermediates (Atkinson, 1997b).

Figure 2.1 presents the typical transformation reactions of VOCs in the troposphere (Atkinson, 2000), including generation of important intermediates such as alkyl or substituted alkyl radicals (R), hydroperoxyl radicals (HO_2), alkoxy radicals (RO), and organic peroxyl radicals (RO_2). Although these detailed reaction mechanisms depend on the specific VOCs, the reactions of VOCs in the atmosphere share many universal sequences. In general, the first step of VOC reactions is either photolysis with OH radicals or NO_3 radicals, which can generate R radicals, or the reaction between the C=C bond and O_3, which can generate RO_2 radicals. Generally, these alkyl or substituted alkyl radicals can be formed in two ways: (i) an H-atom is abstracted from

the C−H bonds or the O−H bond by OH radicals, NO_3 radicals, and Cl radicals (examples shown in equations 2.8 and 2.9), or (ii) the initial C=C bond is broken by NO_3 radical, O_3, and OH radical reactions (examples shown in equation 2.10). The reaction process between VOCs that contain C=C bonds and O_3 is more complicated than those for other radicals (OH, NO_3, and Cl).

$$X + RCH_2R' \rightarrow HX + RC \cdot HR' \quad (2.8)$$

$$X + RCHO \rightarrow HX + R \cdot CO \quad (2.9)$$

$$X + RHC = CHR' \rightarrow RC \cdot H - CH(X)R' \quad (2.10)$$

where X represents OH radicals, NO_3 radicals, or Cl radicals.
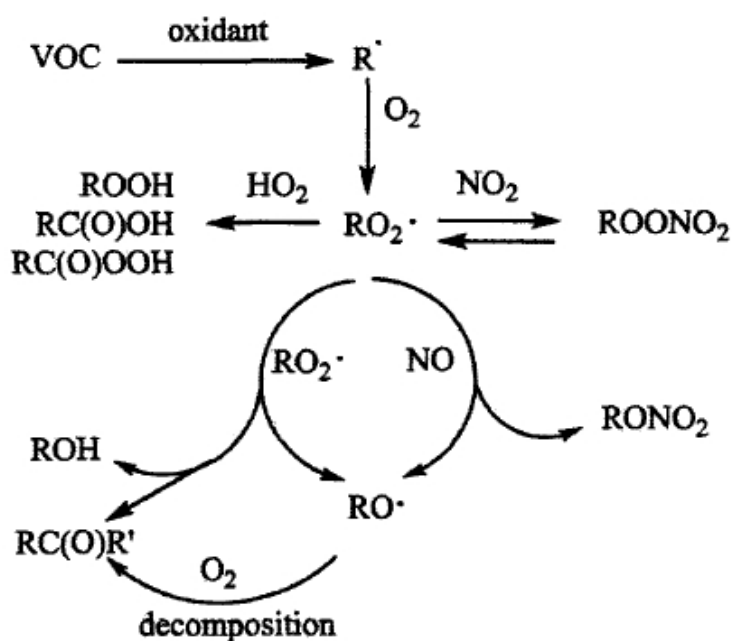
Figure 2.1 Scheme of VOCs' transformation in the troposphere (Atkinson, 2000).

2.2 Characterization of VOCs in Hong Kong and GBA/PRD

2.2.1 Previous field studies on VOCs in Hong Kong and GBA/PRD

Hong Kong, on China's southern coast, is one of the world's most densely populated cities. It has been one of Asia's most developed regions since the early 1990s due to its special administrative status in China. It is a central city in the Guangdong–Hong Kong–Macao Greater Bay Area (GBA) and has approximately 7.5 million residents and more than 900,000 registered vehicles (at the end of 2020). Over the past several years, a number of studies have reported the increased concentration of air pollutants linked to VOC emission (Lee et al., 2002; So and Wang, 2004; Guo et al., 2007, 2006; Chan and Yao, 2008; Lau et al., 2010).

The GBA region was defined in 2017 as including Hong Kong, Macao, and several municipal regions in Guangdong province: Guangzhou, Shenzhen, Zhuhai, Foshan, Huizhou, Dongguan, Zhongshan, Jiangmen, and Zhaoqing. The GBA has become a first-class international bay area and world-class urban agglomeration due to the development of the Pearl River Delta region (PRD). However, rapid industrialization and urbanization have led to many severe air pollution episodes. For example, the O_3 concentration in China's southern coastal area increased at a rate of 0.35 ppbv per year between 1994 and 2018 (Wang et al., 2019).

Hong Kong is a highly urbanized city, and its air quality is influenced by many factors. It has also struggled with huge increases in VOC emissions (Chan et al., 2002; Lee et al., 2002; Cui et al., 2018) and O_3 pollution (So and Wang, 2003; Wang et al., 2017). Several field studies have been conducted in Hong Kong to identify and characterize the ambient VOCs since the early 21st century. Chan et al. (2002) conducted roadside sampling in four districts in January and February 1998 and noted the important roles played by automobile exhaust and the use of organic solvents in urban Hong Kong, as its average concentrations of toluene (77.2 μg m^{-3}), benzene (26.7 μg m^{-3}), and chlorinated VOCs (10.8 μg m^{-3}) are higher than those of other metropolitan areas. Lee et al. (2002) also found that the concentration of VOCs in Hong Kong's urban areas was affected by both vehicular emissions and industrial emissions. In addition, the VOC concentrations were usually higher in winter than in summer. Later, a comprehensive

campaign was conducted in both urban and rural areas of Hong Kong from November 2000 to February 2001 and from June to August 2001 (Guo et al., 2007). The acetylene/CO ratio was higher (5.6 pptv/ppbv) at Tap Mun (a northeastern rural area in Hong Kong) than in Nashville, U.S.A., (Goldan et al., 2000), which suggested that a subtropical city like Hong Kong was influenced by both local and regional pollution.

The complexity of the VOC sources in Hong Kong has been mentioned in many studies (Goldan et al., 2000; Lau and Chan, 2003; Lam et al., 2005). Guo et al. (2004) measured 156 VOC species from January 10 to December 30, 2001, and the results indicated that the photochemical reaction also contributed to Hong Kong's high VOC concentrations. Ho et al. (2004) assessed the relative ages of air parcels during the winter of 2000 and spring of 2001 with the xylene/ethylbenzene ratio (Nelson and Quigley, 1984). The calculated xylene/ethylbenzene ratios (average, 1.2 to 1.7) showed that the VOCs in Hong Kong were affected by photochemical reactions.

The sources of the VOCs in rural areas differ from those of the urban and roadside sites. Guo et al. (2006) conducted a field study from August 2001 to December 2002 at Tai O, a polluted rural/coastal site in the PRD. The source apportionment from the principal component analysis/absolute principal component scores receptor model showed the importance of biomass burning in the rural sites around the PRD during the dry autumn/winter season, which exhibited outcomes contrary to those in urban areas.

2.2.2 Potential impact of OVOCs

OVOCs are a series of VOCs with oxygen-containing functional groups, including aldehydes, ketones, alcohols, ethers, some low-carbon organic acids, and esters. They play a critical role in chemical reactions and processes in the atmosphere, and their emission rate is estimated to be approximately 150 to 500 Tg C yr^{-1} (Singh et al., 2004). Their relatively high chemical reactivity allows OVOCs to participate directly in photochemical reactions and to further produce air pollutants with high oxidizing ability, such as O_3, in the atmosphere (Louie et al., 2013). OVOCs are also the precursors of PAN and SOA (Derwent et al., 2010). For example, methanol and acetone play vital roles in sequestering NOx in the form of PAN and in providing HOx radicals to critical regions of the atmosphere (Folkins and Chatfield, 2000; Singh et al., 1995).

The OVOCs in the atmosphere have various sources, including natural sources (Heiden et al., 2003), anthropogenic sources (Schauer et al., 2001), and the secondary formation process from atmospheric photochemical reactions (Paulot et al., 2012). Biogenic sources are believed to be the largest source of OVOCs (Singh et al., 1994; Jacob et al., 2002); they include direct emissions from plants (Fall, 1999) and agricultural fields (Schade and Custer, 2004) and indirect emissions from O_3 decomposition of the biological fatty acids and the wax on the cuticle of the plant (Fruekilde et al., 1998). It was reported that more than 80% of acetone in a rural environment in the Sierra Nevada

mountains, U.S.A., had biogenic and regional sources (Goldstein and Schade, 2000).

In addition, some of the HCHO, acetaldehyde, and butanone also come directly from

vegetation (Fall, 1999). In contrast, as the number of the vehicles on the road continues

to rapidly increase, automobiles make increasingly significant contributions to the total

emission of OVOCs. In China, the OVOCs contributed 53.8% of total VOCs in the

profiles of heavy-duty diesel vehicle exhaust and 12.4%–46.3% in biomass and

residential coal burning, which indicated the importance of primary OVOCs emissions

from combustion-related sources (Mo et al., 2016). In addition, a large number of

OVOCs emitted from wood combustion were detected, thus indicating another source

of biomass burning (Mcdonald et al., 2000).

In addition to primary emissions such as those from biogenic and anthropogenic sources,

secondary formation from atmospheric chemical reactions also contributes to the

presence of OVOCs. OVOCs are the oxidation products of photochemical reactions of

non-methane hydrocarbons (NMHCs) in the atmosphere (Legreid et al., 2007; Hellén

et al., 2018). OVOCs can further react with free radicals (e.g., OH radicals) to form the

relevant active radicals, which makes the OVOCs critical contributors to oxidation in

the troposphere. Many hydrocarbons from plants (e.g., isoprene and terpene) are

oxidized by free radicals to form OVOCs (Paulot et al., 2012). Moreover, some

carbonyls (e.g. HCHO, acetaldehyde, and acetone) and alcohols with low carbon

numbers can also generate radicals such as HO_2 and RO_2 via photolysis reactions

(Folkins and Chatfield, 2000; Jacob et al., 2002; Singh et al., 2004, 1994).

OVOCs have a significant impact on photochemical smog and atmospheric air pollutants. They are the precursors of free radicals, O_3, and peroxy acetyl nitrates, which influence both human health and plant growth (Singh et al., 1995; Schade and Custer, 2004). Oxidation of OVOCs also leads to damage to the ambient environment. Formic acid and acetic acid, which cause acid rain in remote regions (Galloway et al., 1982), can be generated from the oxidation process of OVOCs (Kesselmeier et al., 1997). Most OVOCs are irritative gases that affect the eyes, skin, and respiratory system and may even cause cancer (Rumchev et al., 2002; He et al., 2015). For instance, HCHO is defined as a carcinogen by the WHO and can lead to various diseases and even death (Szende and Tyihák, 2010).

The study of OVOCs has attracted considerable attention in recent years. Yuan et al. (2010) conducted a field study at a rural site in Guangzhou with proton transfer reaction PTR-MS and found that biomass burning contributed 10% to 18% to reactive NMHCs and OVOCs. Wang et al. (2016) also studied the relationship between biomass burning and OVOCs in the PRD region and used the photochemical age-based parameterization method to show 21% more OVOC emissions from biomass burning than from non-biomass burning plumes. Speciated emissions of OVOCs and VOCs in the PRD region were estimated with the use of sector-based source profiles for anthropogenic sources

and the Model of Emissions of Gases and using Aerosols from Nature for biogenic sources (Ou et al., 2015). The results revealed that OVOCs were composed of 15.9% anthropogenic VOCs, of which methanol, acetone, and ethyl acetate were the major species. Louie and colleagues noted the significant contribution from OVOCs to O_3 formation in Hong Kong, that is, more than one-third of that from all VOCs (Louie et al., 2013). Insufficient attention has been devoted to OVOCs in the atmosphere, and the database of information on OVOCs in Hong Kong and the GBA/PRD region remains scant. Comprehensive field studies of both VOCs and OVOCs in Hong Kong are needed to identify their characteristics and enrich the database.

2.2.3 Potential impact of isoprene

BVOCs are emitted into the atmosphere from plants and vegetation and are a major component of the total VOCs in the atmospheric environment. The reaction of BVOCs and active radicals can lead sequentially to the generation of SOA and particulate matter (Li et al., 2017).

Isoprene (2-methyl-1,3-butadiene, C_5H_8) is considered the most abundant BVOC emitted into the atmosphere (estimated emission rate, ~400 to 660 Tg C yr^{-1}) (Guenther, 1995,2006; Liu et al., 2016a). Isoprene commonly occurs in plants of the families Salicaceae, Fagaceae, and Palmae and the genus *Picea* (spruces), and in diverse ferns (Kesselmeier and Staudt, 1999). It is usually volatilized from plants and emitted into

the atmosphere, as reported in many countries by many groups (Sharkey et al., 1996;

Sharkey and Yeh, 2001; Pétron et al., 2001; Pacifico et al., 2009).

Some studies have also discussed marine emissions of isoprene, which can be produced

by heterotrophic bacteria, marine phytoplankton, and seaweed (Arnold et al., 2009;

Broadgate et al., 2004; Tran et al., 2013), as first reported by Bonsang et al. (1992) in

the Mediterranean Sea and Pacific Ocean. A study conducted on CHINARE cruises

suggested the presence of isoprene in the marine boundary layer and the importance of

oceanic emissions of isoprene (Hu et al., 2013). The estimated emission rate of oceanic

isoprene ranges from 1 to 10 Tg yr^{-1} (Shaw et al., 2010).

Although biogenic emissions are the main source of isoprene in the atmosphere,

anthropogenic contributions to the isoprene concentration also occur (Reimann et al.,

2000). A field experiment conducted at an urban center in northern France from May

1997 to April 1999 revealed the traffic-related origin of isoprene (Borbon et al., 2001).

In Pakistan, a strong correlation was found not only between isoprene and CO but also

between isoprene and acetylene (correlation coefficients, 0.91 and 0.78, respectively).

The diurnal production of isoprene was quite similar to that of other hydrocarbons

related to vehicular sources. The slope of isoprene to CO indicated that 20% of the

isoprene observed in Pakistan came from vehicular emissions (Barletta et al., 2002).

Isoprene has the highest emissions among BVOCs in Hong Kong, with annual average

concentrations of 0.46, 0.30, 0.43, and 0.65 ppbv at rural, residential, industrial, and roadside sites, respectively (So and Wang, 2004). The concentration of isoprene was found to be higher in Hong Kong than in Santiago, U.S.A (0.5 ppbv) (Barletta et al., 2002). The results of principal component analysis suggested that isoprene in rural areas came mainly from biogenic emissions and showed a higher concentration in August, whereas vehicle emissions also dominated significantly in urban areas. In addition, a higher isoprene concentration was observed at the rural site than urban site in Hong Kong, and the concentration rose slightly during summertime, reflecting the influence of biogenic emissions and significant contributions to O_3 formation relative to anthropogenic VOCs (Guo et al., 2007). In addition, isoprene emitted from plants is a major contributor at rural sites and is the key precursor to O_3 formation (So and Wang, 2004). Overall, isoprene plays a crucial role in terms of OH-reactivity and O_3 formation, especially in Hong Kong's rural areas.

The atmospheric concentrations of isoprene range from ppt to several ppb. Its two double bonds and high emitted concentration allow isoprene to react easily with free radicals (e.g., OH radicals, NO_3 radicals, and O_3), and hence it plays an important role in atmospheric chemistry (Clark et al., 2016; Liu et al., 2016b; Santos et al., 2018). The lifetime of isoprene in the atmosphere ranges from a few minutes to hours (Atkinson and Arey, 2003), and it cannot be transported far from its sources before being oxidized (Liakakou et al., 2007). **Figure 2.2** shows the role of isoprene in the tropospheric

environment. **Table 2.1** lists the rate coefficients for isoprene oxidation initiated by OH radicals, O_3, NO_3 radicals, and Cl radicals. The theoretical mechanisms and related chamber studies are reviewed in Section 2.3.2.
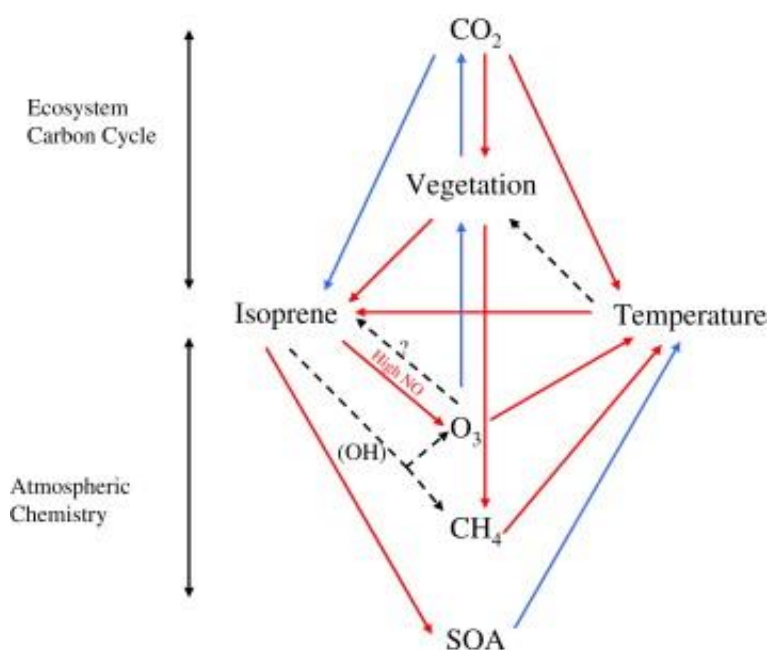
Figure 2.2 Schematic interrelationships for isoprene emissions, SOA formation, and atmospheric chemistry. Red arrows present the positive relationships, blue arrows present the negative relationships, dashed arrows present the uncertain relationships (Pacifico et al., 2009).

Table 2.1 Rate coefficients for isoprene oxidation reported by IUPAC[a].

Radicals	Dominant sink [b]	k (cm^3 molecule^{-1} s^{-1})	T (K)	Reference
OH	1.4 h	2.7×10^{-11}	280-315	(Atkinson et al., 2006)
O$_3$	16.4 h	1.03×10^{-14}	240-360	(Atkinson et al., 2006)
NO$_3$	17.5 h	2.95×10^{-12}	250-390	(Atkinson et al., 2006)
Cl	29 d	4.1×10^{-10}	298	(Sander et al., 2006)

[a] IUPAC: International Union of Pure and Applied Chemistry.
[b] All rate coefficients are reported by IUPAC (Atkinson et al., 2006), where [OH] = 2 $\times 10^6$ molecules cm^{-3}, [O$_3$] = 50 ppbv, [NO$_3$] = 1 pptv and [Cl] = 1 $\times 10^3$ molecules cm^{-3}, respectively.

2.3 Environmental chamber

2.3.1 Overview of environmental chamber

Environmental chambers, also known as smog chambers, have been widely used in recent decades as a practical tool to investigate and infer chemical mechanisms and kinetics. Smog chambers were first used in the 1980s to study the atmospheric chemical processes of air pollutants (Akimoto et al., 1979; Carter et al., 1982).

Several parameters for a new smog chamber system required evaluation and characterization before any experiments can be conducted. Baseline control and wall effects are the major factors that limit the reliability of the results in evaluation of the model and mechanism. For instance, the initial NOx and VOCs concentrations in smog chamber experiments are often higher than those in the atmosphere due to the

limitations of the detection instruments and of background control. In addition, great uncertainties exist for those NOx and VOCs with low concentrations due to the wall loss effect. Therefore, the relatively small surface-to-volume ratio of a large-volume smog chamber can help it avoid the wall effect and reduce the loss of chemicals in both gas and particle phases. The large chamber also allows sufficient reaction time and provides more connection ports for analytical and monitoring instruments.

Both outdoor and indoor chambers have been built in previous research. Outdoor smog chambers use natural light sources whose intensity changes with time and season (Carter et al., 2005; Rohrer et al., 2005) and natural environmental conditions that better reflect diurnal changes and the reaction process. However, it is difficult to conduct repeated experiments due to the uncontrollable light and ambient environmental conditions. In contrast, repeated testing can be carried out under controllable conditions using indoor smog chambers (Cocker et al., 2001; Xu et al., 2006; Wang et al., 2014). Nevertheless, some limitations and uncertainties exist with indoor chambers due to the disparity between natural and artificial light sources.

In the 1980s, Seinfeld and colleagues (Leone and Seinfeld, 1985; Stern et al., 1987) set up a 65-m^3 outdoor smog chamber made of fluorinated ethylene propylene (FEP) at the California Institute of Technology (Caltech) to study aerosol formation from the photo-oxidation of biogenic and aromatic hydrocarbons. Many chamber systems have since

been developed to study gas-phase products and the formation of SOA.

The group at the University of California, Riverside has been working on chambers from 1980s, and eight outdoor and indoor chambers have been constructed (Atkinson et al., 1980; Carter, 1995; Carter et al., 1997). Through years of experimentation and characterization, this group established a highly functional chamber system that consists of two collapsible 90-m^3 FEP Teflon film reactors (Carter et al., 2005). EUPHORE, another representative smog chamber, was a double hemispherical reactor in Valencia, Spain, used to focus on atmospheric chemical reactions in the gas phase and kinetic parameters (Becker et al., 1996; Wang et al., 2014). Smog chamber facilities have been developed in China since the 1980s (Wang et al., 1995; Xu et al., 2006; Wu et al., 2007; Wang et al., 2014). These studies have provided valuable experience in the development of smog chambers to study photochemical kinetics and mechanisms. A series of new chamber systems was recently developed to meet the challenges of air pollution control in China (Zhang et al., 2008; Li et al., 2014; Wang et al., 2014). **Table 2.2** summarizes the details of various chamber systems.

Table 2.2 Summary of chamber systems.

Institutions	Types	Volume (m^3)	Material	Reference
California Institute of Technology, U.S.A.	Indoor	28 (Dual)	FEP	(Cocker et al., 2001)
University of California (Riverside), U.S.A.	Indoor	90 (Dual)	FEP	(Carter et al., 2005)
University Florida, U.S.A.	Outdoor	52 (Dual)	FEP	(Im et al., 2014)
Forschungszentrum Jülich, Germany	Outdoor	27	FEP	(Rohrer et al., 2005)
Toyota Central R&D Labs, Japan	Indoor	2	FEP	(Takekawa et al., 2003)
Paul Scherrer Institut, Switzerland	Indoor	27	FEP	(Dommen et al., 2006)
Forschungszentrum Karlsruhe, Germany	Indoor	84	Metal	(Möhler et al., 2003)
University of North Carolina,U.S.A.	Outdoor	135 (Dual)	FEP	(Lee et al., 2004)
Interuniversity Laboratory of Atmospheric Systems, France	Indoor	4.2	Stainless steel	(Wang et al., 2011)
Commonwealth Scientific and Industrial Research Organisation, Australia	Indoor	18	FEP	(Hynes et al., 2005)
Guangzhou Institute of Geochemistry, Chinese Academy of Sciences, Guangzhou	Indoor	30	FEP	(Wang et al., 2014)
Tsinghua University, Beijing	Indoor	2	FEP	(Wu et al., 2007)
Fudan University, Shanghai	Indoor	4.5	Stainless steel	(Zhang et al., 2008)

Some old chamber systems cannot fulfill all of the requirements for the materials, technologies, wall effect, and control of environmental conditions that allow accurate simulation experiments. Moreover, recent atmospheric chemistry issues have raised new research interests and topics, so enhanced methods should be implemented in chamber studies. For example, state-of-the-art online analytical instruments are needed for observation of intermediates and transient processes. Newly designed chambers have been constructed, and many outdated smog chambers require upgrades to meet these challenging requirements. Leskinen et al. (2015) designed a 29-m^3 collapsible FEP chamber as part of a combustion system to thoroughly study vehicle exhaust, which was combined with dilution systems and cell/animal exposure devices.

2.3.2 Reaction of isoprene in chamber systems

As discussed in Section 2.2.3, isoprene can easily react with free radicals such as hydroxyl radicals (OH), O_3, nitrate radicals (NO_3), and chlorine radicals (Cl), and hence it plays an important role in atmospheric chemistry (Clark et al., 2016; Liu et al., 2016b; Santos et al., 2018) owing to its two double bonds and high concentration in the troposphere. Laboratory studies on the dark and photochemical reactions of isoprene in a chamber system are reviewed in detail below.

The overwhelmingly dominant reaction pathway of isoprene in the atmosphere is oxidation initiated by OH radicals (Wennberg et al., 2018), with an estimated accounts

of approximately 85% of isoprene reaction (Paulot et al., 2012), due to the synchronous diurnal curves between isoprene and OH. As illustrated in **Figure 2.3**, the reaction between isoprene and OH radicals begins from an additive reaction on the unsaturated backbone. Although OH can be added at any of four positions on the conjugated carbon chain of isoprene, the fractions of isomers 1, 2, 3, and 4 are 0.67, 0.02, 0.02, and 0.29, respectively, based on theoretical calculations by Greenwald and colleagues (Greenwald et al., 2007). After the addition of OH to the unsaturated backbone of isoprene, the 1−OH and 4−OH adducts are generated separately as pools of allylic radicals (Peeters et al., 2014, 2009). Peeters et al. (2014) also estimated 0.46 and 0.69 as the fractions of cis allylic radicals and 0.54 and 0.31 as the fractions of *trans*-allylic radicals for 1−OH adducts and 4−OH adducts, respectively. Each OH−isoprene allylic radical will then obtain an oxygen atom to form three distinct isoprene hydroxy peroxyl radicals (ISOPOOs): β−ISOPOO, Z−δ-ISOPOO, and E-δ-ISOPOO (Peeters et al., 2014; Teng et al., 2017). The rate constant of the overall oxygen addition reaction is $k_{ISOPOO\ Addition} = 2.0 \times 10^{-12}$ cm^3 molecule^{-1} s^{-1} at 298 K (Park et al., 2004). Those ISOPOO radicals will continue to react with NO, HO$_2$, or other peroxyl radicals, which can be detected by the degradation of ISOPOO radicals by chemical ionization MS (Zhang et al., 2003) and laser-induced fluorescence (Stevens et al., 1999). Isoprene hydroxy nitrate is generated by both β−ISOPOO and δ−ISOPOO isomers, with branching ratios of 0.067 and 0.24, respectively (Paulot et al., 2009). The rate constant

for the reaction between NO and the ISOPOO radical is $k_{ISOPOO+NO} = 8.8 \pm 1.2 \times$

10^{-12} cm^3 molecule^{-1} s^{-1} at 298 K (Atkinson et al., 2006), which is the sole source of

the production of methyl vinyl ketone (MVK) and methacrolein (MACR). However,

due to the uncertain lifetime of β−ISOPOO, the yields of MVK and MACR from

isoprene oxidation vary and are not confirmed, ranging from 31% to 44.5% when the

NO concentrations changed from 20 ppb to 31.8 ppb, respectively (Liu et al., 2013;

Miyoshi et al., 1994; Paulson and Seinfeld, 1992; Ruppert and Heinz Becker, 2000;

Sprengnether et al., 2002; Tuazon and Atkinson, 1990).

Moreover, HCHO and HO$_2$ are produced in the presence of oxygen, and the yield of

HCHO is equal to the sum of MVK and MACR (Miyoshi et al., 1994; Sprengnether et

al., 2002; Tuazon and Atkinson, 1990). HCHO, MVK, and MACR are the major

products of the reaction of isoprene and OH. The reaction of ISOPOO and HO$_2$

generates the unsaturated hydroxy hydroperoxide named isoprene hydroxy

hydroperoxide (ISOPOOH) with six possible isomers, which was initially reported by

PTR in field measurements from the Amazon basin in Suriname (Crutzen et al., 2000;

Warneke et al., 2001a) and from the savannah in Venezuela (Holzinger et al., 2002).

The rate constant for this reaction is $k_{ISOPOO+HO_2} = 1.74 \pm 0.25 \times 10^{-11}$ cm^3

molecule^{-1} s^{-1} at 298 K (Boyd et al., 2003). As reported in a chamber study (Fabien

Paulot et al., 2009; St Clair et al., 2016), ISOPOOH plays a crucial role in isoprene

oxidation in low-NO$_X$ conditions, as measured by CIMS combined with PTR-MS. In

low-NOx conditions, the self-reactions of RO_2 and cross-reactions with their products

are both important in producing MVK, MACR, HCHO, and ISOPOO (Jenkin et al.,

1998; Jenkin and Hayman, 1995).
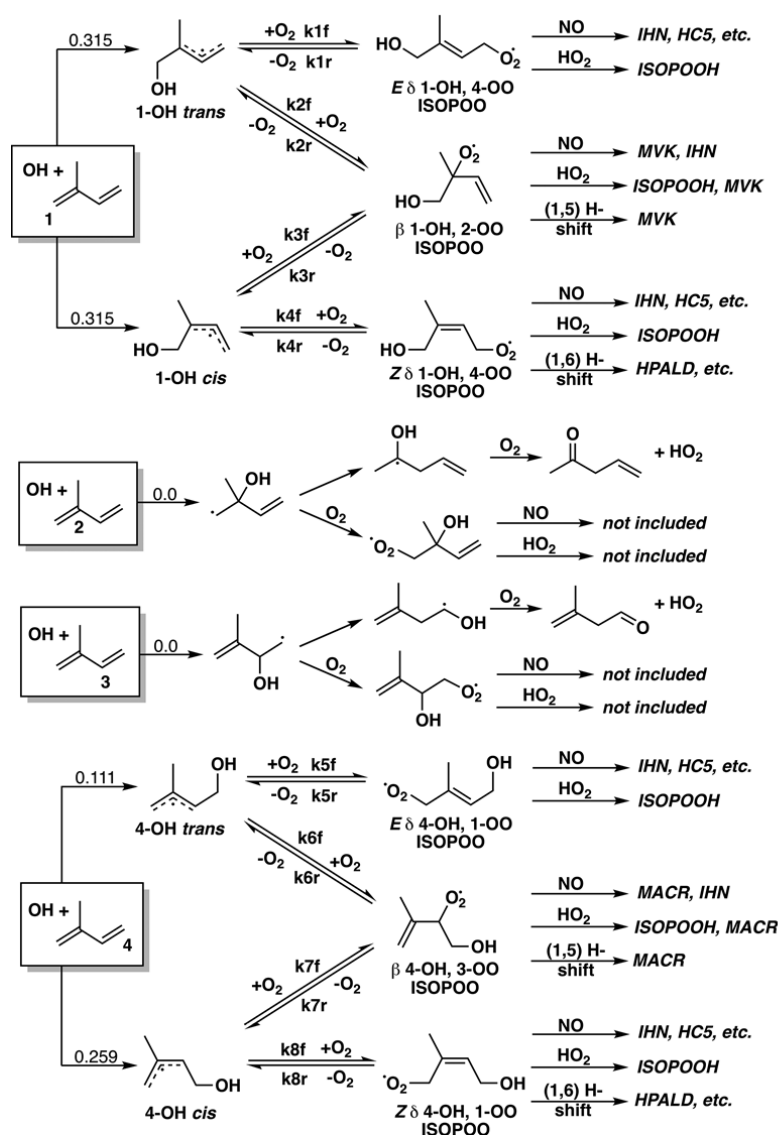
Figure 2.3 Dynamics of the reported isoprene + OH system in the presence of O_2

(Wennberg et al., 2018).

Although the prevailing removal process of isoprene is its reaction with OH radicals, it is estimated that approximately 10% of its loss in the atmosphere is related to reaction with O_3 (Isidorov, 1990). OH radicals, RO_2 radicals, Criegee intermediates, stable gaseous products, and SOA are generated from the complex reaction process between isoprene and O_3 (Biesenthal et al., 1998; Isidorov, 1990; Nguyen et al., 2010). Ozonolysis of isoprene could also become a significant chemical mechanism of O_3 depletion in isoprene-dominant areas (Fiore et al., 2005). The ozonolysis of isoprene is a complex chemical process and includes several steps (**Figure 2.4**). First, the cycloaddition reaction between O_3 and isoprene occurs at one of the two double bonds and then forms either kind of POZ (Zhang et al., 2003). Approximately 60% of the total yields are 3,4-addition POZ, and the rest are 1,2-addition POZ, because in the methyl group the effect of steric hindrance takes precedence over that of electron donation, as reported by Aschmann (1994). The two types of POZ then decompose into different products. The 3,4-addition type becomes MACR or HCHO, whereas the 1,2-addition type produces MVK or HCHO. Both kinds of POZ yield C_1 or C_4 carbonyl oxides with high reactivity; these products are called activated Criegee intermediates (Wennberg et al., 2018). Some of the generated Criegee intermediates further decompose and participate in both bimolecular and unimolecular chemical reactions, and the rest become stabilized Criegee intermediates. Because no alkyl substituent is present in CH_2OO to form a *syn* conformation, CH_2OO has very low unimolecular reactivity.

However, CH_2OO reacts with some gaseous molecules to form HCHO and hydrogen peroxide or highly oxidized multifunctional compounds, water, and formic acid based on its branching ratios (Mentel et al., 2015; Mutzel et al., 2015; Rissanen et al., 2014).
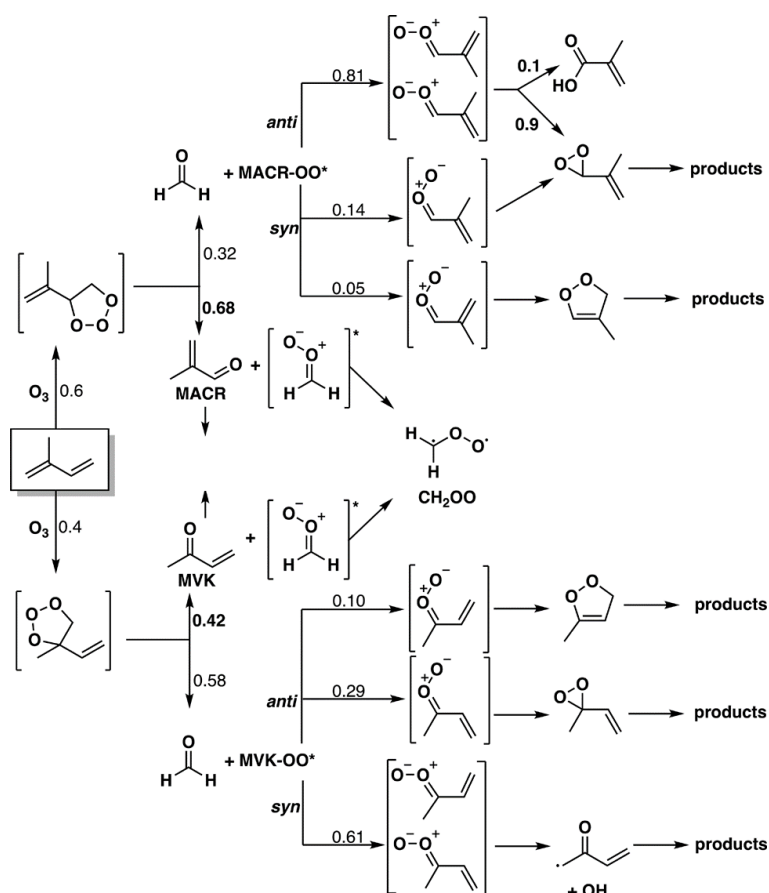
Figure 2.4 Dynamics of the reported ozonolysis of isoprene (Wennberg et al., 2018).

NO_3 radicals undergo photolysis rapidly during daytime, so the reaction of isoprene with NO_3 mostly occurs at night. Although this pathway contributes only a small part

of the isoprene sink (Horowitz et al., 2007), it results in measurably decreased concentrations of isoprene after sunset (Brown et al., 2009; Starn et al., 1998), and is a major source of nitrates (Beaver et al., 2012; Grossenbacher et al., 2004). **Figure 2.5** demonstrates the reactions and products following isoprene + NO_3. The reaction of NO_3 and isoprene begins with addition to the C=C double bond (Berndt and Böge, 1997; Schwantes et al., 2015), which is similar to the reaction of isoprene with O_3. The intermediates continue to gain oxygen and form two kinds of nitrooxy peroxyl radical (INO_2) isomers: $\beta-INO_2$ and $\delta-INO_2$ (Schwantes et al., 2015). Those INO_2 radicals are traditionally assumed to react with HO_2 to produce a series of isoprene nitrates hydroperoxide, but some recent chamber studies have deduced the existence of other pathways. For example, INO_2 radicals can react with NO to form dinitrate and react with NO_3 to form RO radicals, O_2, and NO_2 (Ng et al., 2008; Schwantes et al., 2015). INO_2 radicals can also react with other INO_2 radicals when the experimental conditions favor RO_2 + RO_2. Kwan et al. (2012) conducted related experiments on the Caltech dual 28-m^3 Teflon chamber and found that the products were isoprene hydroxy nitrate and isoprene carbonyl nitrate (59% to 77%), C_{10}-organic peroxide compounds (3% to 4%), and 2INO (19% to 38%). Like in the oxidation of isoprene by OH, INO_2 radicals can produce peroxyl radicals by H-shift isomerization (Schwantes et al., 2015). The detailed mechanism of the reaction between isoprene and NO_3 has not been well investigated. Future experimental studies are needed to address the products and the

mechanism of the reaction between isoprene and NO_3.
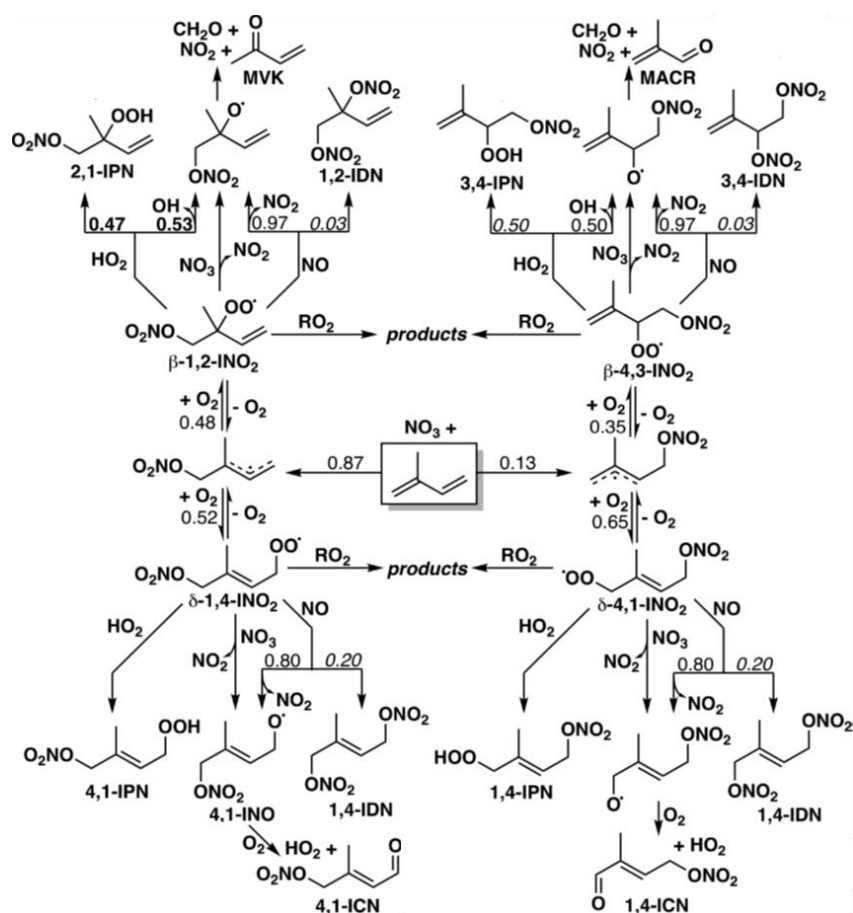
Figure 2.5 Dynamics of the reported isoprene + NO_3 system (Wennberg et al., 2018).

The isoprene sink is also somewhat dependent on oxidation by Cl radicals, although Cl is a minor oxidant. The global average Cl concentration is estimated to be less than 10^3 atoms cm^{-3} (Rudolph et al., 1996), whereas the peak concentration has been inferred to be 10^5 atoms cm^{-3} by considering the marine boundary layer (Singh et al., 1996). Both

the *E* and *Z* stereoisomers of δ−chloro peroxyl radicals are formed from the oxidation of isoprene by Cl radicals. The predominant mechanism for the reaction between isoprene and Cl radicals is an addition reaction, and the addition of Cl at the 4-position is estimated to surpass that at the 1-position, as shown in **Figure 2.6** (Lei et al., 2002a). The carbon-centered radicals produced through oxidation by Cl then react with the O_2 in the atmosphere to rapidly generate peroxyl radicals (Lei et al., 2002b). It remains unclear whether the distribution of allylic radicals to peroxyl radicals forms via the abstraction channel.
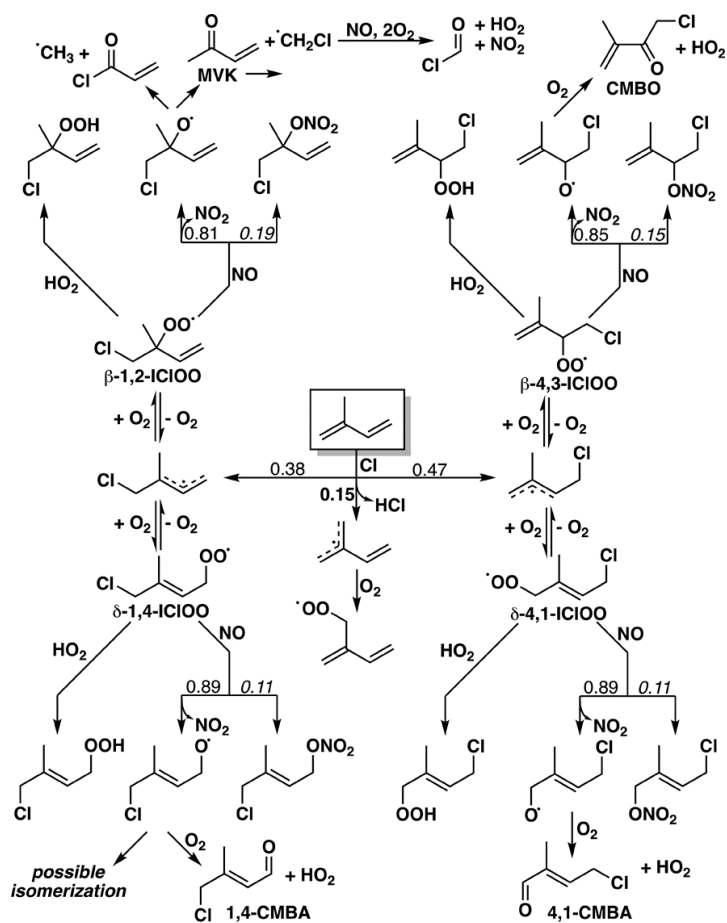
Figure 2.6 Dynamics of the reported isoprene + Cl system (Wennberg et al., 2018).

In summary, the studies reviewed above indicate that although the concentrations and reactions of VOCs in Hong Kong and the GBA/PRD have been investigated, scientific gaps remain to be filled. For example, most studies were performed with offline techniques such as gas chromatography with mass spectrometry (GC-MS) detection, flame ionization detection (FID), and electron capture detection (ECD) and high-performance liquid chromatography (HPLC), which focus on the alkanes, alkenes, and aromatics emitted from vehicles and industries. Scant knowledge is available about the

characteristics of OVOCs, which make a significant contribution to O_3 formation (Louie et al., 2013). In addition, OVOCs are difficult to detect with offline instruments due to their short lifetime and high chemical reactivity. Therefore, in this study, the most recently developed online monitoring equipment, proton transfer reaction quadrupole mass spectrometry (PTR-QMS), was used for the first time at the Hok Tsui site to provide updated information on OVOCs in Hong Kong.

Furthermore, although chambers have been used in several studies and some photochemical and dark oxidation mechanisms of isoprene have been studied in recent years, large gaps remain in elucidating the chemical processes in the complex isoprene reaction system with more than one oxidant. In general, oxidants coexist in the atmosphere and participate in oxidation processes simultaneously (Atkinson et al., 1992; Kwan et al., 2012). However, few studies have investigated the reaction of isoprene in a comprehensive system while considering the synergy among the relevant oxidants in the total oxidation process of isoprene and the highly oxygenated products. Therefore, as described below, a newly developed chamber system at PolyU was used to investigate isoprene oxidation and its contributions to highly oxygenated compounds in a complex system with three types of oxidants (i.e., OH radicals, O_3 and NO_3 radicals).

Chapter 3 Methodology

3.1 Sampling site of field study

The field measurements of VOCs and OVOCs were conducted at the Cape D'Aguilar Supersite Air-Quality Monitoring Station (the HT site; owned by the Hong Kong Environmental Protection Department; 22.22°N, 114.25°E, 60 m above sea level), located at the southeastern tip of Hong Kong Island (**Figure 3.1**). During autumn, the average temperature is 26.7°C, the average relative humidity is 72.5%, and it has a typical subtropical monsoon climate. As a rural coastal site that faces the South China Sea with a sea view of more than 270°, the HT site is affected by southwest wind in summer and northeast wind in autumn. Therefore, it is strongly influenced by oceanic emissions, urban plumes, and biogenic emissions (Wang et al., 2009). Although this station is located in Hong Kong, the HT site has been widely used as an ideal regional background site to investigate air pollution in the GBA and Hong Kong region (Lee et al., 2002; Lui et al., 2017). The field campaigns were conducted during late summer and autumn in 2018 from 27 August to 10 October, which is a common period of photochemical and particulate pollution in Hong Kong and the GBA (Lyu et al., 2020). An extremely powerful and catastrophic tropical cyclone, Typhoon Mangkhut, formed in early September 2018 and caused extensive damage in Hong Kong and GBA in middle-to-late September 2018 (Cheung and Su, 2018). Hence, for safety reasons data

for trace gases and VOCs were not obtained for 15–19 September and 17–25 September,

respectively.
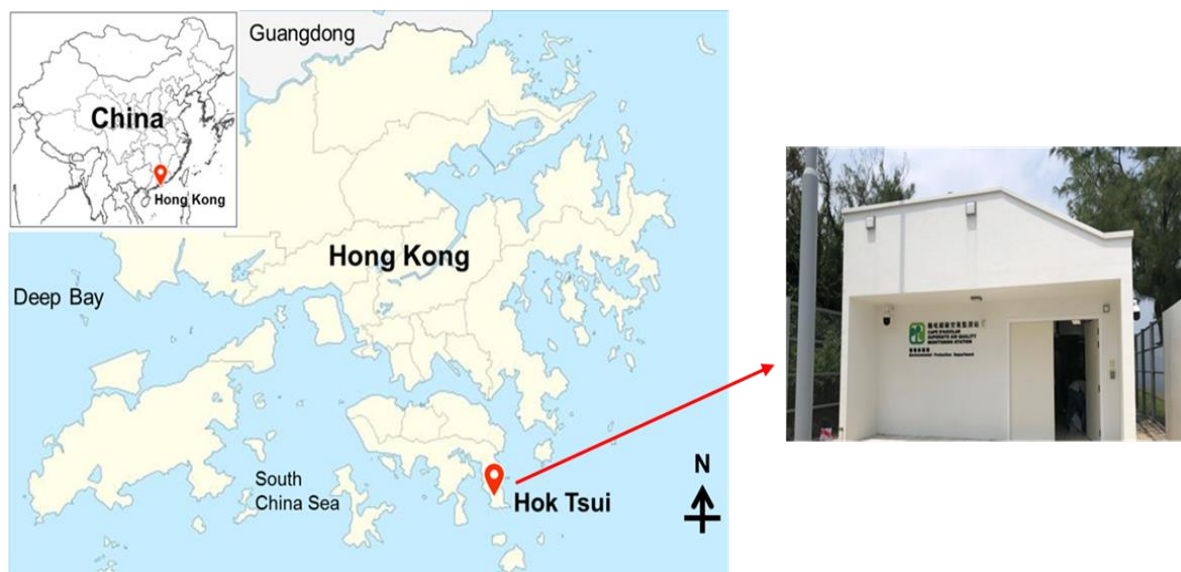
Figure 3.1 Location and appearance of the sampling site in Hok Tsui (HT), Hong

Kong.

3.2 Chamber system

The walk-in indoor environmental chamber located at PolyU comprises a stainless-steel

enclosure of 18.26 m^3 with a pivoted door. In order to achieve the required conditions

such as specific temperature and humidity during the experiment, the chamber system

has been constructed as a box-in-box design. The stainless-steel enclosure acts as outer

environment control box and inside the enclosure a 6-m^3 Teflon bag is set up as an inner

reactor. All reactions occur within the 0.127 mm-thick Teflon PFA
(poly(tetrafluoroethylene-co-perfluoropropyl vinyl ether)) bag. **Figure 3.2** shows the
brief schematic diagram of the PolyU environmental chamber.
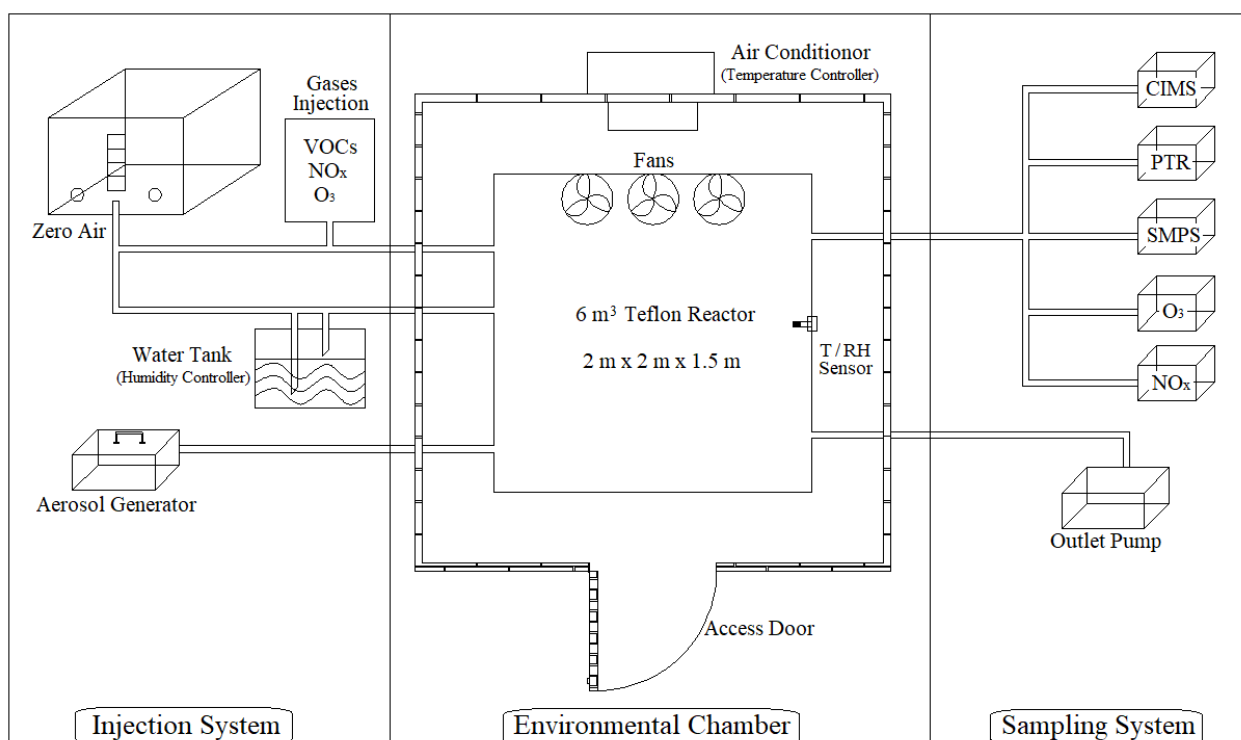
Figure 3.2 Schematic of the PolyU environmental chamber system.

3.2.1 Enclosure

The Teflon reactor is housed in an environmental chamber made by stainless-steel (3.2
m × 3.2 m × 2.5 m) and the effective volume of this stainless-steel chamber is 18.26 m^3
(Lee and Wang, 2006). The material of the inner walls is insulated stainless steel sheet.

The facility has its own air conditioner which can help control the temperature (T) inside the Teflon reactor by a central control system with an adjustable range from 10°C to 40°C ± 1°C. Air humidification system including clean water tank, water level safety switch and water heating element provides clean water vapor for relative humidity (RH) control, which is located beside the stainless-steel enclosure and can be set to a range from 5% to 85% ± 3%.

3.2.2 Teflon reactor

The inner reactor of a chamber system can be made of different materials, such as Al alloy (Tanaka et al., 2003), stainless steel (Lee et al., 2001a; Wang et al., 2011), or FEP (fluorinated ethylene-propylene co-polymer) Teflon film (Carter et al., 2005; Lai et al., 2014; Wang et al., 2014). Because of the stable chemical characteristic and low interfacial free energy, Teflon does not participate in chemical reactions easily, and has a very small adsorption capacity for particulate matters. Therefore, Teflon film is widely used for experimental simulation of chemical reactions for large numbers of smog chambers. As one of the Teflon film, PFA (poly(tetrafluoroethylene-co-perfluoropropyl vinyl ether)) has been extensively used as material for chamber because of its extreme resistance to chemical erosion, optical transparency, and overall flexibility (Bu et al., 2003; Rohrer et al., 2005; Valente et al., 1995). The Teflon bag reactor has a volume of 6 m^3 i.e., 2 m (Length) × 2 m (Width) × 1.5 m (Height) and it is fabricated from 0.127

mm-thick Teflon PFA film. A stainless-steel frame is settled to mount the whole reactor bag with four sets of parallel belt loops. A homogeneous mixing of reactants can be achieved by the installed mixing fans at the center of the ceiling.

There are five Teflon ports fitted on the reactor. Three of them are used for injection of reagents such as zero air, VOC samples (such as isoprene, O_3 and NO_2), water vapor and seed aerosol. The other two ports are housed at the opposite side of the reactor one is used for sampling by connecting with an array of instruments and the other one is linked with an outlet pump. All these ports are equipped with Kynar tube fittings and reinforced with Teflon to keep sealed.

3.2.3 Injection system

A zero air instrument provides clean and dry air, which equips with activated charcoal particle filters and High-Efficiency Particulate Air (HEPA) filters to remove gaseous organics and particles respectively, the allochroic silica gel to remove water. The flow rate of zero air was set to 20 L min^{-1}. The standard of the background air was kept < 1 ppb for non-methane hydrocarbons (NMHCs), < 1 ppb NO_X, O_3 and no detectable particles. The chamber was flushed continuously for over 48 hours with clean air before use.

Gaseous reactants (such as O_3 and NO_2) were injected via a non-absorbent tube, which

was connected to one of the Teflon port on the left side of the reactor. The volume of total gas injection can be calculated by the duration of injection and the air flow rate. A certain volume of isoprene was injected by one port of a three-way tube and carried by zero air injected into the chamber by another port. Ozone was generated by a commercial ultraviolet-light initialed ozone generator (Jelight Model 2001, Jelight Company, U.S.A.). Seed particles were generated by an atomizer (TSI 3079, TSI Inc., U.S.A.) and then passed through a silicone tube to remove water and a neutralizer (TSI 3080, TSI Inc., U.S.A.) to eliminate the charges before introducing into the reactor.

3.3 Instrumentation

3.3.1 Measurement techniques at Hok Tusi site

For the first time, state-of-the-art high-resolution proton transfer reaction quadrupole mass spectrometry (PTR-QMS) (PTR-QMS 500, IONICON Analytik, Austria) was used to comprehensively investigate the photochemical oxidation of VOCs and the formation of secondary organic aerosols at a regional urban background site in Hong Kong. PTR-QMS has been widely used for online VOC measurements in field studies (Li et al., 2019; Yuan et al., 2013). In principle, the continuously introduced VOCs which are injected into the drift tube via a Venturi-type inlet undergoes non-dissociative proton transfer from H_3O^+ ions (from water vapor via hollow cathode discharge) and further ionized as $VOC \cdot H^+$ fragments and then detected by a quadrupole mass filter

(Hewitt et al., 2003). Normally, PTR-QMS can only detect the substance with a proton affinity greater than water (165.2 kcal/mol). During this campaign, the PTR-QMS operation system was operated under H_3O^+ mode, and H_3O^+ primary ions were set to a constant drift tube pressure of 2.2 mbar. The field density ratio (E/N; where E is the electric-field strength, and N is the gas-number density) was 136 Td, and the temperatures of the inside and outside sample inlets were both 60°C. The sampling flow rate was 300 mL min^{-1} for the inlet flow controller and 245 mL min^{-1} for the pressure controller.

A large variety of VOCs and OVOCs were quantified online with PTR-QMS at a high time resolution. The specific species of interest in this study were (1) alkenes, namely *m/z* 69 for isoprene and *m/z* 137 for monoterpenes; (2) aromatic hydrocarbons, namely *m/z* 79 for benzene, *m/z* 93 for toluene, and *m/z* 107 for xylene; (3) OVOCs, namely *m/z* 33 for methanol, *m/z* 45 for acetaldehyde, *m/z* 57 for acrolein, *m/z* 59 for acetone, *m/z* 71 for methyl vinyl ketone (MVK) and methacrolein (MACR), *m/z* 73 for methyl ethyl ketone (MEK), and *m/z* 113 for products from the ozonolysis of terpenes; and (4) others, such as *m/z* 42 for acetonitrile. The data were collected and processed with PTR-MS Viewer version 3.2. The signal of *m/z* 113 was observed in ambient air above a Ponderosa pine forest canopy in California, and the results from chamber experiments confirmed that this ion is consistent with the products of terpene ozonolysis (Lee et al., 2006). Another field study at Mount Tai in China also identified the signal as

representing unsaturated aldehydes or ketones (Inomata et al., 2010). As a result, we attributed this *m/z* 113 signal to the products from the ozonolysis of terpenes (terpenes oxidation products; TOPs). The PTR-QMS program measured the above-mentioned *m/z* values at a time interval of approximately 26 s.

During the campaign, the ambient temperature changed slightly and humidity change contributed little on the major uncertainty in PTR-QMS measurements (Eerdekens et al., 2009; Kari et al., 2018; Warneke et al., 2001b). For quality control, the PTR-QMS was calibrated with a gas calibration unit (GCU, IONICON Analytik, Austria) containing a standard gas canister (RESTEK canister, IONICON Analytik, Austria) containing 27 types of VOCs. Zero air was introduced every day, to check the baseline of VOCs. Calibration was conducted every week, and a five-point curve was used to qualify the concentrations of VOCs. The details of the calibration procedure, including the mixing ratio of the standard gas, the calibration curve, the correlation coefficient, and the detection limits, are listed in **Table 3.1**. All species observed during the field campaign had good correlation coefficients (0.995 to 0.997).

Table 3.1 The calibration curves, mixing ratio, correlation coefficient and detection limits for individual VOCs and OVOCs in gas standard.

Compounds	Mixing ratio (ppmv)	Calibration curve	Correlation coefficient, R^2	Detection limit (pptv)
Methanol	0.99	y = 0.9468x + 0.7201	0.996	162
Acetonitrile	0.99	y = 1.3145x + 0.1951	0.996	17
Acetaldehyde	0.95	y = 0.7047x + 0.2353	0.997	101
Acrolein	1.01	y = 1.0587x + 0.1942	0.997	23
Acetone	0.98	y = 1.0461x + 0.2326	0.997	31
Isoprene	0.95	y = 1.0380x + 0.4258	0.995	40
MVK + MACR	1.01	y = 1.0553x - 0.0652	0.996	25
MEK	0.99	y = 1.0337x + 0.0236	0.997	18
Benzene	0.99	y = 0.9816x + 0.1068	0.996	12
Toluene	0.99	y = 0.9807x + 0.2739	0.997	30
Xylene	1.02	y = 0.9876x + 0.1760	0.997	25
TOPs	1.01	y = 0.9642x + 0.1709	0.997	33
Monoterpenes	1.01	y = 0.8368x + 2.0316	0.996	29

In addition, to integrate the VOC measurements, the concentrations of nitric oxide (NO), nitrogen dioxide (NO_2), O_3, carbon monoxide (CO), and sulfur dioxide (SO_2) were measured every minute. NO and NO_2 were measured with an NOx analyzer (Model 42i-TL, Thermo Fisher Scientific Inc., U.S.A.), and O_3 was measured with an O_3 analyzer (Model 49i, Thermo Fisher Scientific Inc., U.S.A.). CO was measured with an CO analyzer (Model 48i, Thermo Fisher Scientific Inc., U.S.A.), and SO_2 was measured with an SO_2 analyzer (Model 43i, Thermo Fisher Scientific Inc., U.S.A.). The data for

the CO and SO_2 concentrations and for the meteorological conditions (temperature and relative humidity) were provided by the Hong Kong Environmental Protection Department. The sampling inlets of these trace gas analyzers were at the same position as those for PTR-MS, and their flow rates were 1.5 L $min^{-1} \pm 10\%$.

3.3.2 Measurement techniques for chamber system

A variety of gas-phase and aerosol-phase instruments were employed in the chamber system to investigate isoprene oxidation. As an advanced technology, proton transfer reaction-time-of-flight-mass spectrometry (PTR-ToF-MS) has also been used in many chamber studies (Chu et al., 2014; Liu et al., 2015; Wang et al., 2015). Here we applied PTR-ToF-MS (PTR-ToF-MS 1000 ultra, IONICON Analytik, Austria) to detect the concentration of VOCs in real time. The PTR-ToF-MS 1000 ultra combines the latest evolution with the new funnel technology to improve ion transmission leading to a much higher sensitivity, which is as low as 5 ppt. This online VOCs monitoring instrument can be easily used in high-speed applications, even under the situation of very low VOC concentrations, or a large number of sample compounds as well. The PTR-ToF-MS was calibrated with a gas calibration unit (GCU, IONICON Analytik, Austria) containing a standard gas canister (RESTEK canister, IONICON Analytik, Austria) weekly. In addition, a high-resolution time-of-flight-chemical ionization mass spectrometer (ToF-CIMS) using nitric acid-adducts was employed to characterize

multifunctional highly oxygenated compounds. ToF-CIMS is a latest direct, online, reproducible mass spectrometer that is capable for quantifying various classes of OVOCs (Bannan et al., 2019; Lee et al., 2014; Zhao et al., 2017).

For other gases, O_3 was measured by an O_3 analyzer (Model 49i, Thermo Fisher Scientific Inc., U.S.A.), and Model 42i nitrogen oxide analyser (Model 42i-TL, Thermo Fisher Scientific Inc., U.S.A.) was used to measure the concentration of NO, NO_2 and NOx. And the sampling flow rates were 1.5 L min^{-1} ± 10% for both. All instruments were located close to the chamber system and connected to the sampling port of the inner reactor directly.

For aerosol monitoring, particle number concentrations and size distributions were obtained from scanning mobility particle sizer (SMPS) (TSI 3080; TSI Inc., U.S.A.). Aerosol sampling flow rate was 3.0 L min^{-1} and the size distribution ranged from 15 nm to 680 nm was measured within 240 s. The particle number concentration accuracy of the SMPS is ± 10%. A temperature and humidity sensor (HBO; Inc., U.S.A.) is equipped inside the Teflon reactor to ensure that the temperature and RH are within the required range.

3.4 Model used in this study

3.4.1 Photochemical reactivity of VOCs

VOCs are important precursors of ground-level ozone (Seinfeld et al., 2016). OFP is extensively used to estimate the contribution of individual VOC compounds to O_3 generation (Huang et al., 2008), as it reflects the relative contribution of various VOCs to the generation of O_3. The OFP was developed by implementing the box model simulation with different scenarios, and the maximum incremental reactivity (MIR) is used to reflect the ozone production which is more sensitive to the variation of VOCs than NO_X. As a rural coastal site, the peak ozone concentration at HT is controlled by both VOCs and NO_X in different seasons. But during the sample period, VOCs play a more sensitive role in ozone formation (Jin and Holloway, 2015). In addition, the MIR was also used for the estimation of OFP at HT (So and Wang, 2004) and PRD rural areas (Tang et al., 2007) in previous studies. This is then used to determine the key sources and precursors of O_3, and specific MIR and VOC concentrations are used for OFP calculations, as follows (equation 3.1):

$$OFP\ (j) = Concentration(j) \times MIR(j) \quad (3.1)$$

where $OFP\ (j)$ is the OFP for the specific VOC species j; $Concentration(j)$ is the concentration of the VOC species j (in $\mu g/m^3$); and MIR (in grams of O_3 per gram of

organic compound) is the maximum incremental reactivity coefficient of the VOC species j, as developed and obtained by Carter (Carter, 2010).

3.4.2 Positive matrix factorization model

Source apportionment techniques generally use a receptor model based on intrinsic statistical features of ambient measurement data (Watson et al., 2001). The receptor model is used to estimate the source contributions of pollutions and to evaluate the bottom-up emission inventories, although these are difficult to establish due to significant uncertainties (Zhang et al., 2009). PMF is an advanced multivariate receptor model recommended by the United States Environmental Protection Agency (US EPA), and is thus widely used for site-specific calculations of source profiles and the time series of these sources, including in cases where little is known about the source profiles (Brown et al., 2007; Cai et al., 2010; Guo et al., 2011; Huang et al., 2015; Yuan et al., 2012). EPA PMF version 5.0 was used in this field study to characterize and identify the sources of VOC species.

Theoretically, PMF presents the contribution of n chemical species from p independent sources with the following chemical mass equation 3.2 (Miller et al., 1972):

$$x_{ij} = \sum_{k=1}^{p} g_{ik} f_{kj} + e_{ij} \quad (3.2)$$

where x_{ij} represents the concentration of jth species in ith chemical sample; g_{ik} represents the contribution of the kth source to the ith sample; f_{kj} represents the score matrix of the jth species on the kth source factor; e_{ij} represents the residual factor for the jth species at the ith chemical sample (Paatero, 1997), and p represents the total number of independent sources, which is determined by several normalized factors, such as the residual distribution for a specific VOC sample, factor scores of the measured concentrations of a VOC, and the error squares of concentration for a specific VOC (Anderson et al., 2001). A minimized object function Q (see equation 3.3) is introduced into this receptor model to yield the solution, which is based on uncertainties (u).

$$Q = \sum_{i=1}^{m} \sum_{j=1}^{n} \left(\frac{e_{ij}}{s_{ij}} \right)^2 \quad (3.3)$$

where e_{ij} represents the residual factor for the jth species at the ith chemical sample, and s_{ij} represents the uncertainty of the jth species at the ith chemical sample, which is calculated using the error fraction and method detection limit (Polissar et al., 1998). Poirot et al. (2001) and Hopke (2014) have also developed methods to deal with data that are missing or below the detection limit. The PMF model could extract source contributions from ambient samples without source profile and apportionment.

Chapter 4 Characteristics and Source Apportionment of VOCs and OVOCs at a Coastal Site in Hong Kong

4.1 Introduction

Studies have identified complex VOC sources and contributions in Hong Kong (Guo et al., 2007; Lau et al., 2010; Liu et al., 2008), which is a major metropolis south of China (Chan and Yao, 2008). Hong Kong's air quality is affected by its large population (7.5 million residents) and heavy traffic (nearly 880,000 registered vehicles). Emissions from solvents and vehicles are the key contributors to O_3 formation in the urban area of Hong Kong (Lam et al., 2013; Lau et al., 2010; Ling and Guo, 2014). Hong Kong is also affected by the Asian monsoon, which comprises marine wind from the southwest in summer and continental wind from the northeast in winter. The northern winds from the continent also reduce the air quality in autumn and winter (Lyu et al., 2020). In addition, the significant contribution from OVOCs on ozone formation in Hong Kong was estimated, which was more than one-third of that from VOCs alone (Louie et al., 2013). There is insufficient attention on OVOCs in atmosphere, and the database and information on OVOCs is scant in Hong Kong.

In general, the O_3 formation potential (OFP) reflects the contribution of VOC species to O_3 generation, and may be used to evaluate the key VOC species in O_3 episodes.

Identifying and quantifying the contributions from each source is also crucial for air pollution abatement and for the formulation of control measures and strategies. Positive matrix factorization (PMF) is one of the receptor models which has been widely used to study the source VOC profiles (Anderson et al., 2001; Brown et al., 2007; Cai et al., 2010; Guo et al., 2011; Zhu et al., 2018). It is crucial to understand the chemical composition of VOCs, identify major source regions of air pollution, and quantify the relative contribution of each source sector to ambient VOC concentrations, especially for cities such as Hong Kong that experience severe photochemical smog and O_3 pollution.

In this chapter, field measurements were conducted at a coastal site (Hok Tsui; HT) in Hong Kong from August to October 2018. The VOC concentrations were measured using an online high-resolution instrument proton transfer reaction quadrupole mass spectrometry (PTR-QMS). The concentrations of the 13 calibrated species of VOCs and oxygenated VOCs (OVOCs) were determined and thoroughly analyzed. The OFP was used to identify the key species for O_3 generation at the HT site, and PMF was used to apportion the VOCs to their respective sources. The updated source contributions were identified and quantified in Hong Kong and the GBA according to the PMF estimation results.

4.2 VOCs and OVOCs characteristics at Hok Tsui

4.2.1 Observation of VOCs and OVOCs

The time series of the trace gases such as NO, NO_2, O_3, CO, and SO_2, the meteorological conditions, and the representative biogenic VOC isoprene and anthropogenic VOC benzene are shown in **Figure 4.1**. The concentration of VOC and OVOC species at the HT site and a comparison with data from four other suburban sites are shown in **Table 4.1**, including: (1) Tai O (Guo et al., 2006), another coastal area on the southwestern tip of Hong Kong; (2) Changdao (B Yuan et al., 2013), a coastal area between Liaoning Peninsula and Jiaodong Peninsula; (3) the Panyu District of Guangzhou (Zou et al., 2015), which is approximately 15 km south of downtown Guangzhou (a key city in the GBA); and (4) the Huairou District of Beijing (Li et al., 2019), which is approximately 50 km from the North 5th Ring Road and influenced by the urban plume. The geographic locations of these sites are also illustrated in **Figure 4.2**.
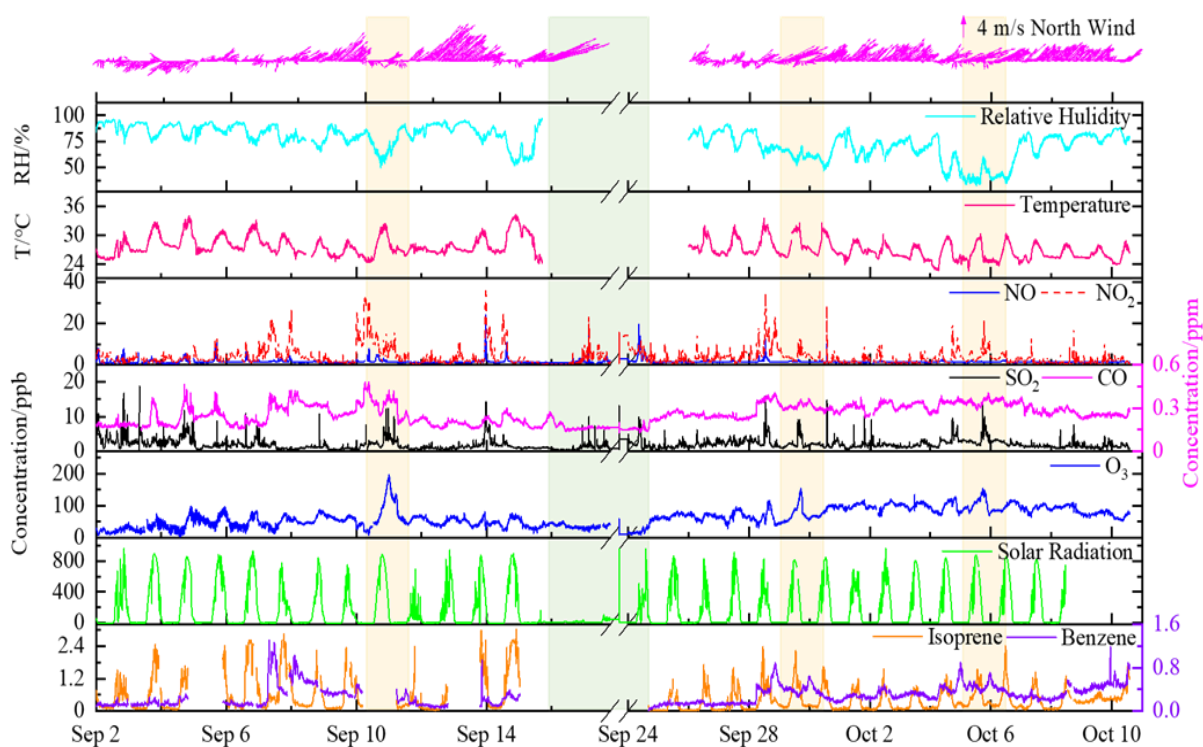
Figure 4.1 Time series of meteorological parameters, SO_2, CO, O_3, NO_X and representative VOC isoprene and benzene at the HT site. The yellow shaded-areas highlight the O_3 episodes; the green shaded-area marked as super typhoon Mangkhut landfall period.

Table 4.1 Average concentration of VOCs at HT site and comparison to other studies[a].

VOCs species	This study	Tai O, coastal	Changdao, rural	Panyu, rural	Huairou, rural
Methanol	3.73 ± 3.26	N.A.	5.67 ± 4.80	N.A.	3.42 ± 2.58
Acetonitrile	0.20 ± 0.20	N.A.	0.21 ± 0.12	N.A.	0.11 ± 0.10
Acetaldehyde	0.72 ± 0.59	N.A.	0.63 ± 0.44	3.66	0.83 ± 0.57
Acrolein	0.26 ± 0.23	N.A.	N.A.	N.A.	N.A.
Acetone	2.43 ± 1.43	N.A.	1.85 ± 0.92	N.A.	1.59 ± 1.17
Isoprene	0.47 ± 0.47	0.43 ± 0.73	0.01 ± 0.01	N.A.	0.04 ± 0.04
MVK + MACR	0.11 ± 0.10	N.A.	N.A.	1.14	0.13 ± 0.13
MEK	0.46 ± 0.31	N.A.	0.35 ± 0.22	N.A.	0.38 ± 0.38
Benzene	0.29 ± 0.20	0.87 ± 0.92	0.55 ± 0.36	N.A.	0.91 ± 0.91
Toluene	0.25 ± 0.25	5.67 ± 7.13	0.57 ± 0.51	N.A.	0.73 ± 0.73
Xylene	0.26 ± 0.26	0.38 ± 0.57	N.A.	N.A.	N.A.
TOPs	0.07 ± 0.07	N.A.	N.A.	N.A.	N.A.
Monoterpenes	0.13 ± 0.12	N.A.	0.07 ± 0.06	N.A.	0.04 ± 0.04

N.A. – not available.

[a] The unit of concentration for all VOCs species is ppb.

Figure 4.2 Location of the five rural sampling sites.

The range of average VOC concentrations measured at HT (0.07 ± 0.07 ppb [TOPs] to 3.73 ± 3.26 ppb [methanol]) was similar to that from other rural areas. However, slight differences existed in the concentration ranges of some species measured in these rural areas. For example, the average concentration of isoprene (a representative BVOC) at the HT site was 0.47 ppb, which was similar to that at Tai O. Nevertheless, it is quite high relative to that at Changdao and Huairou. BVOCs play a critical role in the atmosphere and exert a great influence on climate (Fuentes et al., 2000); this has a significant effect on Hong Kong, a hot tropical city located downwind from dense forests (Guenther, 1995). The HT site is part of a marine reserve and is lush with native coastal plants; this large green area may generate high concentrations of isoprene. Besides, isoprene is also produced by marine organisms (Arnold et al., 2009; Broadgate

et al., 2004; Tran et al., 2013) and it was detected in marine air by PTR-MS in southern Indian Ocean (Kameyama et al., 2014) and North Pacific Ocean (Kameyama et al., 2010). A study conducted on the CHINARE cruises suggested the existence of isoprene in the marine boundary layer and the importance of oceanic emissions to isoprene (Hu et al., 2013). As a result, the concentrations of MVK + MACR and MEK were also high, as they are the major intermediate products generated by isoprene oxidation. The same phenomenon was also observed in monoterpenes commonly emitted from plants, whose concentration was approximately 1.9 times and 3.3 times than those measured at Changdao and Huairou, respectively.

Methanol was the most abundant species of the measured VOCs at HT (average concentration, 3.73 ± 3.26 ppb). The value was lower than that at Changdao, but similar to those reported in Barcelona (Filella and Peñuelas, 2006) and in Beijing, whose nearby areas of vegetation are similar to those of the HT site. Methanol mostly originated from biogenic emissions and secondary formation (from oxidation of methane). The dominant sink of methanol was reaction with atmospheric oxidants, such as OH radicals, NO_3 radicals, and O_3. The reactivities were low, which resulted in a relatively high concentration of methanol at the HT site (Atkinson, 2000). Acetone had the second-highest concentration observed during the HT campaigns (average concentration was 2.43 ± 1.43 ppb), which was slightly higher than the concentrations in Changdao (1.85 ppb) and Huairou (1.59 ppb). Similar to methanol, the major source

of acetone was primary biogenic emissions, and it was consumed by photolysis and OH oxidation in the atmosphere. Although acetone showed less reactivity toward atmospheric oxidants than methanol, photodissociation still played an important role in its removal (Atkinson et al., 1999), which led to a lower concentration of acetone than methanol. Benzene, toluene, and xylene are the main components of aromatic VOCs. The average concentrations of these benzene series compound (BTX) were lower than those in other rural sites. As the HT site is a background site of the GBA, the concentrations of VOCs measured at the HT site were typically lower than those found at the Changdao and Beijing rural sites (**Table 4.1**). However, some species were present in high concentrations, which indicated the importance of BVOCs and the key role of photochemical oxidation on OVOCs formation at the HT site.

4.2.2 Diurnal variations

Figure 4.3 shows the diurnal variations in VOC concentrations at the HT site. As shown in **Figure 4.3,** the concentrations of all OVOCs were higher during the daytime than at nighttime, due to the solar radiation and higher temperature during the daytime, while there was no obvious peak in the concentrations of acetaldehyde and acrolein during the daytime. The presence of solar radiation and the higher temperature during the daytime facilitated the photochemical reactions that generate OVOCs, and thus the concentrations of the OVOCs peaked at noon. There were several minor peaks in

methanol concentrations (e.g., at 05:00 and 12:00), which indicates that it had different sources. That 05:00 peak was most likely a result of dew formation. During this period, the increase in methanol was always accompanied by a reduction in the gap between the temperature and the dew point and by a low wind speed (**Figure 4.4**), which indicates that methanol emissions were related to condensation; after the leaves became wet, methanol was dissolved and then released to the atmosphere. This phenomenon has also been described elsewhere (Filella and Peñuelas, 2006; Warneke et al., 1999). The noon peak in methanol concentration due to photochemical reaction was a result of the strongest solar radiation occurring at this point in the day. The concentration of acetone showed a similar diurnal variation to methanol, without an effect from dew formation. There was a slight increase in the concentration of all OVOCs at night, which was attributed (except for acrolein) to the change in the boundary layer height. Aromatic compounds showed several maximum-concentration peaks throughout the day. The 07:00 peak was mainly due to the emissions from commuter traffic from a cable station near the site. The concentrations of benzene, toluene, and xylene decreased during the daytime due to reaction with OH radicals, but the differences in their loss ratios demonstrated the differences in their reaction rates (Seinfeld et al., 1998). Another peak around 20:00 was slightly later than the time of high emissions from normal rush-hour traffic, and thus may have been caused by long-distance transportation from the urban area. Isoprene and monoterpene concentrations exhibited the expected trend consistent

with solar radiation, reached an apex at noon. The concentrations of MVK + MACR, the major photooxidation products of isoprene and monoterpene, and the products from the ozonolysis of terpenes, were greater in the afternoon because the accumulation of oxidated isoprene and monoterpene was lower at night. Acetonitrile, as an inert substance, reacts very slowly with OH radicals (Atkinson et al., 2008). There was a slight increase in the concentration of acetonitrile during the daytime, and a slow decrease after sunset. This curve was similar to that of acetonitrile concentration data from a rural site in New Hampshire, USA (Jordan et al., 2009), and was likely due to dry deposition (Talbot et al., 2005). The specific and detailed source apportionment for VOCs is discussed in Section 4.5.
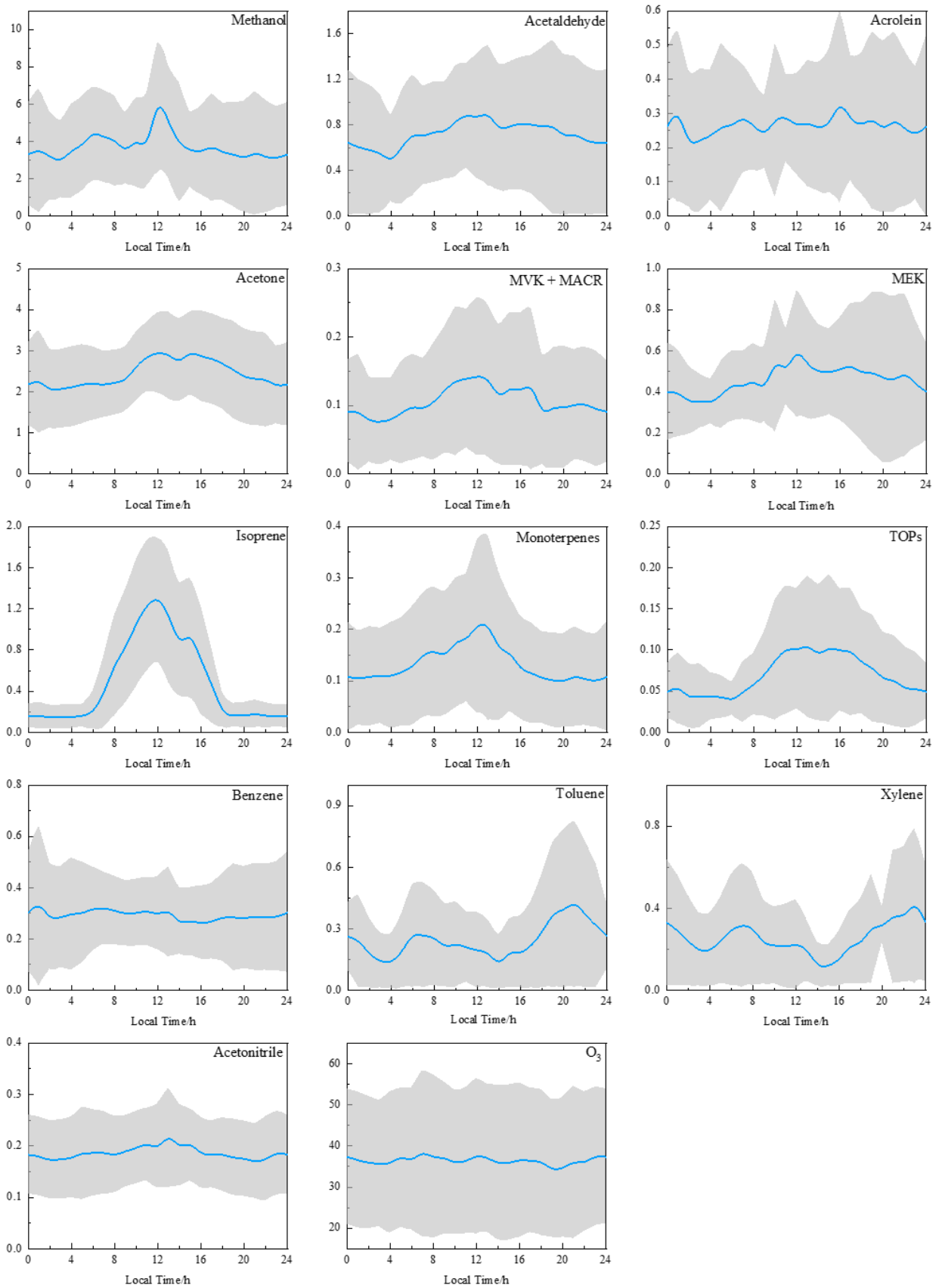
Figure 4.3 Diurnal variations of VOCs and O$_3$ at HT site. The blue lines are average concentrations, and gray areas indicate standard deviations. The unit of concentration for all VOCs species is ppb.
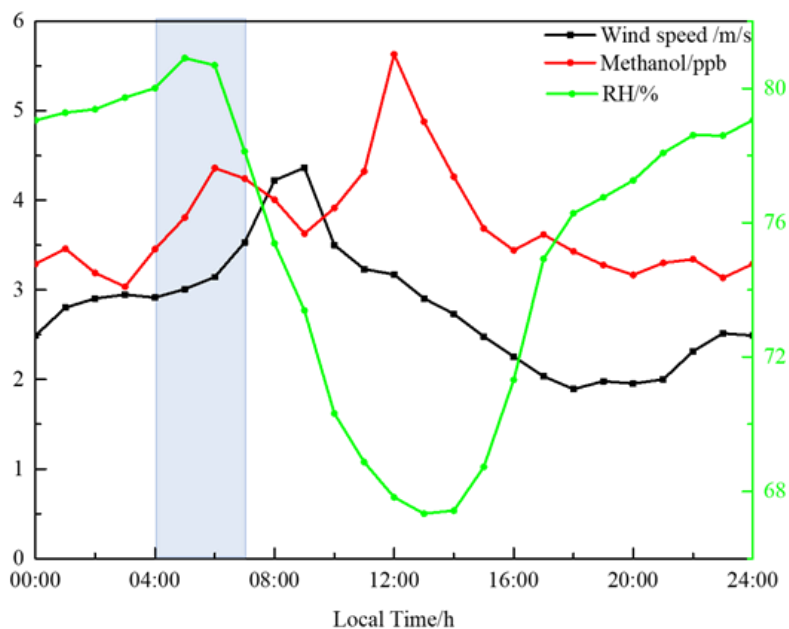
Figure 4.4 Diurnal variations of wind speed, methanol concentration and relatively humidity.

4.3 Comparison with urban site

We previously conducted a study at the Mong Kok (MK) air quality monitoring station, a typical urban station in Hong Kong, using PTR-MS to characterize urban VOCs and OVOCs (Cui et al., 2016). **Figure 4.5** shows a comparison of the VOC concentrations at suburban (HT) and urban (MK) sites and the suburban-to-urban ratios of the average concentrations for each compound. As shown in **Figure 4.5 (a)**, almost 80% of the measured VOCs concentrations at the HT site were lower than those that were

previously recorded at the MK site. The blue line in **Figure 4.5 (b)** shows the average

ratio (0.59) of the suburban and urban concentrations. In general, the concentrations of

hydrocarbons were lower at the HT site than at the MK site because fewer emissions

from vehicles and human activities were present at the former. The concentrations of

the OVOCs acetone, MEK, and methanol were slightly higher at the HT site than those

that were previously found at the MK site. As shown in **Figure 4.5 (b)**, the

concentrations of methanol and acetone at the HT site were 1.13 times higher than those

that were previously found at the MK site. Green plant emissions, including plant

growth and decay, are reportedly the principal sources of methanol (Jacob et al., 2005;

Schade et al., 2011). In addition, the differences in the meteorological conditions during

these two campaigns may have led to an increase in the concentration of methanol. The

measurement at the MK site was conducted during four different months (February,

May, August and November 2013), thus the final obtained concentration was the

average of the measurements from all four seasons. The lower temperature and weaker

solar radiation during MK measurements, especially during February and November

(**Table 4.2**), may have led to a lower level of methanol formation from photochemical

reactions. The concentration of MEK in suburban areas is 1.23 times higher than that

in urban areas. In addition, the HT site is more than 90% covered by vegetation, which

will lead to a high isoprene concentration and the generation of more isoprene-oxidation

products in this area.
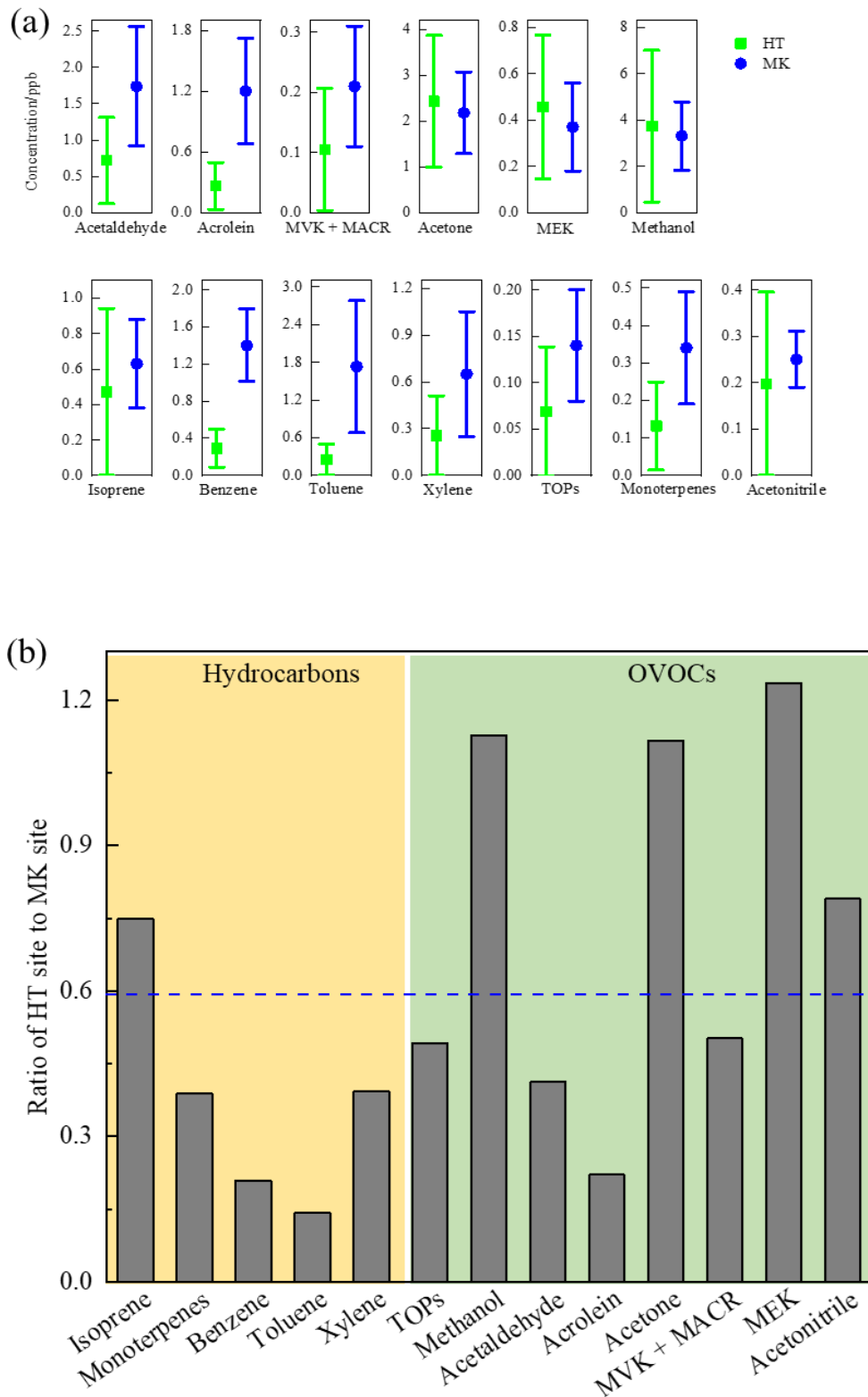
Figure 4.5 Comparison of VOCs between coastal rural (HT) and urban (MK) sites:

(a) the average concentration of these two works, the solid squares are average concentration; the whiskers are standard deviation; (b) ratio of coastal rural site concentration to urban site concentration, the yellow shaded-area marks as hydrocarbon species, the green shaded-area marks as OVOCs species, the blue dot line is the average ratio value.

Table 4.2 Average temperature and solar radiation of MK and HT sites during measurement periods.

Site	Month	Average temperature ($^{\circ}$C)	Average solar radiation (MJ/m^2)
MK	February	19.1	11.5
	May	25.7	12.3
	August	28.6	14.5
	November	21.7	11.1
HT	September	28	15.6
	October	25.3	14.8

4.4 Ozone formation potential of VOCs and OVOCs

Because VOCs and OVOCs are the precursors of O_3, it is important to evaluate their contribution to O_3 formation. The MIR method was developed to calculate and assess the contribution of each VOC to total O_3 production (Carter, 1994). **Table 4.3** presents the OFP of the VOC species measured at the HT site. The results indicate that the contributions of alkanes, aromatic hydrocarbons, and OVOCs to O_3 formation were 26.54%, 20.45%, and 53.02%, respectively, which indicates that OVOCs were the dominant species that contributed to O_3 formation at the HT site. OVOCs have also

been found to be the major contributors to O_3 formation at rural sites rather than at urban sites (Luo et al., 2011). The top five VOC species (in order) that contributed to O_3 formation were isoprene, MEK, xylene, acetaldehyde, and acrolein (**Figure 4.6**). Isoprene had the highest OFP (13.46 $\mu g/m^3$) of the measured VOCs, which accounted for 21.47% of the OFP of all measured VOC species. Previous field studies showed that biogenic emissions remain major contributors to O_3 formation if only isoprene is considered (Lu et al., 2010; Xie et al., 2008).

Table 4.3 Ozone formation potential of VOCs species at HT[a].

VOCs	Concentration (ug/m^3)*	MIR (g O^3/g VOCs)	OFP (ug/m^3)
Methanol	4.89	0.65	3.18
Acetaldehyde	1.30	6.34	8.22
Acrolein	0.60	7.24	4.32
Acetone	5.77	0.35	2.02
Isoprene	1.31	10.28	13.46
MVK+MACR (average)	0.32	7.615	2.40
MEK	1.36	9.39	12.74
Benzene	0.93	0.69	0.64
Toluene	0.94	3.88	3.66
Xylene (average)	1.13	7.55	8.52
TOPs	0.32	1.1	0.35
Monoterpenes	0.72	4.38	3.17

[a] The concentrations are the average concentration of VOCs at HT site.
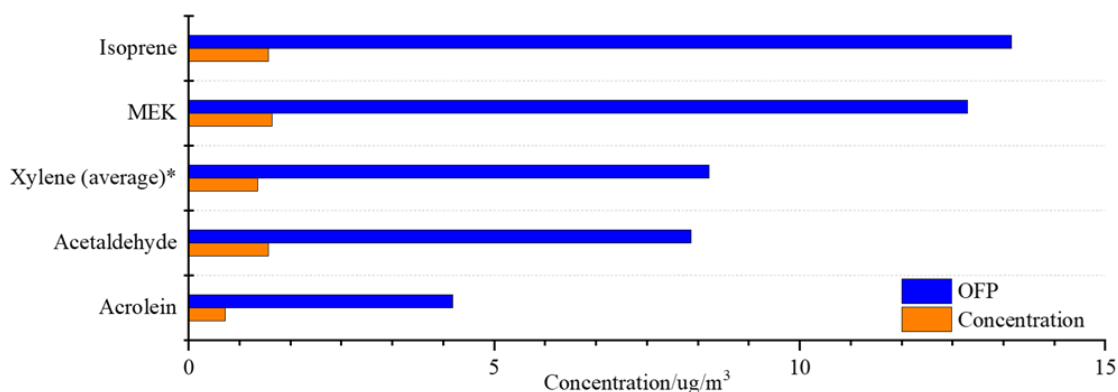
Figure 4.6 Top five VOC species in emission concentration and corresponding OFP at HT site.

4.5 Source identification

In this section, the receptor model PMF version 5.0 was used to analyze the measured VOC data sets for the HT site. The VOC species measured with online PTR-MS (N = 2597) were used to base run into the PMF model. Factor numbers 2 to7 were explored to resolve the best solution for the PMF results, and various random SEEDs points were used to minimize the results for each factor number (Paatero, 1997). In an attempt to generate rotational ambiguity, the fPeak values were changed from -3 to 3. To confirm the optimal values of the sources, **Figure 4.7** shows the trials of the theoretical Q value with the function of factor sizes. The value of Q/Q_{exp} decreased by 31% from factor 2 to factor 3, and by 41% from factor 3 to factor 4. As the number of factors continued to increase to 5, the value of Q/Q_{exp} changed from 1.51 (factor 4) to 1.14 (factor 5), and the decrease was then not obvious. The additional factors in PMF decrease the Q/Q_{exp}

values gradually, and Q/Q_{exp} values should be approximately equal to the number of degrees of freedom or the total number of data points (Guo et al., 2011). Finally, five source factors were selected for our analysis of Q/Q_{exp} values.
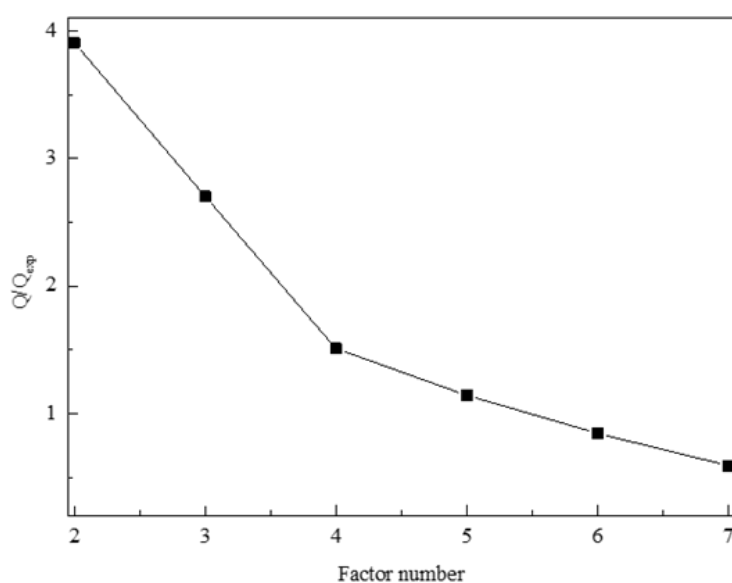
Figure 4.7 Q/Qexp values against number of factors in PMF base runs.

Figure 4.8 shows the source profiles as the percentage of each species mapped in each respective factor and in terms of source apportionment. Factor 1 comprised high percentages of the aromatic hydrocarbons benzene (26.95%), toluene (89.22%), and xylene (79.17%). Because the industrial use of benzene has been forbidden and toluene is a common ingredient in solvents, the ratio of toluene to benzene (T/B) is a valuable

indicator for the identification of emission sources (Zhang et al., 2013). The T/B ratio

shows a wide range in various studies. Normally, a relatively high T/B value is observed

in a typical industrial area (Sahu et al., 2016; Tiwari et al., 2010), and the ratio would

decreases as the contribution of vehicle emissions increases (Sahu et al., 2020). When

the T/B ratio falls below 1, biomass burning is the dominant source of emissions (Liu

et al., 2008). **Figure 4.9** presents a scatterplot of toluene to benzene; the T/B slope at

the HT site of factor 1 was 3.2, which fell between the range of industrial and roadside

emission. The 72-h backward trajectories indicate that winds from mainland China

passed through many cities on the ground during the high T/B period from 19:00 to

21:00 on September 28 (**Figure 4.10**). This result suggests that factor 1 may reflect the

mix of industrial and automotive emissions.
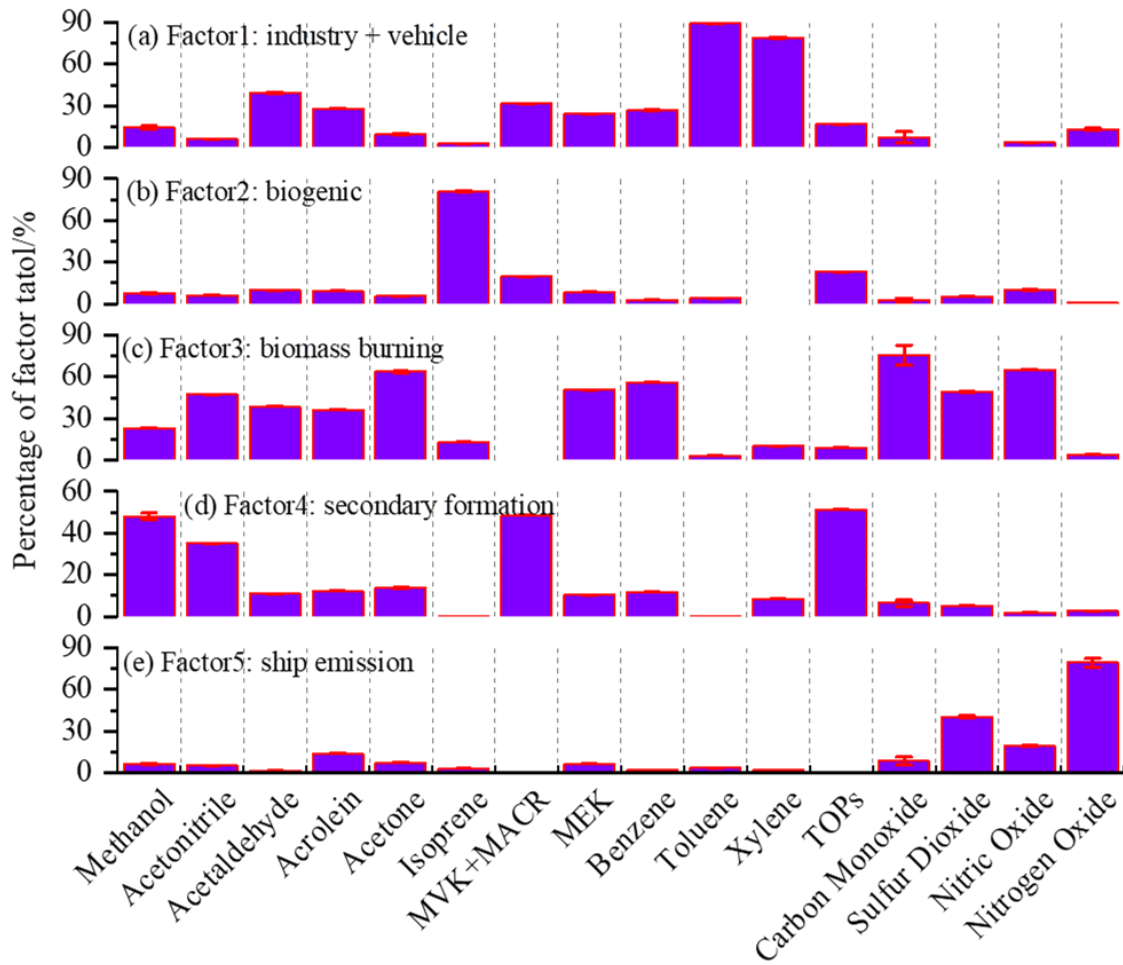
Figure 4.8 Source profiles (percentage of factor total) resolved from PMF at HT site.
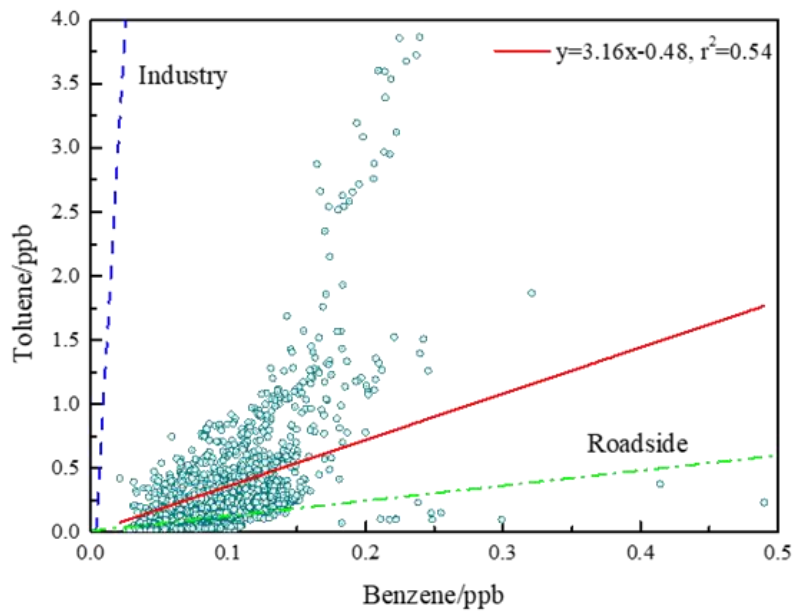
Figure 4.9 Scatterplots of toluene to benzene at HT site in factor 1. Red line presents the T/B ratio in this study, blue dash line presents a study at Qingxi industrial township in Dong Guan, Guangdong province (Tang et al., 2007), green dash dot line presents a study from Mong Kok roadside station in Hong Kong (Cui et al., 2016).
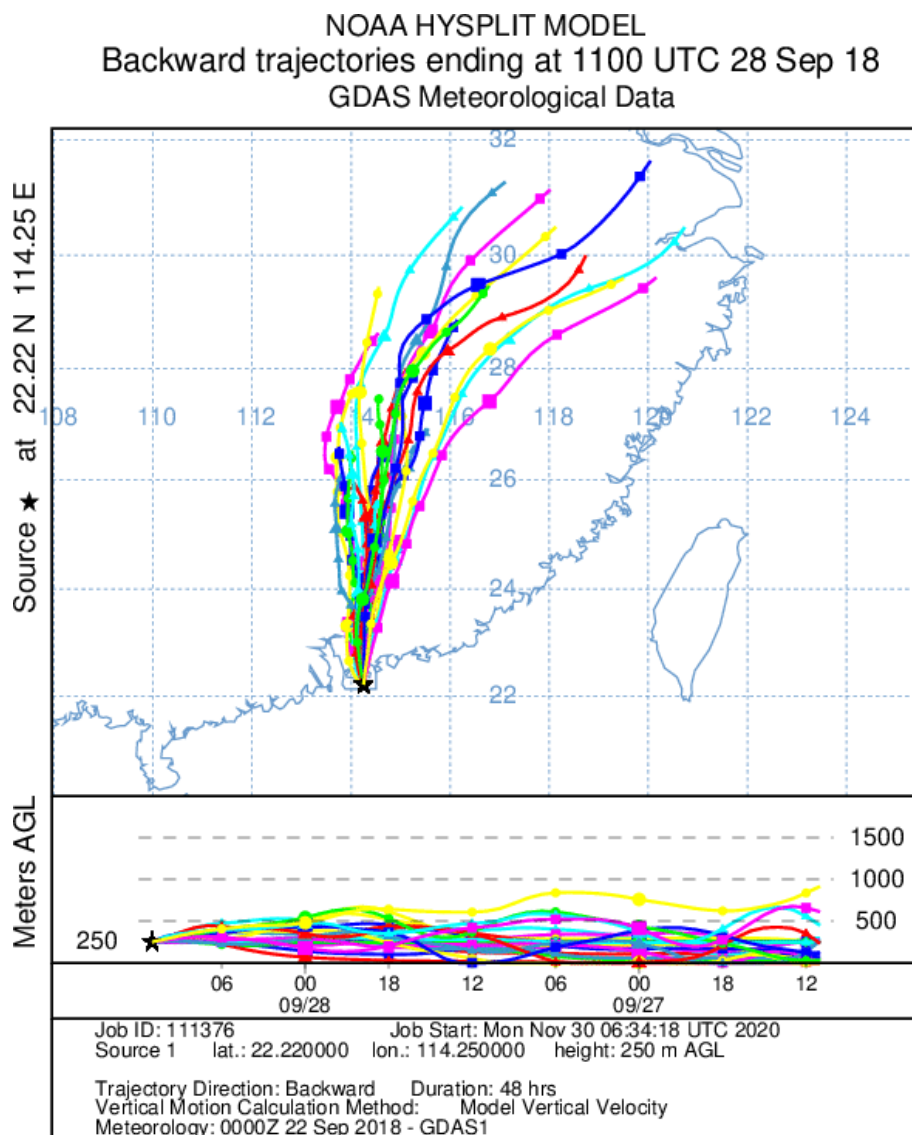
Figure 4.10 72-hours backward trajectories during high T/B period based on HYSPLIT model, arriving HT site at 21:00 on September 28 (UTC 11:00 on September 28).

The major species of factor 2 were isoprene, comprising more than 80% of its total concentration, and its oxidation products (MVK + MACR). TOPs also contributed more than 20% of this factor. Moreover, factor 2 peaked during the afternoon and decreased

at night, which formed a similar diurnal curve with biogenic signals due to photosynthesis. Therefore, factor 2 was related to biogenic emissions.

Factor 3 was dominated by CO (75.5%), benzene (56.13%), acetonitrile (47.4%), and OVOCs (acetone, acetaldehyde, MEK, and acrolein). CO is an excellent tracer of combustion emissions, which are discharged from various sources, such as biomass (Wu et al., 2016), industry (Taiwo et al., 2014), vehicles (Watson et al., 2001), and residences (Gros and Sciare, 2009). Acetonitrile is a typical marker of biomass burning (de Gouw et al., 2003; L. Li et al., 2014). To better explain the trend and correlation, **Figure 4.11** illustrates the time series of acetonitrile and CO concentrations. As depicted in **Figure 4.11**, these two pollutants showed similar concentration variations during the field study. The time at which acetonitrile and CO reached their peak concentrations was almost identical, and three notable peaks that occurred on September 28, October 4, and October 8 are framed by a green dashed line. **Figure 4.12** shows the 72-h backward trajectories and fire plots when the concentrations of acetonitrile and CO clearly increased. This reveals the pathways of the air masses that accompanied large numbers of fire plots at the HT site, which came mainly from mainland China during the period of high acetonitrile/CO concentrations. The pollutants that are generated by biomass burning are likely transported to the HT site by the continental wind. Biomass burning has been verified as the major contributor to benzene emissions (Andreae and Merlet, 2001; Liu et al., 2008), and large

concentrations of OVOCs, such as acetone, acetaldehyde, acrolein, and methanol, are also generated by this process (Karl et al., 2007; Read et al., 2012). Also, acetone and MEK had a high contribution to this factor of 63.6% and 50.6%, respectively. A field study at a rural site in north China revealed that primary emissions such as biomass burning were also a significant source of some OVOCs, such as acrolein, acetone, and MEK (Zhang et al., 2020). Lyu at al. (2020) also proved that biomass burning is the largest contributor of organic aerosols at the HT site when the wind comes from the continent. Therefore, the VOC species in factor 3 resulted from biomass burning.
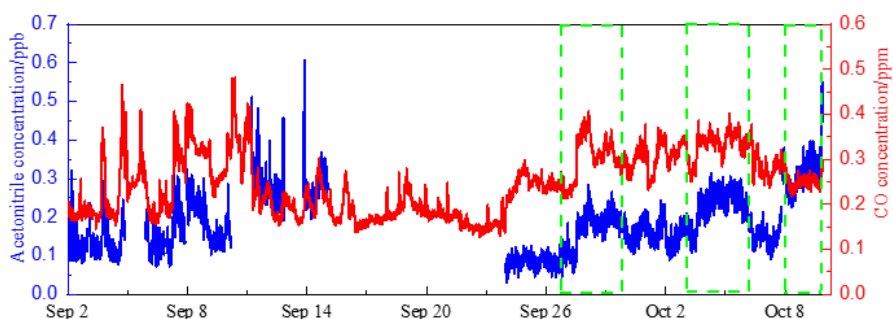
Figure 4.11 Time series of acetonitrile and CO, the green dash line circles three significant increases of acetonitrile and CO at HT site during campaign.
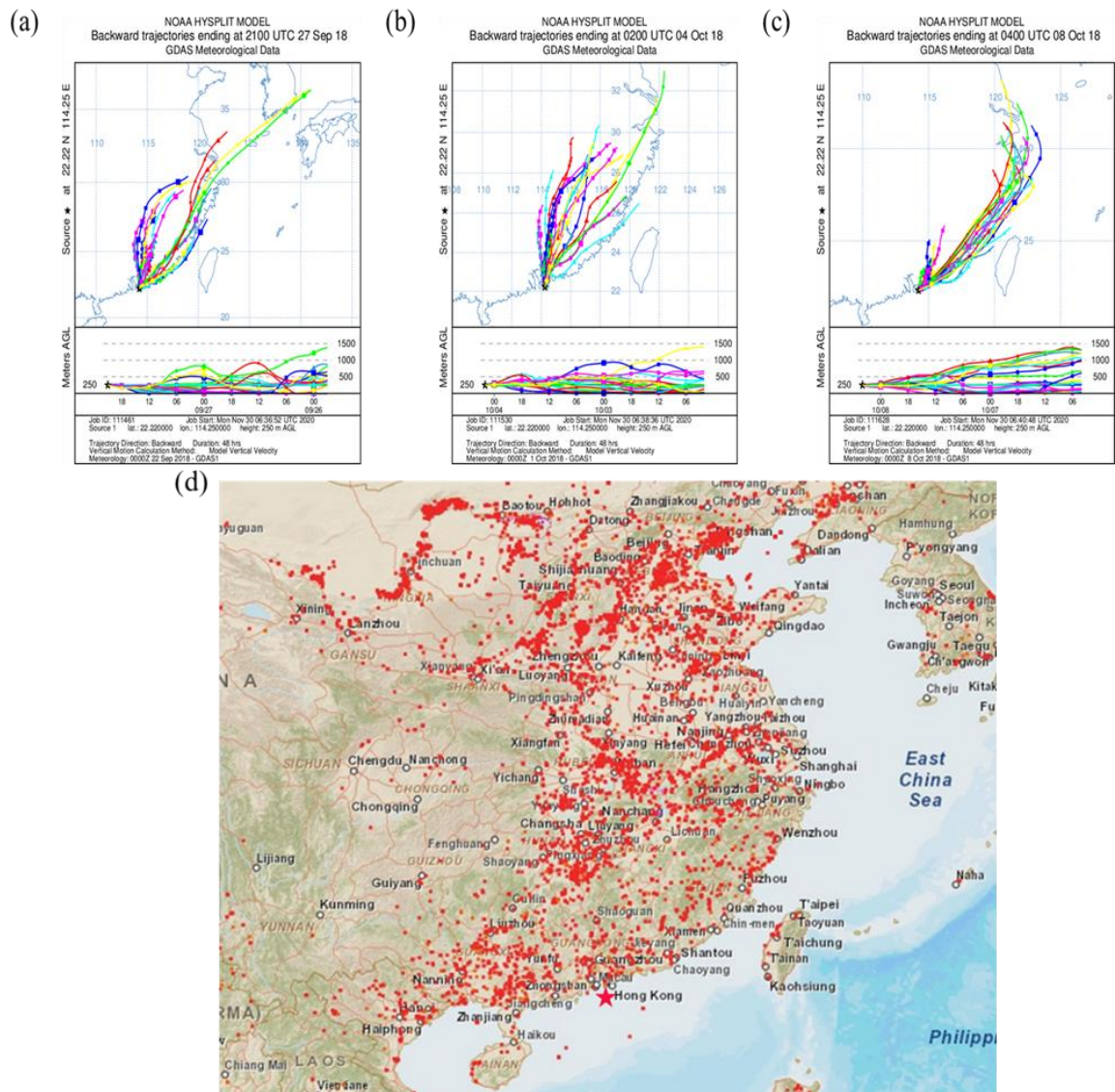
Figure 4.12 72-hours backward trajectories for peaks of acetonitrile and CO based on HYSPLIT model, arriving HT site at (a) 05:00 on September 28 (UTC 21:00 on September 27); (b) 10:00 on October 4 (UTC 02:00 on October 4) and (c) 12:00 on October 8 (UTC 04:00 on October 8). (d) fire plots retrieved from Fire Information for Resource Management System (FIRMS) based on NASA's Moderate Resolution Imaging Spectroradiometer (MODIS) during September 28 to October 4.

A positive correlation was found between factor 4 and secondary formed tracers O_X (O_3 + NO_2; correlation coefficient, $R^2 = 0.59$) (**Figure 4.13**), and factor 4 was distinguished by its high percentage of oxidation products. For example, the percentages of oxidation products contributed by isoprene and terpenes were 48.51% and 51.26%, respectively. In addition, the diurnal variation in factor 4 showed a maximum concentration in the afternoon and early evening. Hence, the high concentration of OVOCs was attributed mainly to secondary formation in factor 4.
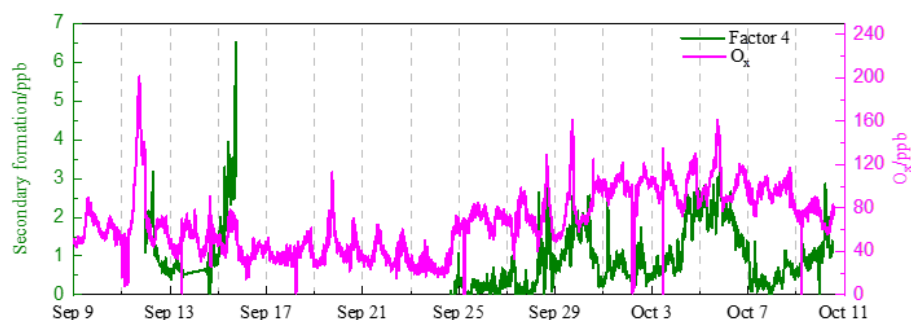
Figure 4.13 Time series of resolved factor 4 and O_X (O_3+NO_2) from PMF at HT site during campaign.

Factor 5 at the HT site was characterized by high percentages of SO_2, NO_2, and NO. SO_2 and NO_X are important constituents of the marine boundary layer (Davis et al., 2001). Because the HT site is a coastal corner with a sea view of more than 270°, **Figure**

4.14 demonstrates that the concentration of SO_2 increased as the wind originated from the seaside. Acrolein, which contributed 13% to factor 5, is released when biodiesel is heated or burned (Stevens and Maier, 2008). Thus, factor 5 was primarily related to shipping emissions.
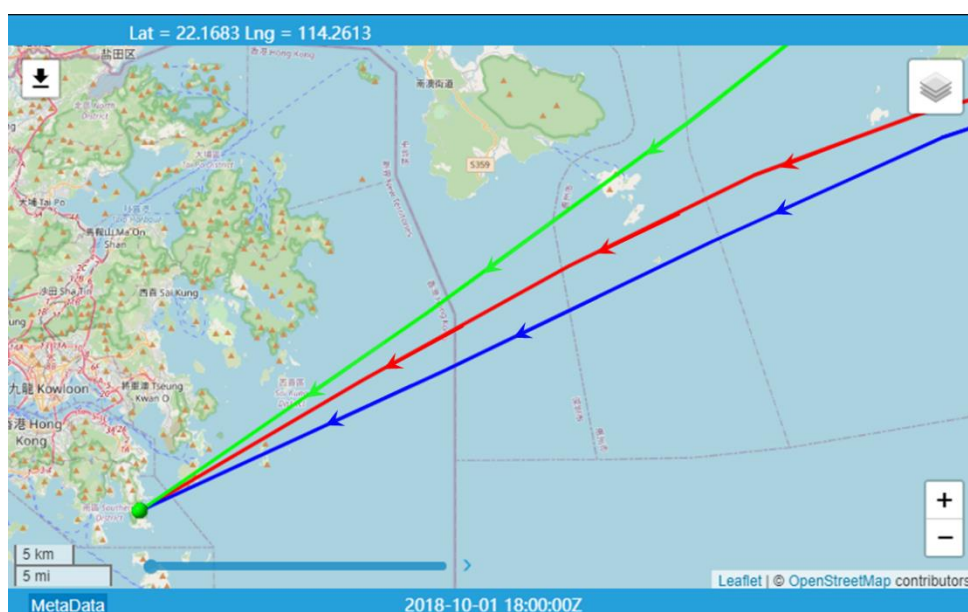
Figure 4.14 6-hours backward trajectories when the level of SO_2 increased based on HYSPLIT model, arriving HT site at 18:00 on October 01. The three different color lines show different altitudes of 100 (red line), 500 (blue line), and 1000 (green line) meters, the directions of arrow represent the vectors of wind.

Based on the discussion above, five factors were identified from the PMF results at the HT site in Hong Kong. **Figure 4.15** illustrates the contributions of the five major

emission sources to the measured VOC concentrations. Generally, the most significant source was biomass burning, which contributed to 63.7% of the measured VOC concentrations. The second-largest source was ship-related emissions, which accounted for 13.5% of the measured VOC concentrations. Secondary formation, a mix of industrial and vehicle emissions and biogenic emissions, contributed 9.2%, 8.1%, and 5.5% of the measured VOC concentrations during the campaign, respectively.
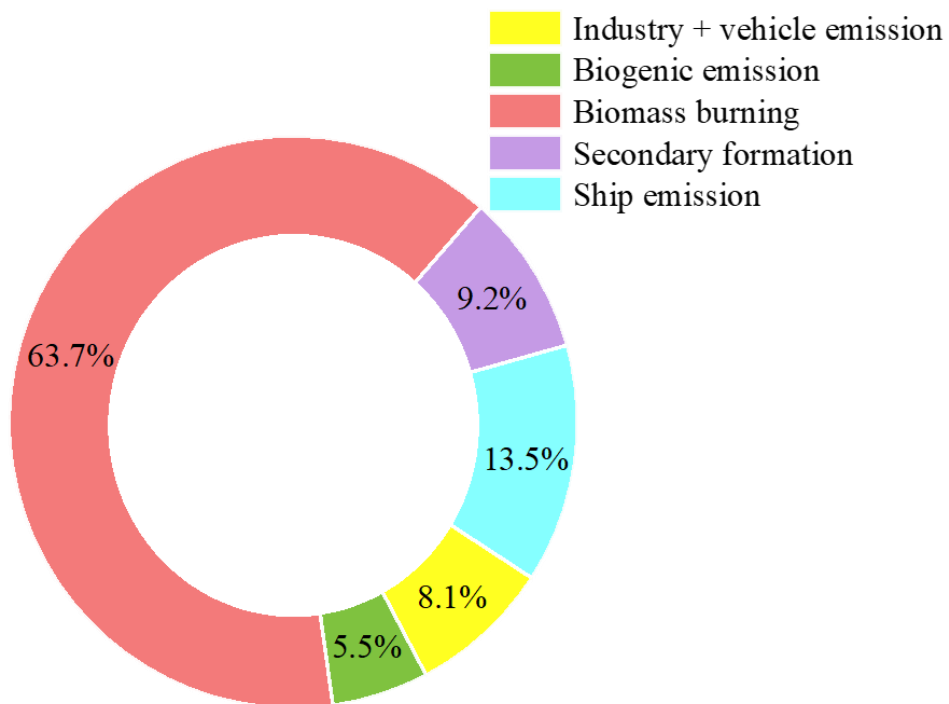
Figure 4.15 Source apportionment results from PMF at HT site.

4.6 Summary

In the chapter, the concentrations of VOCs and OVOCs were measured by PTR-MS during autumn in Hong Kong and their emission characteristics, OFP, and relative contributions from various sources were explored. Methanol was found to be the most abundant species among the measured VOCs (average concentration, 3.73 ± 3.26 ppb). The concentration of isoprene and MEK in HT was higher than that previously observed in other rural studies, suggesting besides biogenic emissions, the distinct oceanic emissions contribute to BVOCs as well. A VOC data set was collected to estimate the OFP. According to the MIR method, the top five contributors to O_3 formation in Hong Kong (in order) were isoprene, MEK, xylene, acetaldehyde, and acrolein, and isoprene accounted for 21.47% of all measured VOC species. OVOCs were the dominant species at the HT site with the potential for O_3 formation.

The receptor model PMF was also used to identify possible sources and to evaluate the dominant sources of emissions. Five factors were extracted to identify the sources of VOCs in Hong Kong, namely biomass burning (63.7%), ship-related emissions (13.5%), secondary formation (9.2%), industry-related and vehicle-related sources (8.1%), and biogenic emissions (5.5%). The results indicate that the air pollution in Hong Kong was strongly influenced by urban plumes from GBA/PRD and by oceanic emissions during autumn.

Chapter 5 Characterization of the Environmental Chamber

5.1 Introduction

As mentioned in Chapter 2, VOCs can react in the atmosphere with various active radicals such as OH radicals, NO_3 radicals, O_3, and Cl radicals (Barletta et al., 2005; Biesenthal et al., 1998; Middleton, 1995). These complex chemical reactions can form intermediates or products that contain one or more polar functional groups, such as aldehydes, ketones, alcohols, nitro compounds, peroxyl nitrates, and hydroperoxides (Atkinson et al., 1980; Carter et al., 1997; Kamens et al., 1982). These chemicals tend to be less volatile and can easily transfer to the particulate phase to form secondary organic aerosols (SOA) (Ng et al., 2008; Tsigaridis and Kanakidou, 2003; Tuazon and Atkinson, 1990). Meanwhile, some second-generation products can also be further oxidized (Wennberg et al., 2018). Effective testing and scientific prediction are needed to understand the pathway and mechanism of the reaction of VOCs and free radicals.

However, because thousands of VOCs species are present in the ambient air, both the large number of intertwined reactions and the meteorological conditions have an unpredictable impact on these transformations. It is thus difficult to identify the scientifically reasonable pathways and mechanisms solely by observation of the real atmospheric chemical processes. However, temperature, humidity, light, the precursor

concentration, and even meteorological factors can be controlled in a chamber system (Carter et al., 1997; 2005; Cocker et al., 2001). Therefore, chamber simulation experiments are effective in studying the mechanisms of atmospheric pollution and could be further used to develop solutions for pollution control.

The first indoor environmental chamber in Hong Kong was newly established at The Hong Kong Polytechnic University (PolyU) and is described in this chapter. This chamber facility was designed to study the mechanisms of reactions between isoprene and free radicals and their contribution to SOA by implementing state-of-the-art online gas and particle monitoring instruments, such as proton transfer reaction-time-of-flight-mass spectrometry (PTR-ToF-MS) and high-resolution time-of-flight-chemical ionization mass spectrometer (ToF-CIMS). Characterization of a new chamber system is necessary to evaluate its performance and to calibrate the results of future experiments (Wang et al., 2014). Therefore, a set of characterization experiments were performed to evaluate the performance of the new facility, and the impact of the walls inside the reactor on gas-phase reactivity and secondary aerosol formation is discussed.

5.2 Temperature control and its homogeneity

Maintenance of the stability and uniformity of the temperature inside the reactor during an experiment is very important to obtain ideal experimental results. A separate central air conditioning system is incorporated in this chamber to control the temperature,

which can be adjusted from 10°C to 40°C ± 1°C. In addition, a stand-alone sensor (HBO, Inc., U.S.A.) is installed inside the Teflon reactor to monitor and record the temperature each minute. A set of mixing fans is installed at the center of the chamber ceiling to achieve homogeneous mixing of the reactants. The surfaces of the fan blades are coated with Teflon to prevent the fan blades from polluting the air in the reactor and adsorbing the particles. **Figure 5.1** shows the evolution of the average temperatures inside the reactor over 4 h when the temperatures are set to 10°C, 25°C, and 40°C, respectively, and the average temperatures stabilize in approximately 45, 10, and 30 min, respectively, when the outside temperature is approximately 25°C. The standard deviations of the average temperatures are all within ±1°C, the demonstrating the ability to control the temperature inside the Teflon reactor.
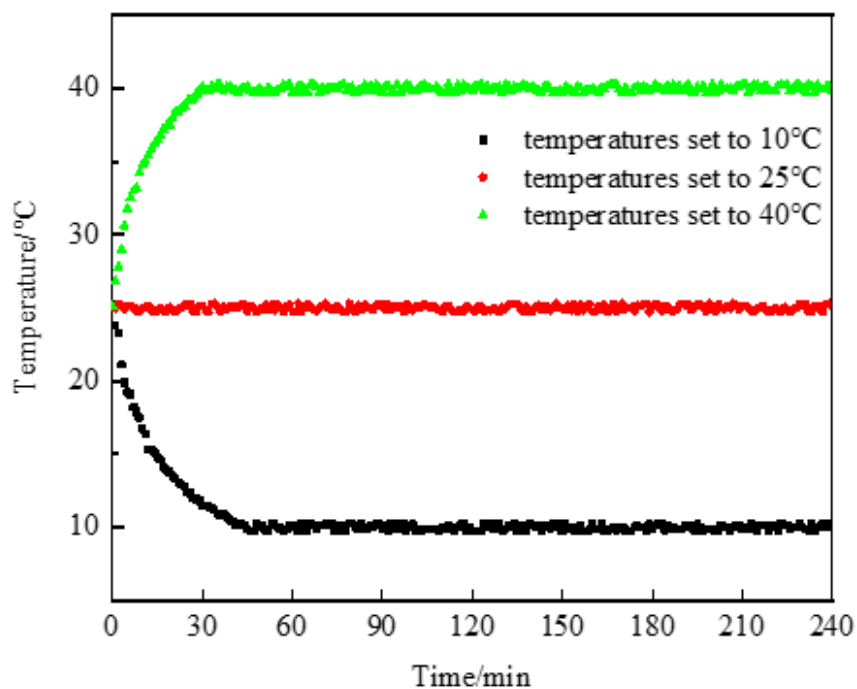
Figure 5.1 Evolution of the average temperatures inside the chamber.

5.3 Mixing and dilution

To avoid the influence of partially concentrated chemicals during the experiment, the homogeneity of the reactants must be maintained with the Teflon-coated fans at all times. Isoprene was chosen as a tracer to test the gas-phase mix inside the reactor, 100 ppb of which was injected into the chamber at a rate of 2 L min^{-1}. To achieve a balance between low wall loss and even mixing (Carter et al., 2005; Wang et al., 2014), the fans' rotation speed was set to 800 rpm. **Figure 5.2 (a)** illustrates that isoprene can be well mixed in 15 min, which is much shorter than the duration of a typical experiment, which is normally longer than 4 h. A similar short mixing time was also achieved for O$_3$ and NO$_2$. The chamber volume showed a slight decrease due to the continuous sampling by

various instruments, which may have caused a dilution effect. CH_3CN, a low-reactive

VOC, was chosen as the tracer to test the dilution effect, but dilution was not detectable

and could be excluded due to the uncertainty of the instrument, as shown in **Figure 5.2**

(b).
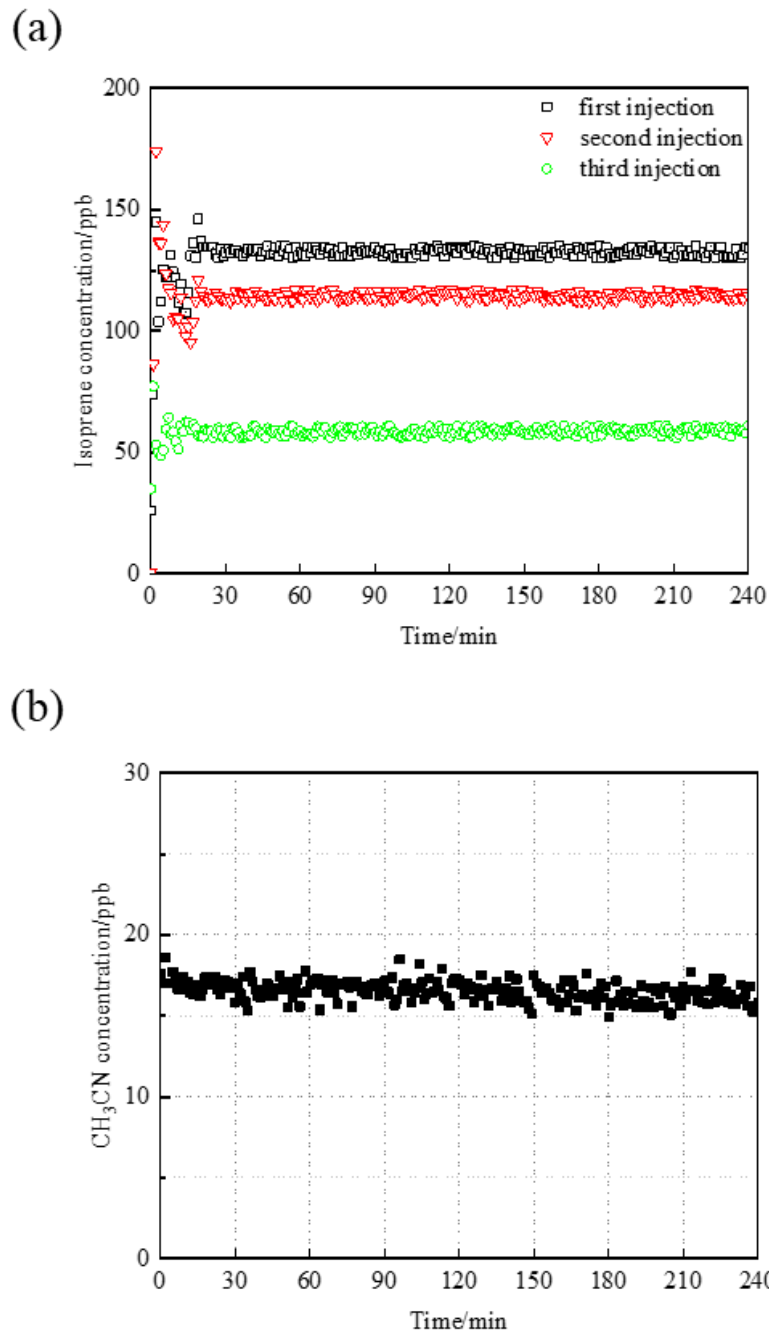
Figure 5.2 Evolutions of mixing and dilution of chamber: (a) mixing of isoprene; (b) concentration of CH_3CN.

5.4 Purity of inlet air

Clean dry air was provided by an air cleaning system generating zero air. The purification system was equipped with activated-charcoal particle filters and high-efficiency particulate air filters to remove gaseous organics and particles, respectively. The flow rate of zero air was set to 20 L min^{-1}, and the standards of the background air were kept below 1 ppb for non-methane hydrocarbons (NMHCs), less than 1 ppb NO$_X$ and O$_3$, and no detectable particles (**Figure 5.3**). The chamber was flushed continuously with clean air for more than 48 h before use.
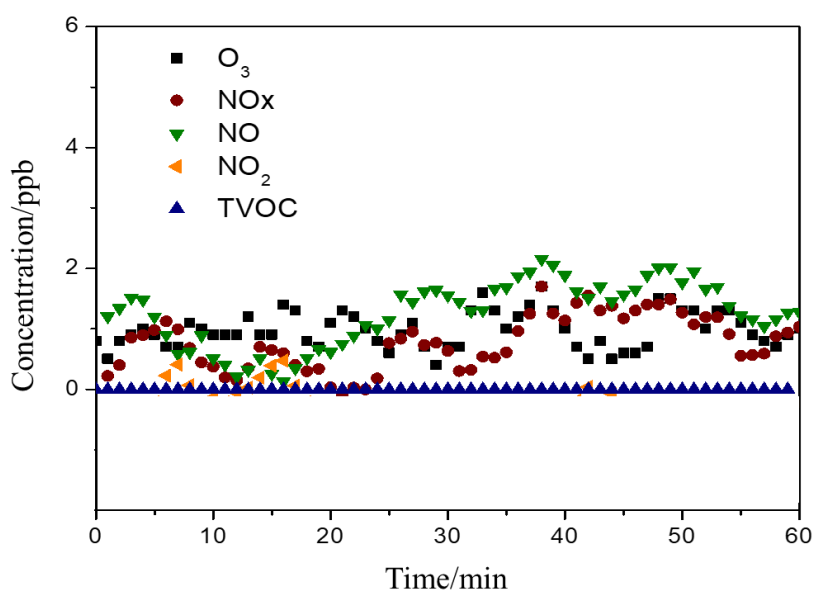
Figure 5.3 Purity of inlet air.

5.5 Wall loss of gas species

During the experimental process in the environmental chamber, the loss of gaseous reactants and products can occur on the reactor's inner surface due to a deposition effect or conversion to other species (McMurry and Grosjean, 1985). The correction factor to account for the loss on chamber walls is important in explaining the experimental results and parameterizing the simulation results, and it is also required to accurately calculate the SOA yield. The loss process is generally considered to follow first-order kinetics, and its reaction rate is as given in equation 5.1 (Cocker et al., 2001),

$$\frac{d[X]}{dt} = -K_{w,x}[X] \quad (5.1)$$

where $[X]$ is the concentration of the target compound, and $-K_{w,x}$ is the wall loss rate constant of the target compound.

Various experiments were performed to determine the wall-loss rate constant for O_3, NO_2, and the representative biogenic VOC, isoprene. The objective species (i.e., O_3, NO_2, and isoprene) were injected into the chamber. Their concentrations were monitored continuously in dark conditions. **Figure 5.4** shows the changes in the concentrations and their index curves with time. The index curves of O_3, NO_2, and isoprene demonstrated a strong correlation with time (R^2 = 0.979, 0.932, and 0.991 respectively), which indicates that wall loss for this chamber is a first-order kinetic

process.
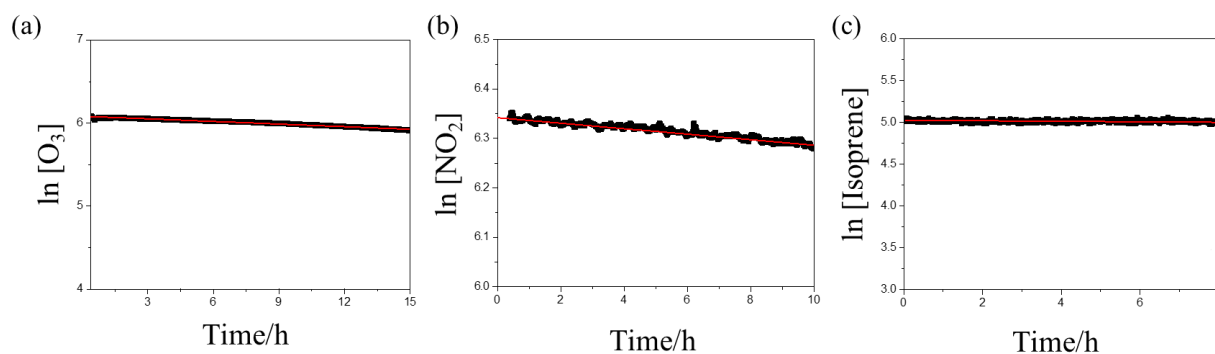
Figure 5.4 Index curves of concentrations and reaction times for (a) O_3, (b) NO_2, and (c) isoprene.

The wall loss of gaseous chemicals in smog chambers has been widely studied due to the significant role it plays (Rollins et al., 2009; Wang et al., 2014; Wu et al., 2007). **Table 5.1** summarizes the wall loss rate constants of gases in the PolyU environmental chamber and the constants of the smog chambers reported in other studies. It can be concluded from **Table 5.1** that the wall loss rate constants of our chamber were reasonable. The wall loss rate constant of isoprene in our work was 2.8×10^{-7} s^{-1} (lifetime, 52.08 d), which was the lowest of the species and indicates that wall loss of isoprene can be neglected in subsequent experiments.

Table 5.1 Comparison of the loss rate on walls of gaseous species between the PolyU chamber and other chamber systems.

Institution	Volume (m^3)	Material	Wall loss rate constant		References
			O$_3$	NO$_2$	
GIG-CAS	3	Teflon FEP	$2.2 \times 10^{-6}\,\text{s}^{-1}$	$1.4 \times 10^{-4}\,\text{s}^{-1}$	(Wang et al., 2014)
ERT	3.9	Teflon FEP	$3 \times 10^{-6}\,\text{s}^{-1}$	$0\text{--}5 \times 10^{-4}\,\text{s}^{-1}$	(Rollins et al., 2009)
Tsinghua	2	Teflon FEP	$1 \times 10^{-6}\,\text{s}^{-1}$	$4.2 \times 10^{-4}\,\text{s}^{-1}$	(Wu et al., 2007)
PolyU	6	Teflon PFA	$2 \times 10^{-6}\,\text{s}^{-1}$	$9.3 \times 10^{-4}\,\text{s}^{-1}$	This work

5.6 Wall loss of particles

Suspended particles are lost on the walls of environmental chambers through several mechanisms, including electrostatic attraction, turbulence, Brownian diffusion, and gravitational sedimentation. An accurate evaluation of the particulate matter lost on the surface of a reactor is necessary to estimate the total mass of the product in the particle phase. The particle loss rate on the walls is proportional to the initial concentration of particulate matter and also depends on the particle size. The wall loss rate of the particles can be described by first-order kinetics as in equation 5.2 (Cocker et al., 2001),

$$\frac{dN(d_p,t)}{dt} = -k(d_p) \times N(d_p,t) \quad (5.2)$$

where $N(d_p, t)$ is the concentration of the particles, d_p is the diameter of the particles,

and $k(d_p)$ is the wall loss rate constant of particles.

To evaluate the loss rate constant on the walls of the smog chamber, an aerosol generator with a certain concentration of $(NH_4)_2SO_4$ atomization flow (0.5 mol L^{-1} $(NH_4)_2SO_4$ solution) was introduced into the smog chamber. Meanwhile, the distribution of the particle size was measured continuously with a scanning mobility particle sizer (SMPS) continuously, as shown in **Figure 5.5**. An $(NH_4)_2SO_4$ seed was injected into the chamber at the beginning of the experiment. After injection, the particles appeared with an average diameter of 100 nm. Owing to coagulation behavior and the probable high loss rate of small particles, the size of small particles changed to approximately 250 nm over the following hours.
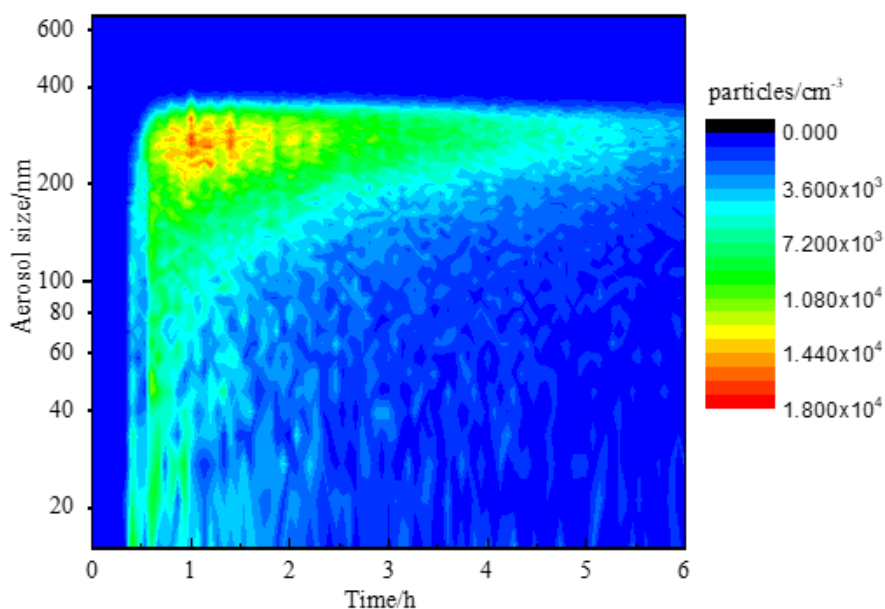
Figure 5.5 Distribution of particle size of $(NH_4)_2SO_4$ in chamber.

According to the relationship between the total concentration of particulate matter and the particle size, the wall loss rate constant for particles can be obtained for a cuboid chamber with equation 5.3 (Takekawa et al., 2003).

$$k_{dep}(dp) = a \times d_p^b + \frac{c}{d_p^d} \quad (5.3)$$

The values of a, b, c, and d for this work were 6.52×10^{-2}, 7.55×10^{-2}, 41.21, and 1.19, respectively. The wall loss rate constant for particles in the PolyU chamber was 0.27 h^{-1}, as determined from this equation. **Figure 5.6** compares the particle wall-loss rate constants between the PolyU chamber and other chambers. The loss rate constant in our study was similar to others (Wang et al., 2014; Wu et al., 2007) and lower than that described by Takekawa et al. (2003). The low loss rates on the walls for gas species and particles demonstrated the stable and traceable losses of gases and particles on the walls of the chamber system.
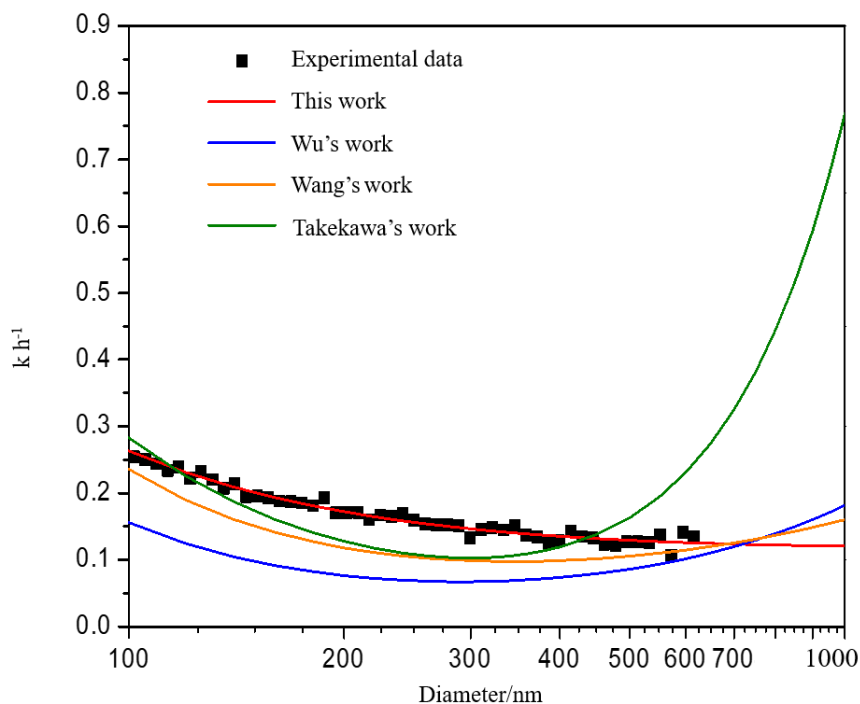
Figure 5.6 Comparison of the particle wall loss rate constant between the PolyU chamber and other chambers.

5.7 Preliminary results from isoprene dark ozonolysis

An experiment to study the dark ozonolysis of isoprene was performed with the chamber system characterized above. In this experiment, 66 ppb of isoprene was first injected into the chamber, followed by the introduction of 440 ppb of O_3 under dry conditions (relative humidity < 5%) with the temperature set at 25°C ± 1°C. **Figure 5.7** shows the mass spectra of gaseous products obtained by PTR-ToF-MS. At the beginning of the experiment, an *m/z* of 69, as the signal of isoprene, was identified (see red bar in **Figure 5.7(a))**. The peak of isoprene disappeared after 6 h of reaction with

an excess of ozone (O_3), accompanied by other peaks (see black bars in **Figure 5.7(a)**).

The results indicated that the reaction of isoprene with O_3 produced a series of gaseous

products. As shown in **Figure 5.7(a)**, strong ion signals at *m/z* values of 31, 47, 59, 61,

and 71 were detected after isoprene dark ozonolysis. The full mass spectrum of gaseous

products, labeled with the formula for each peak, is displayed in **Figure 5.7(b)**. The

strongest peak at *m/z* of 31 was identified as HCHO, and the relatively strong ion signal

at *m/z* of 71 was attributed to methacrolein (MACR) and methyl vinyl ketone (MVK).

As reviewed in Section 2.3.2, isoprene ozonolysis can form ozonides via two pathways

involving the addition of O_3 to the C=C bond, and every ozonide can be decomposed

into MACR or MVK. Many other studies have noted that MVK and MACR are major

first-generation products of isoprene ozonolysis (Edney et al., 1986; Holloway et al.,

2005). Hence, both compounds are major oxidation products of the reaction of isoprene

initiated by O_3 (Haofei Zhang et al., 2011). A battery of highly reactive OVOCs was

also formed during the reaction, indicated by the ion signals at *m/z* of 47, 61, 75, and

87, which are attributed to CH_2O_2, $C_2H_4O_2$, $C_3H_6O_2$, and $C_4H_6O_2$, respectively. These

OVOCs are all C_1–C_4 species and can be classified as aldehydes, ketones, and acids (or

esters), as summarized in **Table 5.2**. The results are in agreement with those of the

previous chamber studies and model simulations reviewed in Chapter 2 (Kamens et al.,

1982; Rollins et al., 2009; Wennberg et al., 2018).
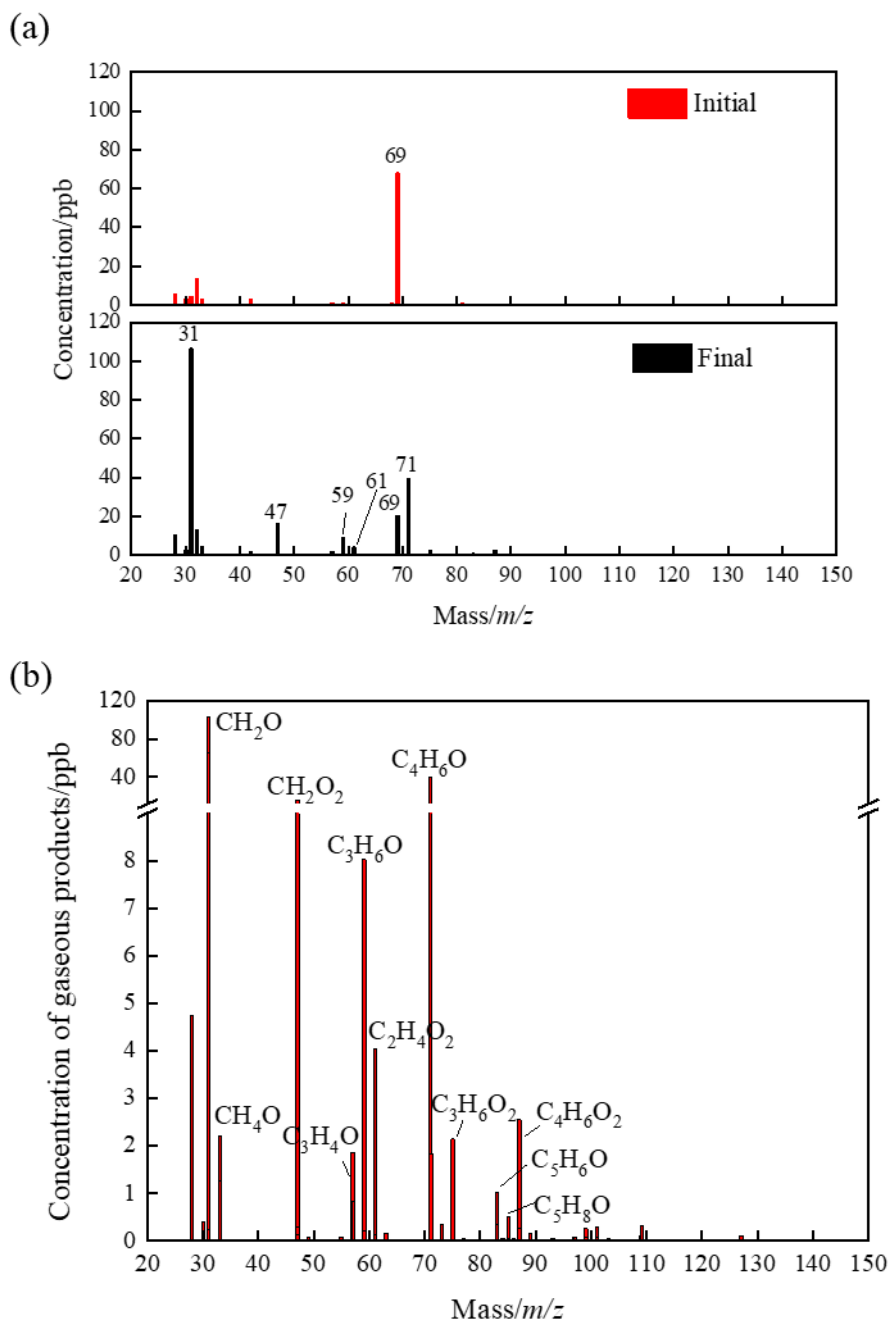
Figure 5.7 Mass spectra of gaseous products detected by PTR-ToF-MS: (a) differences in mass spectra before and after the reaction; (b) Full mass spectrum of gaseous products of isoprene reaction with O_3.

Table 5.2 Summary of C_1–C_4 OVOCs detected during dark ozonolysis of isoprene.

Category	Aldehyde (CH₃)ₙCHO		Ketone (CH₃)ₙCO		Acid/Ester CₙH₂ₙO₂			
Formula	CH_2O	C_4H_6O	C_3H_6O	C_4H_6O	CH_2O_2	$C_2H_4O_2$	$C_3H_6O_2$	$C_4H_6O_2$
Structure	HCHO	MACR: CH₃C=CH₂CHO	CH₃COCH₃	MVK: CH₃COCH=CH₂	HCOOH	CH₃COOH	CH₃CH₂COOH	CH₃COCH=CH₂

5.8 Summary

An environmental chamber was constructed and commissioned at PolyU, and the characterization experiments described in this chapter demonstrate that the chamber has the capacity to carry out simulations to provide valuable data for gas-phase chemical reactions and the formation of secondary aerosols. The temperature and relative humidity are controllable and can be set to range from 10°C to 40°C ($\pm$ 1°C) and from 5% to 85% ($\pm$3%), respectively. An air purification system provides zero air for the chamber with non-methane hydrocarbon concentrations of less than 1 ppb, NO_X and O_3 concentrations of less than 1 ppb, and particle concentrations of less than 10^2 particles cm^{-3}. The average wall loss rate constants for O_3 and NO_2 were 2.92×10^{-6} s^{-1} and 9.3×10^{-4} s^{-1}, respectively, and the particle wall loss rate constant was 0.27 h^{-1}. The relatively low loss rate constants of both gas species and particles reflect the long lifetimes of these species, confirming that the wall effect in this environmental chamber is negligible. C_1–C_4 OVOCs such as HCHO, MACR, and MVK were identified with

PTR-ToF-MS during the reaction between isoprene and O_3. These results illustrate the

chamber's utility for further evaluation of gas-phase chemical mechanisms. The

chamber system was subsequently used to investigate and simulate gaseous chemistry

and secondary aerosol formation.

Chapter 6 Chamber Simulation of Nocturnal Isoprene Oxidation

6.1 Introduction

As reviewed in Chapter 2, isoprene is the most abundant biogenic VOC in the atmosphere. It can be oxidized by OH radicals, O_3, NO_3 radicals, and Cl radicals (Clark et al., 2016; Liu et al., 2016b; Santos et al., 2018), and it further influences air quality and climate by contributing to the formation of OVOCs, O_3, and secondary organic aerosols (SOA) (Ng et al., 2008; Wennberg et al., 2018). The results from Chapter 4 indicated that isoprene had a higher concentration at a rural site in Hong Kong than in other rural sites, and it is also the major contributor to O_3 formation. The complexity of the isoprene oxidation process limits chamber experiments to focus on a simplified reaction system with only one oxidant. Several studies have been conducted to investigate the products, mechanisms, and effects of isoprene oxidation with a single oxidant (Clark et al., 2016; Dommen et al., 2006; Hynes et al., 2005; Kamens et al., 1982; Li et al., 2017; Liu et al., 2016a; Wennberg et al., 2018). As discussed in Section 2.3.2, reactions with OH radicals and NO_3 radicals were identified as the main pathways for sinking of isoprene during the daytime and nighttime, respectively. However, oxidants generally coexist in the atmosphere at the same time. It is therefore important to investigate how the concomitant oxidants affect the oxidation process of isoprene.

O_3 is a photochemical product that is considered to be an important atmospheric oxidant during both daytime and nighttime (Wennberg et al., 2018). NO_3 radicals generated from the reaction between O_3 and NO_2 contribute to the oxidation process of organics at nighttime (Ng et al., 2008; Schwantes et al., 2015; Starn et al., 1998). It has been reported that OH radicals can be generated in the oxidation process of isoprene by NO_3 radicals and O_3, although the concentration of the regenerated OH radicals at nighttime was lower than that seen in the daytime (Atkinson et al., 1992; Kwan et al., 2012). Therefore, it should be possible that OH radicals, O_3, and NO_3 radicals contribute concurrently to the oxidation of isoprene at night in areas with photochemical pollution. In addition, NO_2 has been reported to participate in the cycles of the mentioned oxidants and can cause SOA formation in isoprene oxidation (Schwantes et al., 2015; Tuazon and Atkinson, 1990). Therefore, NO_2 also plays vital roles in various oxidation pathways.

The diversity of meteorological and geographical conditions often leads to variations in the relative humidity (RH) in the real atmosphere. Several studies have investigated the effects of changes in RH on isoprene oxidation (Pankow and Chang, 2008; Volkamer et al., 2009; Wenxing et al., 1995). Zhang et al. (2011) described the importance of RH in SOA formation. The formation of SOA was shown to be enhanced by a low RH (15% to 40%) relative to a high RH (40% to 90%). Lewandowski also obtained a decreased aerosol yield of 85% with absolute humidity increasing from 2 to

12 g m^{-3} for isoprene (Lewandowski et al., 2015). However, the opposite results were obtained from experiments conducted in the Caltech environmental chambers (Nguyen et al., 2016). Major products of isoprene ozonolysis such as HCHO, methacrolein (MACR), and methyl vinyl ketone (MVK) did not exhibit strong dependence on RH as it was increased from 4% to 76%. Because no general conclusion has yet been reached, it is necessary to re-evaluate the influence of RH on isoprene oxidation, especially on the major products.

The oxidation of isoprene can be summarized into two main pathways: one leads to decomposition of the parent structure into small molecules, which are mostly present in the gas phase (Berndt and Böge, 1997), and the other causes highly oxygenated compounds with low volatility to condense into the particle phase (Ng et al., 2008). To gain a full understanding of the oxidation mechanisms of isoprene, both small molecules and the highly oxygenated compounds generated from the process should be measured and analyzed. Analysis of the highly oxygenated compounds could be especially important for reducing the knowledge gap regarding SOA formation.

This chapter describes a series of chamber experiments conducted with various NO$_2$ concentrations to investigate the nocturnal oxidation of isoprene. Small molecules and highly oxygenated compounds were detected by proton transfer reaction-time-of-flight-mass spectrometry (PTR-ToF-MS) and high-resolution time-of-flight-chemical

ionization mass spectrometer (ToF-CIMS), respectively. The products from various oxidants were identified to evaluate the contribution of each oxidant to isoprene oxidation. SOA formation was also measured, and the contributions of the detected highly oxygenated compounds to its formation were analyzed. The influence of NO_2 on the products, the proportions of various oxidants, and SOA formation was investigated. The oxidation of isoprene in the complex system was explored to provide an updated mechanism for isoprene oxidation.

6.2 Products detected by PTR-MS and ToF-CIMS

Figure 6.1 exhibits the evolutions of isoprene, NO_2, O_3, and SOA formation. The concentrations of these gaseous reactants decreased after mixing, and SOA was gradually generated during the oxidation process of isoprene. Several OVOC products were formed in the oxidation process of isoprene. **Figure 6.2** illustrates typical time series of OVOC products with high intensities detected by PTR-ToF-MS, that is, the OVOCs with one carbon atom to five carbon atoms (C_1 to C_5). Because hundreds of signals were detected during the reaction, we selected only the products with final concentrations in the top ten. As the reaction progressed, the concentrations of most C_1 to C_5 OVOCs including HCHO, CH_2O_2, $C_2H_4O_2$, C_3H_4O, C_4H_6O (MVK + MACR), C_4H_8O (methyl ethyl ketone, MEK), C_5H_8O, and $C_5H_{10}O$, increased, while the concentrations of C_2H_6O and C_3H_6O first increased and then decreased slightly and

remained constant. HCHO and MVK + MACR were the major products with the

highest signal intensities, which is in agreement with previous findings (Nguyen et al.,

2016; Wennberg et al., 2018).
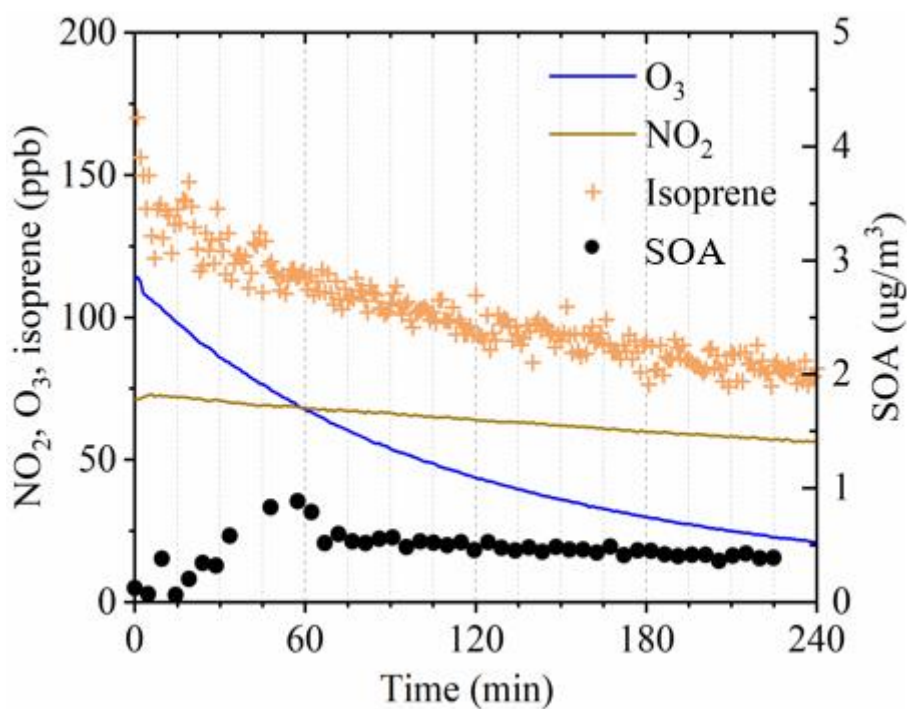
Figure 6.1 Evolution of isoprene, NO_2, O_3, and SOA formation.
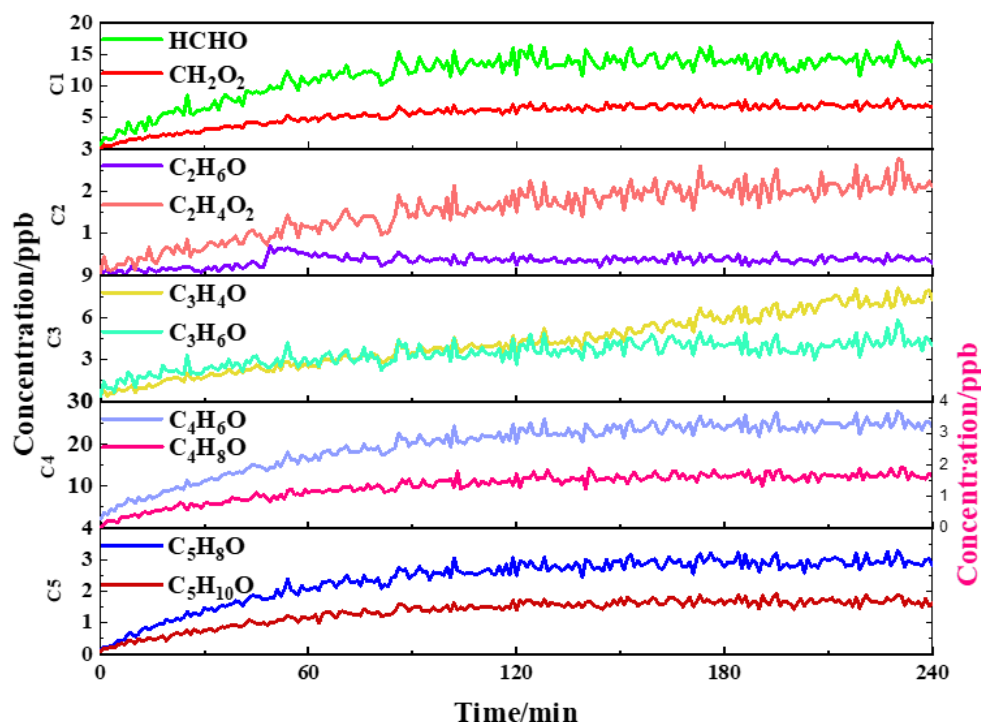
Figure 6.2 Time series of OVOCs with high intensities detected by PTR-ToF-MS.

Numerous oxygenated compounds were identified by ToF-CIMS (**Figure 6.3**). Generally, most detected compounds continued to increase in concentration throughout the oxidation process, as shown in **Figure 6.4**. However, the concentrations of these products were all at the ppt level, that is, lower than those detected by PTR-ToF-MS. For the detected compounds, compounds with five carbons number (C_5) were the most dominant HOMs (40%-60%). It was noted that the compounds with nine and ten carbons (C_9 and C_{10}) were also produced with high concentration despite their low volatilities (**Figure 6.6(a)**). $C_5H_{10}N_2O_8$, marked in red in **Figure 6.3**, was the most

abundant of the compounds detected by ToF-CIMS, regardless of the concentration of

NO$_2$. A further discussion is presented in Section 6.3.
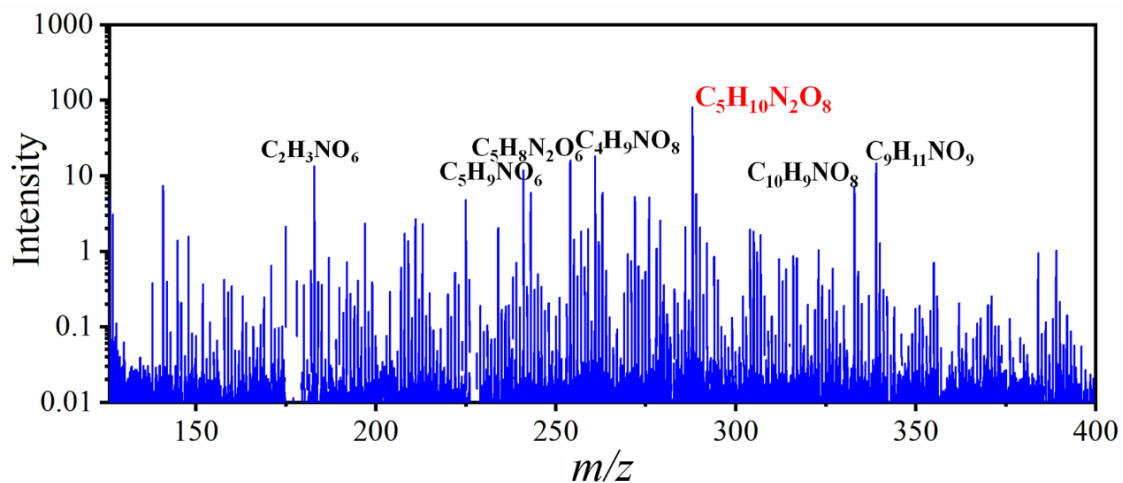
Figure 6.3 Full spectrum of ToF-CIMS at the end of the oxidation of isoprene.
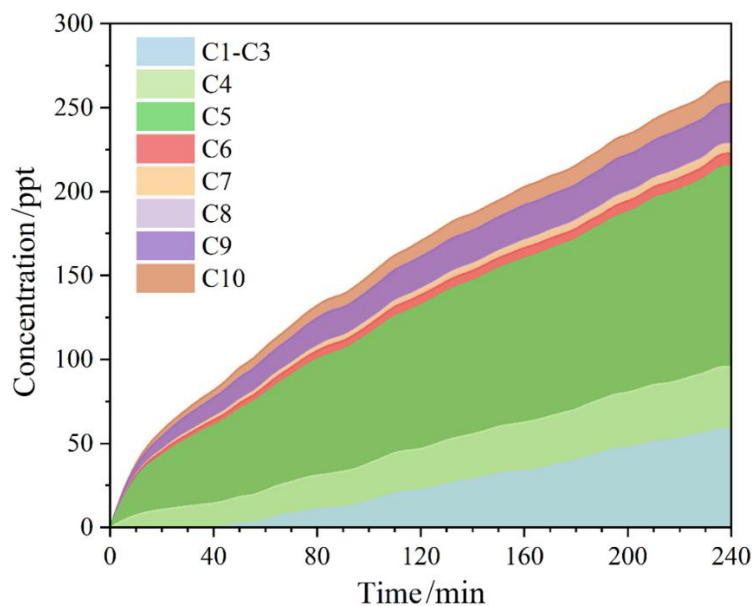
Figure 6.4 Evolution of products with various carbon numbers detected by ToF-CIMS.

6.3 Influence of NO$_2$ concentration on isoprene oxidation

The yields of OVOCs with low carbon numbers (C$_1$–C$_4$) that were detected by PTR-ToF-MS under various concentrations of NO$_2$ are illustrated in **Figure 6.5**. The yields of gaseous species with one, two, three and four C atoms were calculated using equation (6.1) (Pandis et al., 1992),

$$Y = \frac{\Delta[\text{OVOCs}]}{\Delta[isoprene]} \quad (6.1)$$

where $\Delta[\text{OVOCs}]$ was calculated according to the generated OVOCs, and $\Delta[isoprene]$ is the reduced amount of isoprene. **Figure 6.5** indicates that MVK + MACR achieved the highest yield among the products and that the yield decreased from

79% to 43% when the NO_2 concentration was increased from 20 ppb to 800 ppb. The second-highest yield was that of HCHO, but as the concentration of NO_2 increased, its yield first increased and then began to decrease when the NO_2 concentration exceeded 150 ppb. The concentrations of CH_2O_2, C_2H_6O, C_4H_6O, and $C_4H_8O_2$ decreased as the NO_2 concentration increased, but the opposite trends were seen with $C_3H_6O_2$ and MEK. The yield of C_3H_4O was maximized with the lowest concentration of NO_2. The discrepant trends among the OVOCs may indicate variations in the contributions of oxidants to isoprene oxidation with different concentrations of NO_2.
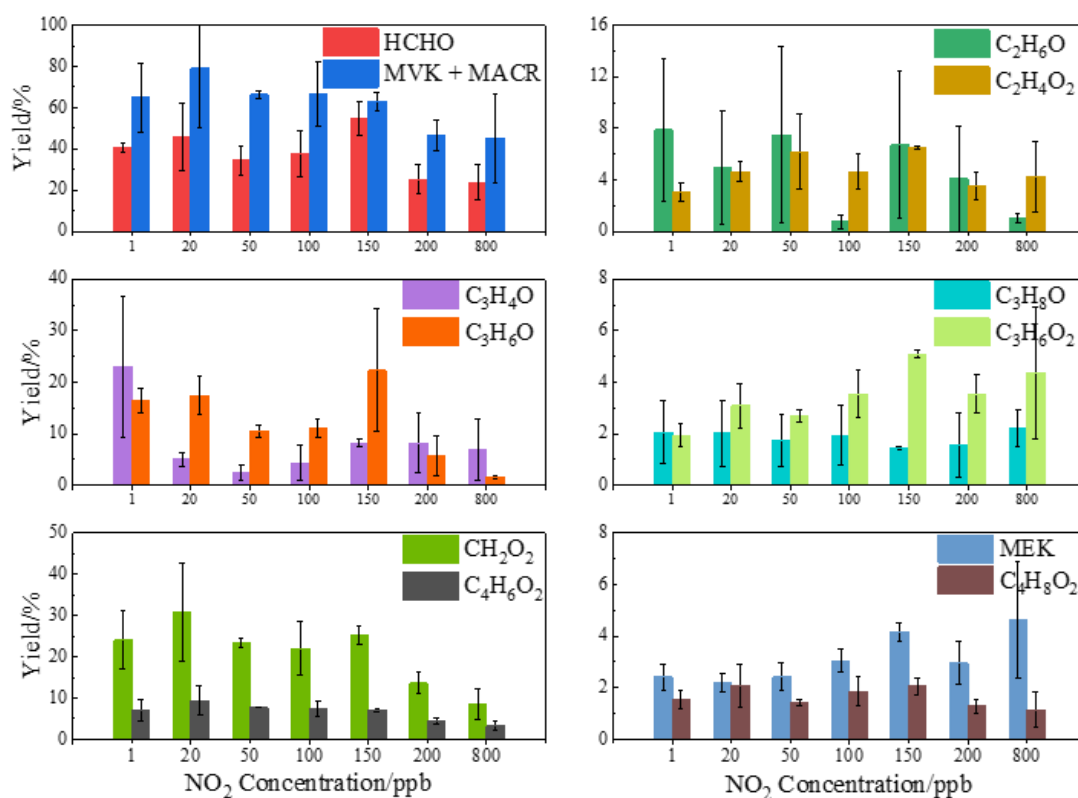
Figure 6.5 Influence of NO_2 on C_1–C_4 OVOC yields.

Table 6.1 lists the top ten compounds with five or more carbon atoms detected by ToF-CIMS. It is obvious that the products were also influenced by the NO_2 concentration, as their concentrations increased with the NO_2 concentration (**Figure 6.6(b)**). It should be noted that most products detected by ToF-CIMS contained nitrate groups, which were assumed to be generated from the reaction between RO_2 and NO or from the addition of NO_3 radicals to the double bond of isoprene. Because NO was not injected into the system and NO_3 would hinder its secondary formation, the formation pathway for organic nitrate should be dominated by the NO_3 oxidation process. The increased yields and concentrations of these compounds indicated that the proportion of products of oxidation by NO_3 increased as the NO_2 concentration increased.

Table 6.1 Top ten compounds under various NO_2 concentrations detected by ToF-CIMS.

[NO$_2$]	1 ppb	5 ppb	20 ppb	50 ppb	100 ppb	150 ppb	200 ppb	700 ppb
1	$C_5H_{10}O_8N_2$	$C_5H_{10}O_8N_2$	$C_5H_{10}O_8N_2$	$C_5H_{10}O_8N_2$	$C_5H_{10}O_8N_2$	$C_5H_{10}O_8N_2$	$C_5H_{10}O_8N_2$	$C_5H_{10}O_8N_2$
2	$C_{10}H_9O_8N_1$	$C_{10}H_9O_8N_1$	$C_5H_8O_6N_2$	$C_4H_9O_8N_1$	$C_4H_9O_5N_1$	$C_5H_9O_6N_1$	$C_4H_9O_5N_1$	$C_4H_9O_5N_1$
3	$C_{10}H_{11}O_8N$	$C_4H_9O_8N_1$	$C_4H_9O_8N_1$	$C_2H_3O_5N_1$	$C_2H_3O_5N_1$	$C_2H_3O_5N_1$	$C_5H_8O_6N_2$	$C_5H_8O_6N_2$
4	$C_9H_9O_6N_1$	$C_5H_8O_6N_2$	$C_{10}H_9O_8N_1$	$C_5H_9O_6N_1$	$C_5H_9O_6N_1$	$C_4H_9O_5N_1$	$C_2H_3O_5N_1$	$C_5H_9O_6N_1$
5	$C_5H_9O_9N_1$	$C_4H_9O_5N_1$	$C_7H_5O_6N_1$	$C_5H_8O_6N_2$	$C_5H_8O_6N_2$	$C_{10}H_9O_8N_1$	$C_5H_9O_6N_1$	$C_2H_3O_5N_1$
6	$C_5H_{10}O_7N_2$	$C_7H_5O_6N_1$	$C_5H_9O_6N_1$	$C_{10}H_9O_8N_1$	$C_4H_9O_8N_1$	$C_5H_{11}O_6N_1$	$C_9H_9O_6N_1$	$C_{10}H_9O_8N_1$
7	$C_5H_8O_6N_2$	$C_5H_{10}O_7N_2$	$C_5H_{10}O_7N_2$	$C_4H_9O_5N_1$	$C_{10}H_9O_8N_1$	$C_5H_8O_6N_2$	$C_{10}H_9O_8N_1$	$C_9H_{13}O_{12}N_1$
8	$C_{10}H_{13}O_5N_1$	$C_{10}H_{11}O_8N$	$C_5H_{11}O_6N_1$	$C_7H_5O_6N_1$	$C_9H_9O_6N_1$	$C_5H_9O_7N_1$	$C_5H_9O_9N_1$	$C_5H_8O_8N_2$
9	$C_6H_5O_3N$	$C_7H_7O_6N_1$	$C_7H_7O_6N_1$	$C_5H_{11}O_6N_1$	$C_5H_9O_9N_1$	$C_9H_9O_6N_1$	$C_4H_9O_8N_1$	$C_9H_9O_6N_1$
10	$C_6H_{12}O_9$	$C_5H_9O_9N_1$	$C_9H_9O_6N_1$	$C_9H_9O_6N_1$	$C_5H_{11}O_6N_1$	$C_5H_9O_9N_1$	$C_5H_{11}O_6N_1$	$C_5H_9O_9N_1$
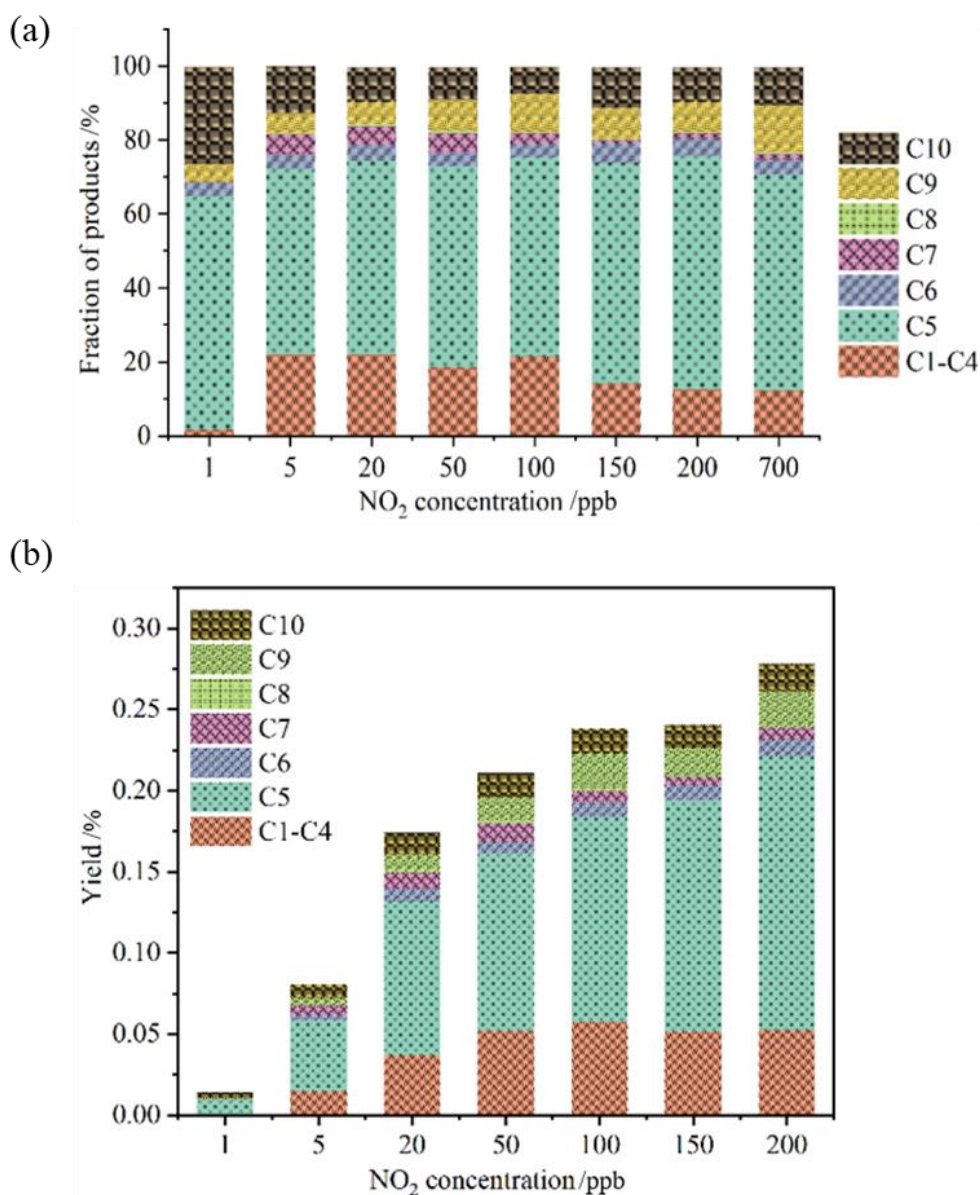
Figure 6.6 Influence of NO$_2$ on products with different carbon number under different NO$_2$ conditions: (a) fraction; (b) yield.

To investigate the changes in the contributions of various oxidants to isoprene oxidation as the NO$_2$ concentration increased, tracers were selected for various oxidation

pathways. As discussed above, organic nitrate can only be generated from the oxidation of isoprene by NO_3 radicals (Ng et al., 2008). Therefore, $C_5H_{10}N_2O_8$ was selected as the tracer for oxidation by NO_3 radicals. Although MVK + MACR were the major products of isoprene oxidation, they could not be selected as the tracers for any reaction pathways because they could be generated via the O_3, OH radical, or NO_3 radical oxidation processes (Wennberg et al., 2018). For oxidation of isoprene by OH radicals, the tracer should include the skeleton of isoprene in its structure without a nitrate group. Therefore, $C_5H_{10}O_3$ was selected as the tracer for the OH radical oxidation pathway. The difference between the oxidation of isoprene by O_3 and by NO_3 radicals or OH radicals was that Criegee intermediates were generated in reactions that involved O_3, which could further react with H_2O, SO_2, or NO_2 (Nguyen et al., 2016). In our study, we found the CH_2OO Criegee intermediate and the MACR-OO + MVK-OO Criegee intermediate (C_4 Criegee, $C_4H_6O_2$). It has been reported that hydroxymethyl hydroperoxide (CH_4O_3) is produced from the reaction between CH_2OO Criegee intermediates and H_2O, which was unique in the system (Chen et al., 2016). Hence, CH_4O_3 was used as the tracer for the O_3 oxidation process. In addition to the individual oxidation by a single oxidant, the combined oxidation process of isoprene by various oxidants was also observed. We found a series of products with ten carbons and only one nitrate substituent group. Those compounds should be generated from the reaction of two RO_2 radicals as shown in equation 6.2, where $C_5H_gNO_h$ should be generated

from the NO$_3$ radical process and $C_5H_{x\text{-}g}O_{y\text{-}h}$ should be formed from the OH radical process.

$$C_5H_gNO_h + C_5H_{x\text{-}g}O_{y\text{-}h} \rightarrow C_{10}H_xNO_y \quad (6.2)$$
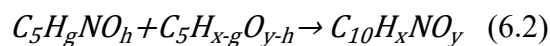
The influence of NO$_2$ on the yields of the tracers, which reflects the influence on the oxidation pathways, is plotted in **Figure 6.7**. As the NO$_2$ concentration increased, the O$_3$ oxidation pathway decreased, whereas the NO$_3$ oxidation pathway increased due to enhanced NO$_3$ radical formation. However, the OH oxidation pathway first increased and then decreased; it subsequently increased slightly, which implied that the influence of NO$_2$ on OH radicals may also follow this trend. The combined oxidation by OH radicals and NO$_3$ radicals first increased and then decreased slightly. These results indicated that the oxidation processes by O$_3$, OH radicals, and NO$_3$ radicals, and the combined oxidation by NO$_3$ radicals and OH radicals, co-existed in the reaction system under the studied conditions, and they were affected by the concentration of NO$_2$.
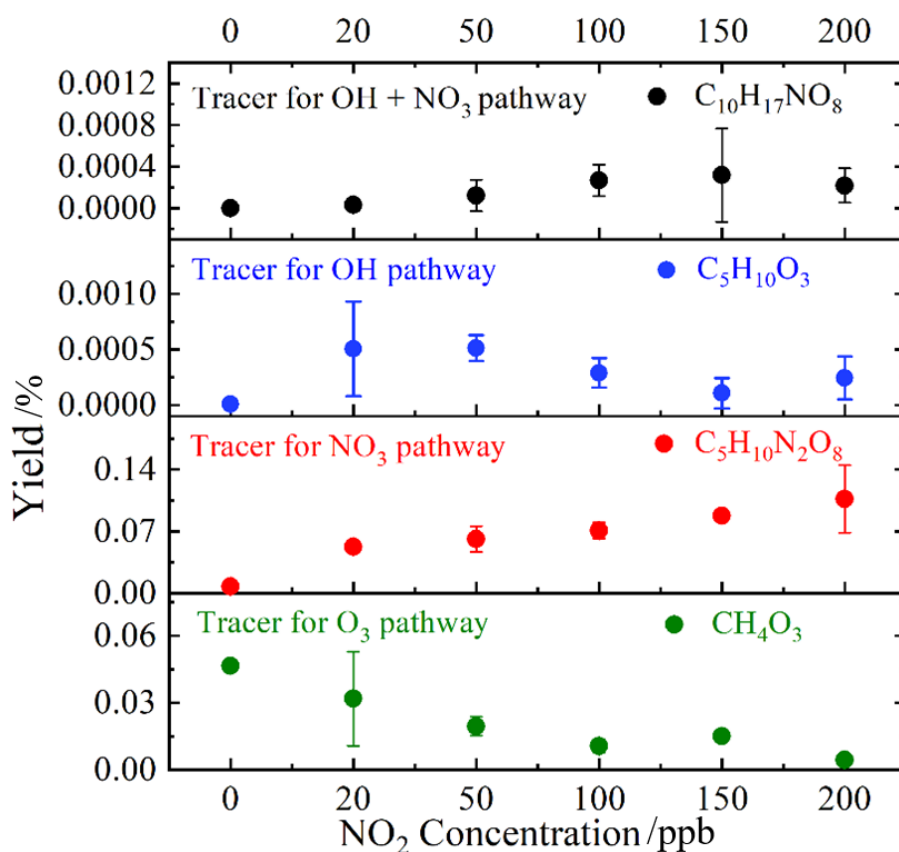
Figure 6.7 Influence of NO_2 on the yields of tracers of various oxidants.

6.4 Humidity-dependent product yields

A series of experiments was carried out to investigate how changes in RH affect the formation and yield of OVOCs. The RH was controlled from 5% to 60% in the chamber system. **Figure 6.8** compares the dry condition (RH < 5%) and the humid condition (RH = 60%). Higher concentrations were observed for the products under dry conditions. For example, the concentration of CH_2O_2 decreased from 13.76 ppb to 5.53 ppb as the RH increased from <5% to 60%. With the decline in the HCHO concentration under humid conditions, the hydrophilicity of HCHO could result in its adsorption and

transformation into the particle phase (Vlasenko et al., 2010). Ketone products like C_3H_6O and MVK + MACR changed only slightly, although lower concentrations were found with an RH of 60%. The results of these experiments suggested that the formation of OVOCs was RH-dependent. An increase in the generation of oxidation products would contribute to SOA formation due to the effects of the liquid water content on SOA yields.
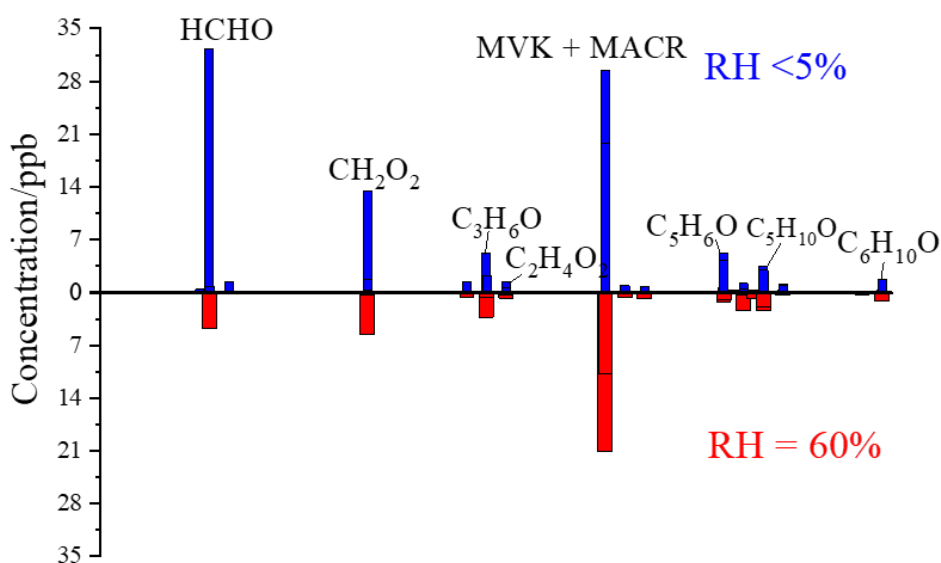
Figure 6.8 Comparison of OVOC concentrations among various RH values. Blue bar (upper): RH < 5% and red bar (lower): RH = 60%.

6.5 SOA formation

SOA was generated in the system during the reactions (**Figure 6.9**). The yields of SOA

under the studied conditions varied from 0.002% to 0.3% and increased as the NO_2/O_3

concentration ratio increased, as presented in **Figure 6.10**. Products with low volatility

should contribute to SOA formation (Presto et al., 2010). We therefore examined the

volatility of the measured products. All of the products measured by PTR-ToF-MS were

VOCs, and the corresponding volatility measurements are shown in **Figure 6.11(a)**. For

the compounds detected by ToF-CIMS, the volatility ranged from values typical of

VOCs to those of extremely low-volatility organic compounds (ELVOC) (**Figure**

6.11(b)). Semi-volatile organic compounds (SVOC) accounted for the largest

proportion, because $C_5H_{10}N_2O_8$, the most abundant compound among those products,

belonged to this type.

The contributions of the detected products to the formation of SOA were calculated

based on the methods proposed by Troestl et al. (2016). For compounds with volatility

(log C) lower than −1, the condensation method was used to calculate the contribution

to the formation of SOA, whereas for compounds with log C greater than −1, the gas–

particle partition method was used. **Figure 6.12** shows a typical result that reflects the

contributions of compounds with different levels of volatility to the formation of SOA

under conditions of 150 ppb NO_2. In this case, approximately 90% of SOA could be

explained by our detected products. Compounds with log C lower than −2 dominated

the formation of SOA, and more than 90% of these compounds existed in the particle

phase. Although $C_5H_{10}N_2O_8$ was the most abundant highly oxygenated compound

detected, its contribution to SOA was less than 2%. These phenomena indicated the importance of detecting the highly oxygenated compounds with low volatility. Because of their low volatility, their gas-phase concentrations were low, which hinders their detection and prevents a deeper understanding of SOA formation.
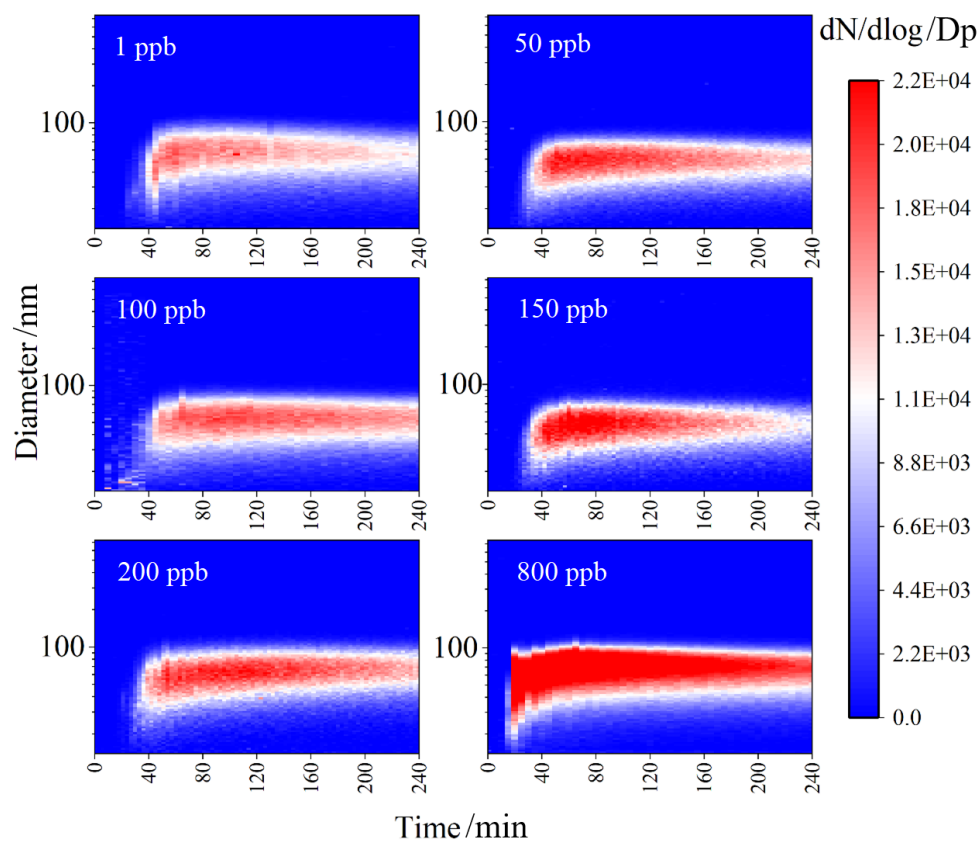
Figure 6.9 Distribution of SOA with the reaction processes under different NO$_2$ concentrations.
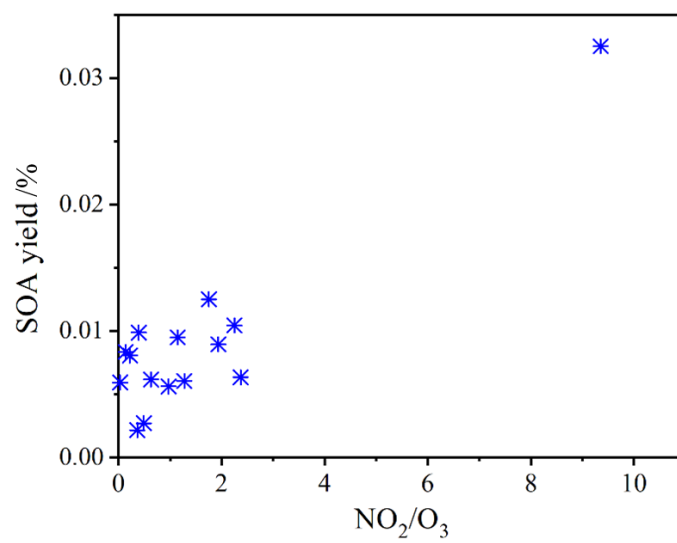
Figure 6.10 SOA yield as a function of NO_2/O_3 concentration ratio.
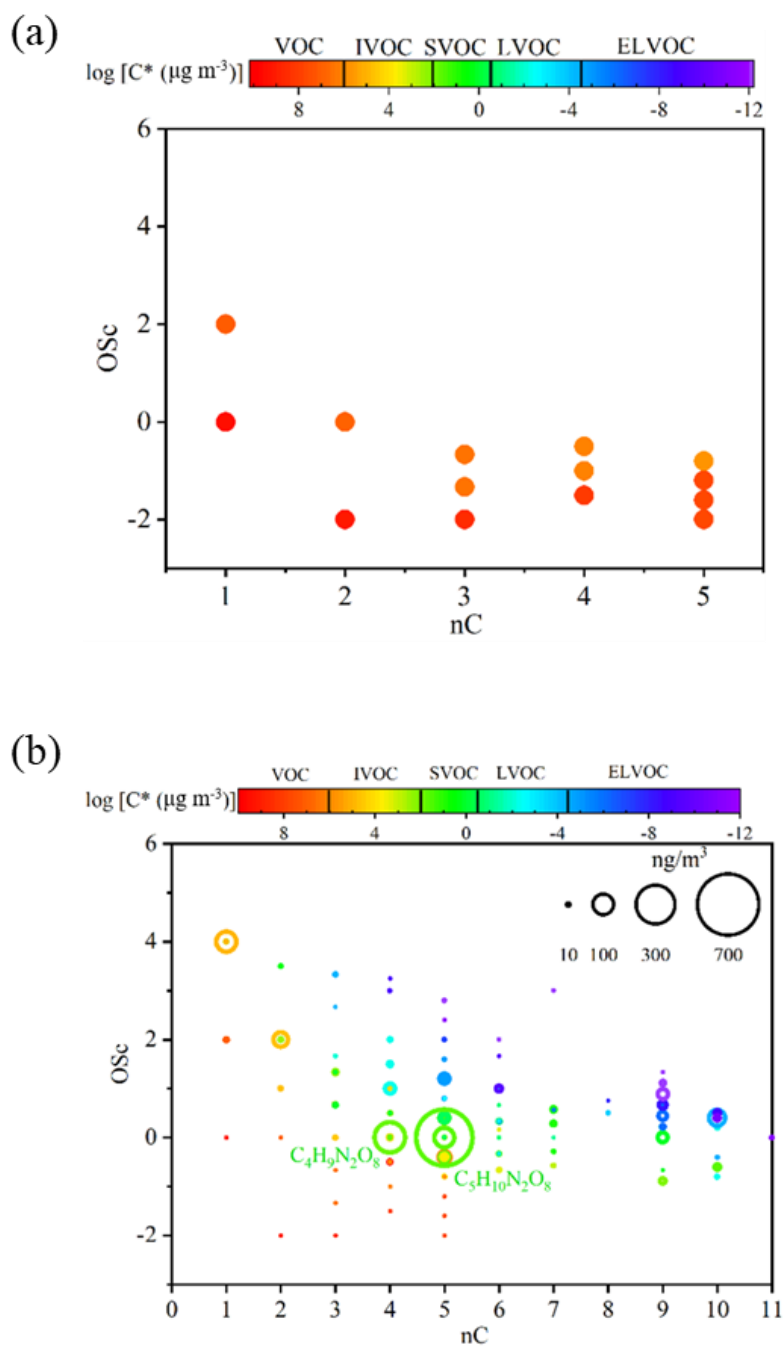
Figure 6.11 State of oxidation and volatility of products detected by (a) PTR-ToF-MS and (b) ToF-CIMS. Where IVOC is for intermediate volatile organic compounds, SVOC is for semi-volatile organic compounds, LVOC is for low-volatility organic compounds, ELVOCs is for extremely low-volatility organic compounds and OSc is for oxidation saturations.

(a)

(b)
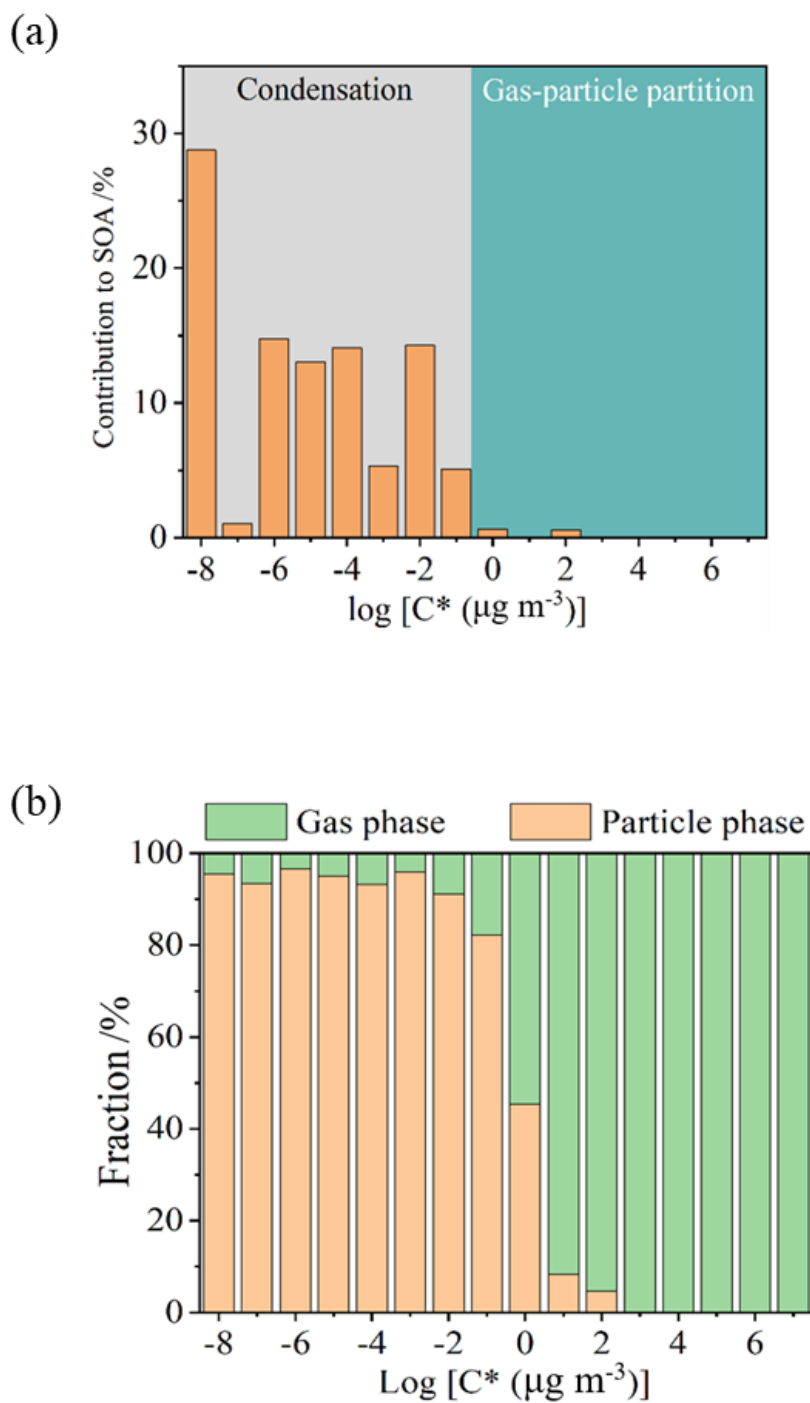
Figure 6.12 (a) Calculation of the contribution of the detected highly oxygenated compounds to the formation of SOA; (b) distribution of highly oxygenated compounds in the gas phase and in the particle phase.

6.6 Carbon balance

The carbon balance in the oxidation process of isoprene was calculated based on the identified products. **Figure 6.13** shows that the carbon balance varied from 37.2% to 60.4% and was controlled by the NO_2 concentration. As discussed in Section 6.2, the concentrations of the products detected by ToF-CIMS were at the ppt level, which accounted for only a fraction of the consumption of isoprene. The carbon balance was almost entirely accounted for by the products detected by PTR-ToF-MS, such as HCHO, MACR + MVK, and other OVOCs. Therefore, the trend of the carbon balance as the NO_2 concentration increased was affected by the yields of products with low carbon compounds. However, the carbon balances were lower than 100%, which has several possible causes. First, the contribution of SOA to the carbon balance was not considered. Second, CO and CO_2, as the end products of the oxidation of isoprene, were not detected in our study and made uncertain contributions to the carbon balance. Third, several gaseous organic products were not measured by PTR-ToF-MS or ToF-CIMS, most likely including organic peroxides, hydroxyl-containing compounds, and high-molecular-weight compounds (Huang et al., 2011).
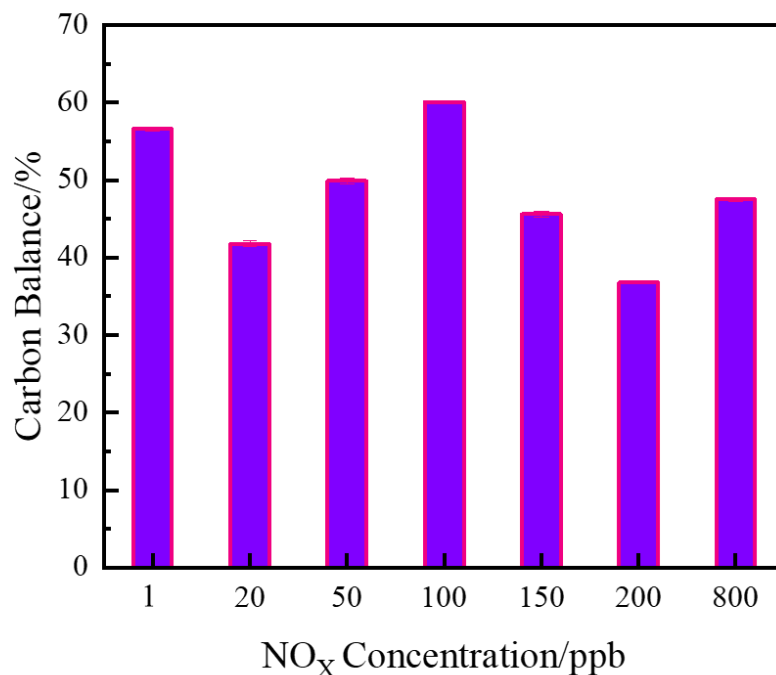
Figure 6.13 Carbon balance in the oxidation of isoprene at various NO_2
concentrations.

6.7 Summary

In the experiments described in this chapter, the nocturnal oxidation reactions of

isoprene by OH radicals, O_3, and NO_3 radicals in a 6-m^3 chamber were investigated

with PTR-ToF-MS and ToF-CIMS. The combination of these two state-of-the-art

online instruments allows us to better understand the oxidation mechanisms in a

complex system. Numerous oxygenated compounds with *m/z* values between 31 and

400 were identified in the oxidation process, wherein MVK + MACR accounted for the

highest yield, ranging from 43% to 79% with various concentrations of NO_2. HCHO

was the second largest product and showed significant RH-dependent properties. A decline in the yield of HCHO was observed from 20% to 5% when the RH was increased from < 5% to 60%. Unexpectedly, $C_5H_{10}N_2O_8$ was the most abundant compound among the highly oxygenated compounds under various concentrations of NO_2. The contributions of various oxidants to isoprene oxidation were estimated, which indicated that the oxidation processes by OH radicals, O_3, and NO_3 radicals and the combined oxidation by OH + NO_3 radicals existed concurrently in the reaction system under all studied conditions, and the pathways were affected by the NO_2 concentration. In addition, the yield of SOA was influenced by NO_2 concentration. Highly oxygenated compounds with low volatility were the dominant species for SOA formation, which comprised more than 90% of SOA. The carbon balance in the oxidation of isoprene varied from 37.2% to 60.4% with the changes in the NO_2 concentration.

Chapter 7 Conclusions

VOCs and OVOCs are the precursors of O_3 and aerosol pollution, which are among the world's most emergent environmental problems. They can react with O_3, OH radicals, NO_3 radicals, and halogens such as Cl radicals and play a vital role in the atmosphere. A comprehensive field study was carried out from August 27 to October 10, 2018, in a rural coastal site in Hong Kong. In this study, the concentrations of VOCs and OVOCs were measured with proton transfer reaction quadrupole mass spectrometry (PTR-QMS) for the first time. Meanwhile, their emission characteristics, O_3 formation potential, and relative contributors from various sources were studied. Methanol was the most abundant species among the measured VOCs (average concentration, 3.73 ± 3.26 ppb), and higher concentrations of isoprene were detected at the Hok Tsui site than those reported in studies of atmospheric chemistry in rural areas. Evident diurnal variations in the concentrations were observed for various VOC species, which indicates the influence of photochemical reactions on the VOC concentrations. The amount of potential O_3 formation was estimated based on the maximum incremental reactivity scale of the VOCs. The top five contributors to O_3 formation in Hong Kong (in the order of amount) were isoprene ($13.46 \ \mu g/m^3$), methyl ethyl ketone ($12.74 \ \mu g/m^3$), xylene ($8.52 \ \mu g/m^3$), acetaldehyde ($8.22 \ \mu g/m^3$), and acrolein ($4.32 \ \mu g/m^3$), which suggests that OVOCs were the dominant species at the Hok Tsui site with the potential for O_3

formation. In addition, the receptor model of positive matrix factorization was used to identify possible emission sources and evaluate their proportions. Five major VOC sources were identified from positive matrix factorization analysis, including (1) biomass burning (63.7%), (2) ship-related emissions (13.5%), (3) secondary formation (9.2%), (4) industry-related and vehicle-related sources (8.1%), and (5) biogenic emissions (5.5%). The source apportionment results showed that the measurements taken at the sampling site at the southeastern tip of Hong Kong were strongly influenced by urban plumes from the Guangdong–Hong Kong–Macao Greater Bay Area/Pearl River Delta region and by oceanic emissions during autumn.

A new environmental chamber was constructed and characterized at PolyU to provide a better understanding of the formation and impact of OVOCs in Hong Kong, where the concentrations of isoprene and oxygenated VOCs were high. The chamber consisted of a 6-m^3 Teflon PFA film reactor inside a stainless-steel enclosure with a pivoted door. The box-in-box design provided controllable and stable reaction conditions, as the temperature and relative humidity (RH) could be set between 10°C and 40°C (±1°C) and between 5% and 85% (±3%), respectively. An air purification system provided zero air into the chamber with a concentration of non-methane hydrocarbons (NMHCs) of less than 1 ppb, concentrations of NO_X and O_3 of less than 1 ppb, and a particle concentration of less than 10^2 particles cm^{-3}. Characterization experiments were performed at 298 K in dry conditions, wherein the average wall-loss rate constants for

O_3 and NO_2 were observed as 2.92×10^{-6} s^{-1} and 9.3×10^{-4} s^{-1}, respectively, and the particle number wall loss rate was measured as 0.27 h^{-1}. The characterization results of isoprene dark ozonolysis revealed OVOC products similar to those found in other chamber studies. The results of the characterization experiments demonstrated the chamber's performance and utility for evaluation of chemical mechanisms. The chamber system can be further used to investigate and simulate gaseous chemical reactions and the formation of secondary aerosols.

Furthermore, a series of chamber experiments was carried out to investigate the nocturnal oxidation of isoprene by OH radicals, O_3, and NO_3 radicals under various concentrations of NO_2. The full spectrum of both small molecules and the highly oxygenated compounds with *m/z* values between 31 and 400 was identified by proton transfer reaction-time-of-flight-mass spectrometry (PTR-ToF-MS) and high-resolution time-of-flight-chemical ionization mass spectrometer (ToF-CIMS). Methyl vinyl ketone (MVK) plus methacrolein (MACR) showed the highest yield (43% to 79%) among these products when the NO_2 concentration changed from 800 ppb to 20 ppb. HCHO was the second largest generator of OVOCs and presented significant dependence on the RH due to its high degree of hydrophilicity. A decrease in the HCHO yield from 20% to 5% was observed when the RH was increased from the dry condition (< 5%) to 60%. In addition, $C_5H_{10}N_2O_8$ was the most abundant substance among the highly oxygenated compounds detected by high-resolution ToF-CIMS.

The contributions of various oxidants to the oxidation of isoprene were estimated under different NO_2 concentrations. Tracers were selected for various oxidation pathways, and the concentrations varied with the NO_2 concentration. The oxidation processes by OH radicals, O_3, and NO_3 radicals and the combined oxidation by OH + NO_3 radicals existed concurrently in the reaction system under the studied conditions, and the pathways were affected by the NO_2 concentration. Secondary organic aerosols (SOA) were also influenced by the changes in the concentration of NO_2. The yield of SOA increased from 0.002% to 0.3% as the NO_2 concentration increased from 1 ppb to 800 ppb. Moreover, it was found that highly oxygenated compounds with low volatility were the dominant species that caused the formation of more than 90% of SOA. Finally, the carbon balance in the oxidation of isoprene was shown to vary from 37.2% to 60.4% with the change in the concentration of NO_2.

Overall, the concentrations, diurnal variations, potential for O_3 formation, and dominant sources of emissions for VOCs and OVOCs were investigated via field measurements at a coastal site in Hong Kong with PTR-MS. It could be concluded that OVOCs were the dominant O_3 precursors in Hong Kong with high photochemical reactivity and great potential for O_3 formation. A series of chamber simulations was conducted to further explore the formation and impact of OVOCs. Nocturnal oxidation of isoprene by OH radicals, O_3, and NO_3 radicals was investigated in a complex system. In-depth analysis of both small molecules and highly oxygenated compounds indicated that multiple

oxidation processes could co-exist in the reaction system and that the pathways were affected by the NO_2 concentration. MVK + MACR and HCHO were the major products, and $C_5H_{10}N_2O_8$ showed an unexpectedly high yield. The formation of SOA from isoprene oxidation was controlled by highly oxygenated compounds with low volatility. In a word, OVOCs play important roles in Hong Kong's atmosphere, and isoprene makes a large contribution to their formation.

Chapter 8 Significance and Suggestions for Future Research

8.1 Significance

This work presents a combined study that includes both a field campaign and laboratory experiments. The latest updated information regarding VOCs and OVOCs from the field study will allow an informed interpretation of the in-chamber experimental results. The nocturnal reaction of isoprene with various radicals was demonstrated in the newly constructed chamber.

The novelty and significance of this study include but are not limited to the following aspects:

a) Proton transfer reaction quadrupole mass spectrometry (PTR-QMS) was used for the first time to investigate the characteristics of air pollutants at a coastal site in Hong Kong; this provides a more accurate measurement and understanding of OVOCs;

b) An updated emission profile for VOCs and OVOCs was obtained by making continuous measurements from August to October 2018, which will help to address the deficiency in our knowledge of these pollutants in Hong Kong and the Greater Bay Area/Pearl River Delta;

c) A newly developed chamber coupled with an array of state-of-the-art online instruments was applied in Hong Kong for the first time to understand the chemical mechanisms of nocturnal oxidation of isoprene, which provide a controllable and repeatable condition for the investigation and simulation of its gaseous chemical reactions and secondary aerosol formation;

d) The online equipment, namely, proton transfer reaction-time-of-flight-mass spectrometry (PTR-ToF-MS) and high-resolution time-of-flight-chemical ionization mass spectrometer (ToF-CIMS), were coupled and installed in the chamber system, providing a full picture of OVOCs generated from nocturnal isoprene oxidation;

e) A comprehensive reaction system with three kinds of oxidants (OH radicals, O_3, and NO_3 radicals) was studied for the first time, which will help to estimate the contributions of various oxidants to isoprene oxidation in real situations;

f) The importance of highly oxygenated compounds with low volatility to the formation of secondary organic aerosols was identified, which will provide a deep understanding of this process.

8.2 Suggestions for future research

Although this work has filled some knowledge gaps in the field of OVOC formation

and chamber simulation of isoprene oxidation by OH radicals, O_3 and NO_3 radicals, many questions must still be addressed in future studies:

a) PTR-QMS was used for field studies to measure VOCs and OVOCs, but isomers and isobars could not be distinguished with this analytical technique;

b) The field study was only conducted in autumn, whereas the long-term data of VOCs and OVOCs, including spring, summer, and winter, should be collected to complete the database;

c) Isoprene oxidation was only studied under nocturnal conditions, but the photochemical reactions of isoprene are recommended to add in the future studies to obtain a comprehensive understanding of its oxidation process;

d) Particulate matter was detected only by SMPS in a chamber system. The results indicated that other products not detected in this study still account for a large part of the carbon balance. More advanced techniques with high time resolutions are recommended for further chamber simulation, including aerosol mass spectrometer (AMS), thermal-desorption aerosol gas-chromatograph (TAG), and gas chromatograph coupled with flame ionization detection (GC-FID).

REFERENCES

Akimoto, H., Sakamaki, F., Hoshino, M., Inoue, G., Okuda, M., 1979. Photochemical Ozone Formation in Propylene-Nitrogen Oxide-Dry Air System. Environ. Sci. Technol. 13, 53–58. https://doi.org/10.1021/es60149a005

Anderson, M.J., Miller, S.L., Milford, J.B., 2001. Source apportionment of exposure to toxic volatile organic compounds using positive matrix factorization. J. Expo. Anal. Environ. Epidemiol. 11, 295–307. https://doi.org/10.1038/sj.jea.7500168

Andreae, M.O., Merlet, P., 2001. Emission of trace gases and aerosols from biomass burning. Global Biogeochem. Cycles 15, 955–966. https://doi.org/10.1029/2000GB001382

Arnold, S.R., Spracklen, D. V, Williams, J., Yassaa, N., Sciare, J., Bonsang, B., Gros, V., Peeken, I., Lewis, A.C., Alvain, S., Alvain, M., 2009. Evaluation of the global oceanic isoprene source and its impacts on marine organic carbon aerosol. Atmos. Chem. Phys. 9, 1253–1262. https://doi.org/10.5194/acp-9-1253-2009

Aschmann, S.M., Atkinson, R., 1994. Formation Yields of Methyl Vinyl Ketone and Methacrolein from the Gas-Phase Reaction of O3 with Isoprene. Environ. Sci. Technol. 28, 1539–1542. https://doi.org/10.1021/es00057a025

Atkinson, R., 2000. Atmospheric chemistry of VOCs and NO(x). Atmos. Environ. 34,

REFERENCES

2063–2101. https://doi.org/10.1016/S1352-2310(99)00460-4

Atkinson, R., 1997a. Atmospheric reactions of alkoxy and β-hydroxyalkoxy radicals.
Int. J. Chem. Kinet. 29, 99–111. https://doi.org/10.1002/(SICI)1097-4601(1997)29:2<99::AID-KIN3>3.0.CO;2-F

Atkinson, R., 1997b. Gas-phase tropospheric chemistry of volatile organic
compounds: 1. Alkanes and alkenes. J. Phys. Chem. Ref. Data 26, 215–290.
https://doi.org/10.1063/1.556012

Atkinson, R., Arey, J., 2003. Atmospheric Degradation of Volatile Organic
Compounds. Chem. Rev. 103, 4605–4638. https://doi.org/10.1021/cr0206420

Atkinson, R., Aschmann, S.M., Arey, J., Shorees, B., 1992. Formation of OH radicals
in the gas phase reactions of O3 with a series of terpenes. J. Geophys. Res. 97,
6065–6073. https://doi.org/10.1029/92JD00062

Atkinson, R., Baulch, D.L., Cox, R.A., Crowley, J.N., Hampson, R.F., Hynes, R.G.,
Jenkin, M.E., Rossi, M.J., Troe, J., 2006. Evaluated kinetic and photochemical
data for atmospheric chemistry: Volume II - Gas phase reactions of organic
species. Atmos. Chem. Phys. 6, 3625–4055. https://doi.org/10.5194/acp-6-3625-2006

Atkinson, R., Baulch, D.L., Cox, R.A., Crowley, J.N., Hampson, R.F., Hynes, R.G.,

REFERENCES

Jenkin, M.E., Rossi, M.J., Troe, J., Wallington, T.J., 2008. Evaluated kinetic and photochemical data for atmospheric chemistry: Volume IV - Gas phase reactions of organic\newline halogen species. Atmos. Chem. Phys. 8, 4141–4496. https://doi.org/10.5194/acp-8-4141-2008

Atkinson, R., Carter, W.P.L., Darnall, K.R., Winer, A.M., Pitts, J.N., 1980. A smog chamber and modeling study of the gas phase NOx–air photooxidation of toluene and the cresols. Int. J. Chem. Kinet. 12, 779–836. https://doi.org/10.1002/kin.550121102

Azuma, K., Uchiyama, I., Uchiyama, S., Kunugita, N., 2016. Assessment of inhalation exposure to indoor air pollutants: Screening for health risks of multiple pollutants in Japanese dwellings. Environ. Res. 145, 39–49. https://doi.org/10.1016/j.envres.2015.11.015

Bannan, T.J., Le Breton, M., Priestley, M., Worrall, S.D., Bacak, A., Marsden, N.A., Mehra, A., Hammes, J., Hallquist, M., Alfarra, M.R., Krieger, U.K., Reid, J.P., Jayne, J., Robinson, W., McFiggans, G., Coe, H., Percival, C.J., Topping, D., 2019. A method for extracting calibrated volatility information from the FIGAERO-HR-ToF-CIMS and its experimental application. Atmos. Meas. Tech. 12, 1429–1439. https://doi.org/10.5194/amt-12-1429-2019

Barletta, B., Meinardi, S., Rowland, F.S., Chan, C.Y., Wang, X., Zou, S., Lo, Y.C.,

REFERENCES

Blake, D.R., 2005. Volatile organic compounds in 43 Chinese cities. Atmos.

Environ. 39, 5979–5990. https://doi.org/10.1016/j.atmosenv.2005.06.029

Barletta, B., Meinardi, S., Simpson, I.J., Khwaja, H.A., Blake, D.R., Rowland, F.S.,

2002. Mixing ratios of volatile organic compounds (VOCs) in the atmosphere of

Karachi, Pakistan. Atmos. Environ. 36, 3429–3443.

https://doi.org/10.1016/S1352-2310(02)00302-3

Beaver, M.R., St. Clair, J.M., Paulot, F., Spencer, K.M., Crounse, J.D., Lafranchi,

B.W., Min, K.E., Pusede, S.E., Wooldridge, P.J., Schade, G.W., Park, C., Cohen,

R.C., Wennberg, P.O., 2012. Importance of biogenic precursors to the budget of

organic nitrates: Observations of multifunctional organic nitrates by CIMS and

TD-LIF during BEARPEX 2009. Atmos. Chem. Phys. 12, 5773–5785.

https://doi.org/10.5194/acp-12-5773-2012

Berndt, T., Böge, O., 1997. Gas-phase reaction of NO3 radicals with isoprene: A

kinetic and mechanistic study. Int. J. Chem. Kinet. 29, 755–765.

https://doi.org/10.1002/(SICI)1097-4601(1997)29:10<755::AID-

KIN4>3.0.CO;2-L

Biesenthal, T.A., Bottenheim, J.W., Shepson, P.B., Li, S.M., Brickell, P.C., 1998. The

chemistry of biogenic hydrocarbons at a rural site in eastern Canada. J. Geophys.

Res. Atmos. 103, 25487–25498. https://doi.org/10.1029/98JD01848

REFERENCES

Blacet, F.E., 1952. Photochemistry in the lower atmosphere. Ind. Eng. Chem. 44,

1339–1342.

Bonsang, B., Polle, C., Lambert, G., 1992. Evidence for marine production of

isoprene. Geophys. Res. Lett. 19, 1129–1132.

https://doi.org/10.1029/92GL00083

Borbon, A., Fontaine, H., Veillerot, M., Locoge, N., Galloo, J.C., Guillermo, R.,

2001. An investigation into the traffic-related fraction of isoprene at an urban

location. Atmos. Environ. 35, 3749–3760. https://doi.org/10.1016/S1352-

2310(01)00170-4

Boyd, A.A., Flaud, P.M., Daugey, N., Lesclaux, R., 2003. Rate constants for RO2 +

HO2 reactions measured under a large excess of HO2. J. Phys. Chem. A 107,

818–821. https://doi.org/10.1021/jp026581r

Broadgate, W.J., Malin, G., Küpper, F.C., Thompson, A., Liss, P.S., 2004. Isoprene

and other non-methane hydrocarbons from seaweeds: A source of reactive

hydrocarbons to the atmosphere. Mar. Chem. 88, 61–73.

https://doi.org/10.1016/j.marchem.2004.03.002

Brown, S.G., Frankel, A., Hafner, H.R., 2007. Source apportionment of VOCs in the

Los Angeles area using positive matrix factorization. Atmos. Environ. 41, 227–

REFERENCES

237. https://doi.org/10.1016/j.atmosenv.2006.08.021

Brown, S.S., Degouw, J.A., Warneke, C., Ryerson, T.B., Dubé, W.P., Atlas, E., Weber, R.J., Peltier, R.E., Neuman, J.A., Roberts, J.M., Swanson, A., Flocke, F., McKeen, S.A., Brioude, J., Sommariva, R., Trainer, M., Fehsenfeld, F.C., Ravishankara, A.R., 2009. Nocturnal isoprene oxidation over the Northeast United States in summer and its impact on reactive nitrogen partitioning and secondary organic aerosol. Atmos. Chem. Phys. 9, 3027–3042. https://doi.org/10.5194/acp-9-3027-2009

Bu, X., Wang, T., Hall, G., 2003. Determination of halogens in organic compounds by high resolution inductively coupled plasma mass spectrometry (HR-ICP-MS). J. Anal. At. Spectrom. 18, 1443–1451. https://doi.org/10.1039/b306570g

Cai, C., Geng, F., Tie, X., Yu, Q., An, J., 2010. Characteristics and source apportionment of VOCs measured in Shanghai, China. Atmos. Environ. 44, 5005–5014. https://doi.org/10.1016/j.atmosenv.2010.07.059

Carter, A., L Fitz, W.P., Cocker III, D., 2005. UC Riverside Recent Work Title Development of a Next-Generation Environmental Chamber Facility for Chemical Mechanism and VOC Reactivity Research Permalink https://escholarship.org/uc/item/6tn5524f Publication Date.

REFERENCES

Carter, W.P.L., 2010. Development of the SAPRC-07 Chemical Mechanism and

Updated Ozone Reactivity Scales, Report to the California Air Resources Board,

Contracts No. 03-318, 06-408, and 07-730.

Carter, W.P.L., 1995. Computer modeling of environmental chamber measurements

of maximum incremental reactivities of volatile organic compounds. Atmos.

Environ. 29, 2513–2527. https://doi.org/10.1016/1352-2310(95)00150-W

Carter, W.P.L., 1994. Development of ozone reactivity scales for volatile organic

compounds. J. Air Waste Manag. Assoc. 44, 881–899.

https://doi.org/10.1080/1073161x.1994.10467290

Carter, W.P.L., Atkinson, R., Winer, A.M., Pitts, J.N., 1982. Experimental

investigation of chamber-dependent radical sources. Int. J. Chem. Kinet. 14,

1071–1103. https://doi.org/10.1002/kin.550141003

Carter, W.P.L., Cocker, D.R., Fitz, D.R., Malkina, I.L., Bumiller, K., Sauer, C.G.,

Pisano, J.T., Bufalino, C., Song, C., 2005. A new environmental chamber for

evaluation of gas-phase chemical mechanisms and secondary aerosol formation.

Atmos. Environ. 39, 7768–7788. https://doi.org/10.1016/j.atmosenv.2005.08.040

Carter, W.P.L., Luo, D., Malkina, I., 1997. Environmental chamber studies for

development of an updated photochemical mechanism for VOC reactivity

assessment 1–92.

Chan, C.K., Yao, X., 2008. Air pollution in mega cities in China. Atmos. Environ.
https://doi.org/10.1016/j.atmosenv.2007.09.003

Chan, C.Y., Chan, L.Y., Wang, X.M., Liu, Y.M., Lee, S.C., Zou, S.C., Sheng, G.Y.,
Fu, J.M., 2002. Volatile organic compounds in roadside microenvironments of
metropolitan Hong Kong. Atmos. Environ. 36, 2039–2047.
https://doi.org/10.1016/S1352-2310(02)00097-3

Chen, L., Wang, Wenliang, Wang, Weina, Liu, Y., Liu, F., Liu, N., Wang, B., 2016.
Water-catalyzed decomposition of the simplest Criegee intermediate CH2OO.
Theor. Chem. Acc. 135, 131. https://doi.org/10.1007/s00214-016-1894-9

Chen, Y., Yan, H., Yao, Y., Zeng, C., Gao, P., Zhuang, L., Fan, L., Ye, D., 2020.
Relationships of ozone formation sensitivity with precursors emissions,
meteorology and land use types, in Guangdong-Hong Kong-Macao Greater Bay
Area, China. J. Environ. Sci. (China) 94, 1–13.
https://doi.org/10.1016/j.jes.2020.04.005

Cheung, T., Su, X., 2018. Typhoon Mangkhut officially Hong Kong's most intense
storm since records began. SCMP 17 Sept.

Chu, B., Liu, Y., Li, J., Takekawa, H., Liggio, J., Li, S.M., Jiang, J., Hao, J., He, H.,

2014. Decreasing effect and mechanism of FeSO4 seed particles on secondary organic aerosol in α-pinene photooxidation. Environ. Pollut. 193, 88–93. https://doi.org/10.1016/j.envpol.2014.06.018

Claeys, M., Graham, B., Vas, G., Wang, W., Vermeylen, R., Pashynska, V., Cafmeyer, J., Guyon, P., Andreae, M.O., Artaxo, P., Maenhaut, W., 2004. Formation of Secondary Organic Aerosols Through Photooxidation of Isoprene. Science (80-.). 303, 1173–1176. https://doi.org/10.1126/science.1092805

Clark, C.H., Kacarab, M., Nakao, S., Asa-Awuku, A., Sato, K., Cocker, D.R., 2016. Temperature Effects on Secondary Organic Aerosol (SOA) from the Dark Ozonolysis and Photo-Oxidation of Isoprene. Environ. Sci. Technol. 50, 5564–5571. https://doi.org/10.1021/acs.est.5b05524

Cocker, D.R., Flagan, R.C., Seinfeld, J.H., 2001. State-of-the-art chamber facility for studying atmospheric aerosol chemistry. Environ. Sci. Technol. 35, 2594–2601. https://doi.org/10.1021/es0019169

Crutzen, P.J., Williams, J., Pöschl, U., Hoor, P., Fischer, H., Warneke, C., Holzinger, R., Hansel, A., Lindinger, W., Scheeren, B., Lelieveld, J., 2000. High spatial and temporal resolution measurements of primary organics and their oxidation products over the tropical forests of Surinam. Atmos. Environ. 34, 1161–1165. https://doi.org/10.1016/S1352-2310(99)00482-3

REFERENCES

Cui, L., Wang, X.L., Ho, K.F., Gao, Y., Liu, C., Hang Ho, S.S., Li, H.W., Lee, S.C.,
Wang, X.M., Jiang, B.Q., Huang, Y., Chow, J.C., Watson, J.G., Chen, L.W.,
2018. Decrease of VOC emissions from vehicular emissions in Hong Kong from
2003 to 2015: Results from a tunnel study. Atmos. Environ. 177, 64–74.
https://doi.org/10.1016/j.atmosenv.2018.01.020

Cui, L., Zhang, Z., Huang, Y., Lee, S.C., Blake, D.R., Ho, K.F., Wang, B., Gao, Y.,
Wang, X.M., Louie, P.K.K., 2016. Measuring OVOCs and VOCs by PTR-MS in
an urban roadside microenvironment of Hong Kong: Relative humidity and
temperature dependence, and field intercomparisons. Atmos. Meas. Tech. 9,
5763–5779. https://doi.org/10.5194/amt-9-5763-2016

Davis, D.D., Grodzinsky, G., Kasibhatla, P., Crawford, J., Chen, G., Liu, S., Bandy,
A., Thornton, D., Guan, H., Sandholm, S., 2001. Impact of ship emissions on
marine boundary layer NOx and SO2 distributions over the Pacific Basin.
Geophys. Res. Lett. 28, 235–238. https://doi.org/10.1029/2000GL012013

de Gouw, J.A., Warneke, C., Parrish, D.D., Holloway, J.S., Trainer, M., Fehsenfeld,
F.C., 2003. Emission sources and ocean uptake of acetonitrile (CH3CN) in the
atmosphere. J. Geophys. Res. Atmos. 108. https://doi.org/10.1029/2002jd002897

Delfino, R.J., Gong, H., Linn, W.S., Hu, Y., Pellizzari, E.D., 2003. Respiratory
symptoms and peak expiratory flow in children with asthma in relation to

volatile organic compounds in exhaled breath and ambient air. J. Expo. Anal.

Environ. Epidemiol. 13, 348–363. https://doi.org/10.1038/sj.jea.7500287

Derwent, R.G., Jenkin, M.E., Utembe, S.R., Shallcross, D.E., Murrells, T.P., Passant,

N.R., 2010. Secondary organic aerosol formation from a large number of

reactive man-made organic compounds. Sci. Total Environ. 408, 3374–3381.

https://doi.org/10.1016/j.scitotenv.2010.04.013

Dommen, J., Metzger, A., Duplissy, J., Kalberer, M., Alfarra, M.R., Gascho, A.,

Weingartner, E., Prevot, A.S.H., Verheggen, B., Baltensperger, U., 2006.

Laboratory observation of oligomers in the aerosol from isoprene/NO x

photooxidation. Geophys. Res. Lett. 33, L13805.

https://doi.org/10.1029/2006GL026523

Edney, E.O., Kleindienst, T.E., Corse, E.W., 1986. Room temperature rate constants

for the reaction of OH with selected chlorinated and oxygenated hydrocarbons.

Int. J. Chem. Kinet. 18, 1355–1371. https://doi.org/10.1002/kin.550181207

Eerdekens, G., Ganzeveld, L., De Arellano, J.V.G., Klüpfel, T., Sinha, V., Yassaa, N.,

Williams, J., Harder, H., Kubistin, D., Martinez, M., Lelieveld, J., 2009. Flux

estimates of isoprene, methanol and acetone from airborne PTR-MS

measurements over the tropical rainforest during the GABRIEL 2005 campaign.

Atmos. Chem. Phys. 9, 4207–4227. https://doi.org/10.5194/acp-9-4207-2009

REFERENCES

Evv-ct-, C., Becker, K.H., 1996. EUPHORE Design and Technical Development of
the European Photoreactor and First Experimental Results Final Report of the
EC-Project. Mediterr. Cent. Environ. Stud. Found.

Fall, R., 1999. Biogenic Emissions of Volatile Organic Compounds from Higher
Plants, in: Reactive Hydrocarbons in the Atmosphere. pp. 41–96.
https://doi.org/10.1016/b978-012346240-4/50003-5

Fantechi, G., Jensen, N.R., Saastad, O., Hjorth, J., Peeters, J., 1998. Reactions of Cl
atoms with selected VOCs: Kinetics, products and mechanisms. J. Atmos. Chem.
31, 247–267. https://doi.org/10.1023/A:1006033910014

Filella, I., Peñuelas, J., 2006. Daily, weekly, and seasonal time courses of VOC
concentrations in a semi-urban area near Barcelona. Atmos. Environ. 40, 7752–
7769. https://doi.org/10.1016/j.atmosenv.2006.08.002

Fiore, A.M., Horowitz, L.W., Purves, D.W., Levy, H., Evans, M.J., Wang, Y., Li, Q.,
Yantosca, R.M., 2005. Evaluating the contribution of changes in isoprene
emissions to surface ozone trends over the eastern United States. J. Geophys.
Res. D Atmos. 110, 1–13. https://doi.org/10.1029/2004JD005485

Folkins, I., Chatfield, R., 2000. Impact of acetone on ozone production and OH in the
upper troposphere at high NOx. J. Geophys. Res. Atmos. 105, 11585–11599.

REFERENCES

https://doi.org/10.1029/2000JD900067

Fruekilde, P., Hjorth, J., Jensen, N.R., Kotzias, D., Larsen, B., 1998. Ozonolysis at vegetation surfaces: A source of acetone, 4-oxopentanal, 6-methyl-5-hepten-2-one, and geranyl acetone in the troposphere. Atmos. Environ. 32, 1893–1902. https://doi.org/10.1016/S1352-2310(97)00485-8

Galloway, J.N., Likens, G.E., Keene, W.C., Miller, J.M., 1982. The composition of precipitation in remote areas of the world. J. Geophys. Res. 87, 8771–8786. https://doi.org/10.1029/JC087iC11p08771

Garcia, J.P., Beyne-Masclet, S., Mouvier, G., Masclet, P., 1992. Emissions of volatile organic compounds by coal-fired power stations. Atmos. Environ. Part A, Gen. Top. 26, 1589–1597. https://doi.org/10.1016/0960-1686(92)90059-T

Goldan, P.D., Parrish, D.D., Kuster, W.C., Trainer, M., McKeen, S.A., Holloway, J., Jobson, B.T., Sueper, D.T., Fehsenfeld, F.C., 2000. Airborne measurements of isoprene, CO, and anthropogenic hydrocarbons and their implications. J. Geophys. Res. Atmos. 105, 9091–9105. https://doi.org/10.1029/1999JD900429

Goldstein, A.H., Schade, G.W., 2000. Quantifying biogenic and anthropogenic contributions to acetone mixing ratios in a rural environment, in: Atmospheric Environment. Elsevier Science Ltd, pp. 4997–5006.

https://doi.org/10.1016/S1352-2310(00)00321-6

Greene, M.J., Gordon, D.M., 2003. Cuticular hydrocarbons inform task decisions.
Nature 423, 32. https://doi.org/10.1038/423032a

Greenwald, E.E., North, S.W., Georgievskii, Y., Klippenstein, S.J., 2007. A two
transition state model for radical-molecule reactions: Applications to isomeric
branching in the OH-isoprene reaction. J. Phys. Chem. A 111, 5582–5592.
https://doi.org/10.1021/jp071412y

Gros, V., Sciare, J., 2009. Volatile organic compounds source apportionment in Paris
in spring 2007, Geophysical Research Abstracts.

Grossenbacher, J.W., Barket, D.J., Shepson, P.B., Carroll, M.A., Olszyna, K., Apel,
E., 2004. A comparison of isoprene nitrate concentrations at two forest-impacted
sites. J. Geophys. Res. D Atmos. 109. https://doi.org/10.1029/2003JD003966

Guenther, Alex, 1995. A global model of natural volatile organic compound
emissions. J. Geophys. Res. 100, 8873–8892. https://doi.org/10.1029/94JD02950

Guenther, A., 1995. A global model of natural volatile organic compound emissions.
J. Geophys. Res. 100, 8873–8892. https://doi.org/10.1029/94JD02950

Guenther, A., Karl, T., Harley, P., Wiedinmyer, C., Palmer, P.I., Geron, C., 2006.

REFERENCES

Estimates of global terrestrial isoprene emissions using MEGAN (Model of

Emissions of Gases and Aerosols from Nature). Atmos. Chem. Phys. 6, 3181–

3210. https://doi.org/10.5194/acp-6-3181-2006

Guo, H., Cheng, H.R., Ling, Z.H., Louie, P.K.K., Ayoko, G.A., 2011. Which

emission sources are responsible for the volatile organic compounds in the

atmosphere of Pearl River Delta? J. Hazard. Mater. 188, 116–124.

https://doi.org/10.1016/j.jhazmat.2011.01.081

Guo, H., So, K.L., Simpson, I.J., Barletta, B., Meinardi, S., Blake, D.R., 2007. C1-C8

volatile organic compounds in the atmosphere of Hong Kong: Overview of

atmospheric processing and source apportionment. Atmos. Environ. 41, 1456–

1472. https://doi.org/10.1016/j.atmosenv.2006.10.011

Guo, H., Wang, T., Blake, D.R., Simpson, I.J., Kwok, Y.H., Li, Y.S., 2006. Regional

and local contributions to ambient non-methane volatile organic compounds at a

polluted rural/coastal site in Pearl River Delta, China. Atmos. Environ. 40, 2345–

2359. https://doi.org/10.1016/j.atmosenv.2005.12.011

Guo, H., Wang, T., Louie, P.K.K., 2004. Source apportionment of ambient non-

methane hydrocarbons in Hong Kong: Application of a principal component

analysis/absolute principal component scores (PCA/APCS) receptor model.

Environ. Pollut. 129, 489–498. https://doi.org/10.1016/j.envpol.2003.11.006

REFERENCES

Hansen, A.B., Palmgren, F., 1996. VOC air pollutants in Copenhagen, in: Science of

the Total Environment. Elsevier B.V., pp. 451–457.

https://doi.org/10.1016/0048-9697(96)05245-X

He, Z., Li, G., Chen, J., Huang, Y., An, T., Zhang, C., 2015. Pollution characteristics

and health risk assessment of volatile organic compounds emitted from different

plastic solid waste recycling workshops. Environ. Int. 77, 85–94.

https://doi.org/10.1016/j.envint.2015.01.004

Heiden, A.C., Kobel, K., Langebartels, C., Schuh-Thomas, G., Wildt, J., 2003.

Emissions of oxygenated volatile organic compounds from plants part I:

Emissions from lipoxygenase activity. J. Atmos. Chem. 45, 143–172.

https://doi.org/10.1023/A:1024069605420

Hellén, H., Praplan, A.P., Tykkä, T., Ylivinkka, I., Vakkari, V., Bäck, J., Petäjä, T.,

Kulmala, M., Hakola, H., 2018. Sesquiterpenes identified as key species for

atmospheric chemistry in boreal forest by terpenoid and OVOC measurements.

Atmos. Chem. Phys. Discuss. 1–39. https://doi.org/10.5194/acp-2018-399

Hewitt, C.N., Hayward, S., Tani, A., 2003. The application of proton transfer

reaction-mass spectrometry (PTR-MS) to the monitoring and analysis of volatile

organic compounds in the atmosphere. J. Environ. Monit.

https://doi.org/10.1039/b204712h

REFERENCES

Ho, K.F., Lee, S.C., Guo, H., Tsai, W.Y., 2004. Seasonal and diurnal variations of

volatile organic compounds (VOCs) in the atmosphere of Hong Kong. Sci. Total

Environ. 322, 155–166. https://doi.org/10.1016/j.scitotenv.2003.10.004

Holloway, A.L., Treacy, J., Sidebottom, H., Mellouki, A., Daële, V., Le Bras, G.,

Barnes, I., 2005. Rate coefficients for the reactions of OH radicals with the

keto/enol tautomers of 2,4-pentanedione and 3-methyl-2,4-pentanedione, allyl

alcohol and methyl vinyl ketone using the enols and methyl nitrite as photolytic

sources of OH. J. Photochem. Photobiol. A Chem. 176, 183–190.

https://doi.org/10.1016/j.jphotochem.2005.08.031

Holzinger, R., Sanhueza, E., von Kuhlmann, R., Kleiss, B., Donoso, L., Crutzen, P.J.,

2002. Diurnal cycles and seasonal variation of isoprene and its oxidation

products in the tropical savanna atmosphere. Global Biogeochem. Cycles 16, 22-

1-22–13. https://doi.org/10.1029/2001gb001421

Hopke, P.K., 2014. A GUIDE TO POSITIVE MATRIX FACTORIZATION Physico-

chemical and toxicological characterization of electronic cigarette exposure

View project A GUIDE TO POSITIVE MATRIX FACTORIZATION,

researchgate.net.

Horowitz, L.W., Fiore, A.M., Milly, G.P., Cohen, R.C., Perring, A., Wooldridge, P.J.,

Hess, P.G., Emmons, L.K., Lamarque, J.F., 2007. Observational constraints on

the chemistry of isoprene nitrates over the eastern United States. J. Geophys. Res. Atmos. 112. https://doi.org/10.1029/2006JD007747

Hu, Q.H., Xie, Z.Q., Wang, X.M., Kang, H., He, Q.F., Zhang, P., 2013. Secondary organic aerosols over oceans via oxidation of isoprene and monoterpenes from Arctic to Antarctic. Sci. Rep. 3, 1–7. https://doi.org/10.1038/srep02280

Huang, D., Zhang, X., Chen, Z.M., Zhao, Y., Shen, X.L., 2011. The kinetics and mechanism of an aqueous phase isoprene reaction with hydroxyl radical. Atmos. Chem. Phys. 11, 7399–7415. https://doi.org/10.5194/acp-11-7399-2011

Huang, S., Shao, M., Lu, S., Liu, Y., 2008. Reactivity of ambient volatile organic compounds (VOCs) in summer of 2004 in Beijing. Chinese Chem. Lett. 19, 573–576. https://doi.org/10.1016/j.cclet.2008.03.029

Huang, Y., Ling, Z.H., Lee, S.C., Ho, S.S.H., Cao, J.J., Blake, D.R., Cheng, Y., Lai, S.C., Ho, K.F., Gao, Y., Cui, L., Louie, P.K.K., 2015. Characterization of volatile organic compounds at a roadside environment in Hong Kong: An investigation of influences after air pollution control strategies. Atmos. Environ. 122, 809–818. https://doi.org/10.1016/j.atmosenv.2015.09.036

Hynes, R.G., Angove, D.E., Saunders, S.M., Haverd, V., Azzi, M., 2005. Evaluation of two MCM v3.1 alkene mechanisms using indoor environmental chamber data.

REFERENCES

Atmos. Environ. 39, 7251–7262. https://doi.org/10.1016/j.atmosenv.2005.09.005

Im, Y., Jang, M., Beardsley, R.L., 2014. Simulation of aromatic SOA formation using
the lumping model integrated with explicit gas-phase kinetic mechanisms and
aerosol-phase reactions. Atmos. Chem. Phys. 14, 4013–4027.
https://doi.org/10.5194/acp-14-4013-2014

Inomata, S., Tanimoto, H., Kato, S., Suthawaree, J., Kanaya, Y., Pochanart, P., Liu,
Y., Wang, Z., 2010. PTR-MS measurements of non-methane volatile organic
compounds during an intensive field campaign at the summit of Mount Tai,
China, in June 2006. Atmos. Chem. Phys. 10, 7085–7099.
https://doi.org/10.5194/acp-10-7085-2010

Isidorov, V.A., 1990. Organic Chemistry of the Earth's Atmosphere, Organic
Chemistry of the Earth's Atmosphere. https://doi.org/10.1007/978-3-642-75094-
6

Jacob, D.J., Field, B.D., Jin, E.M., Bey, I., Li, Q., Logan, J.A., Yantosca, R.M., Singh,
H.B., 2002. Atmospheric budget of acetone. J. Geophys. Res. Atmos. 107.
https://doi.org/10.1029/2001jd000694

Jacob, D.J., Field, B.D., Li, Q., Blake, D.R., de Gouw, J., Warneke, C., Hansel, A.,
Wisthaler, A., Singh, H.B., Guenther, A., 2005. Global budget of methanol:

Constraints from atmospheric observations. J. Geophys. Res. D Atmos. 110, 1–17. https://doi.org/10.1029/2004JD005172

Jenkin, M.E., Boyd, A.A., Lesclaux, R., 1998. Peroxy radical kinetics resulting from the OH-Initiated oxidation of 1,3-butadiene, 2,3-dimethyl-1,3-butadiene and isoprene. J. Atmos. Chem. 29, 267–298. https://doi.org/10.1023/A:1005940332441

Jenkin, M.E., Hayman, G.D., 1995. Kinetics of reactions of primary, secondary and tertiary β-hydroxy peroxyl radicals. J. Chem. Soc. Faraday Trans. 91, 1911–1922. https://doi.org/10.1039/FT9959101911

Jin, X., Holloway, T., 2015. Spatial and temporal variability of ozone sensitivity over China observed from the Ozone Monitoring Instrument. J. Geophys. Res. 120, 7229–7246. https://doi.org/10.1002/2015JD023250

Jordan, C., Fitz, E., Hagan, T., Sive, B., Frinak, E., Haase, K., Cottrell, L., Buckley, S., Talbot, R., 2009. Long-term study of VOCs measured with PTR-MS at a rural site in New Hampshire with urban influences. Atmos. Chem. Phys. 9, 4677–4697. https://doi.org/10.5194/acp-9-4677-2009

Kamal, M.S., Razzak, S.A., Hossain, M.M., 2016. Catalytic oxidation of volatile organic compounds (VOCs) - A review. Atmos. Environ.

REFERENCES

https://doi.org/10.1016/j.atmosenv.2016.05.031

Kamens, R.M., Gery, M.W., Jeffries, H.E., Jackson, M., Cole, E.I., 1982. Ozone–
isoprene reactions: Product formation and aerosol potential. Int. J. Chem. Kinet.
14, 955–975. https://doi.org/10.1002/kin.550140902

Kameyama, S., Tanimoto, H., Inomata, S., Tsunogai, U., Ooki, A., Takeda, S., Obata,
H., Tsuda, A., Uematsu, M., 2010. High-resolution measurement of multiple
volatile organic compounds dissolved in seawater using equilibrator inlet-proton
transfer reaction-mass spectrometry (EI-PTR-MS). Mar. Chem. 122, 59–73.
https://doi.org/10.1016/j.marchem.2010.08.003

Kameyama, S., Yoshida, S., Tanimoto, H., Inomata, S., Suzuki, K., Yoshikawa-Inoue,
H., 2014. High-resolution observations of dissolved isoprene in surface seawater
in the Southern Ocean during austral summer 2010-2011. J. Oceanogr. 70, 225–
239. https://doi.org/10.1007/s10872-014-0226-8

Kang, C.M., Lee, H.S., Kang, B.W., Lee, S.K., Sunwoo, Y., 2004. Chemical
characteristics of acidic gas pollutants and PM2.5 species during hazy episodes
in Seoul, South Korea. Atmos. Environ. 38, 4749–4760.
https://doi.org/10.1016/j.atmosenv.2004.05.007

Kansal, A., 2009. Sources and reactivity of NMHCs and VOCs in the atmosphere: A

REFERENCES

review. J. Hazard. Mater. https://doi.org/10.1016/j.jhazmat.2008.11.048

Kari, E., Miettinen, P., Yli-Pirilä, P., Virtanen, A., Faiola, C.L., 2018. PTR-ToF-MS
product ion distributions and humidity-dependence of biogenic volatile organic
compounds. Int. J. Mass Spectrom. 430, 87–97.
https://doi.org/10.1016/j.ijms.2018.05.003

Karl, T.G., Christian, T.J., Yokelson, R.J., Artaxo, P., Hao, W.M., A.Guenther, 2007.
The Tropical Forest and Fire Emissions Experiment: method evaluation of
volatile organic compound emissions measured by PTR-MS, FTIR, and GC from
tropical biomass burning. Atmos. Chem. Phys. 7, 5883–5897.

Kesselmeier, J., Bode, K., Hofmann, U., Müller, H., Schäfer, L., Wolf, A., Ciccioli,
P., Brancaleoni, E., Cecinato, A., Frattoni, M., Foster, P., Ferrari, C., Jacob, V.,
Fugit, J.L., Dutaur, L., Simon, V., Torres, L., 1997. Emission of short chained
organic acids, aldehydes and monoterpenes from Quercus ilex L. and Pinus pinea
L. in relation to physiological activities, carbon budget and emission algorithms.
Atmos. Environ. 31, 119–133. https://doi.org/10.1016/S1352-2310(97)00079-4

Kesselmeier, J., Staudt, M., 1999. Biogenic Volatile Organic Compounds (VOC): An
Overview on Emission, Physiology and Ecology. J. Atmos. Chem. 33, 23–88.
https://doi.org/10.1023/A:1006127516791

REFERENCES

Khalili, N.R., Scheff, P.A., Holsen, T.M., 1995. PAH source fingerprints for coke ovens, diesel and, gasoline engines, highway tunnels, and wood combustion emissions. Atmos. Environ. 29, 533–542. https://doi.org/10.1016/1352-2310(94)00275-P

Kot-Wasik, A., Dębska, J., Namieśnik, J., 2004. Monitoring of organic pollutants in coastal waters of the Gulf of Gdańsk, Southern Baltic, in: Marine Pollution Bulletin. Pergamon, pp. 264–276. https://doi.org/10.1016/j.marpolbul.2004.02.014

Kwan, A.J., Chan, A.W.H., Ng, N.L., Kjaergaard, H.G., Seinfeld, J.H., Wennberg, P.O., 2012. Peroxy radical chemistry and OH radical production during the NO 3-initiated oxidation of isoprene. Atmos. Chem. Phys. 12, 7499–7515. https://doi.org/10.5194/acp-12-7499-2012

Lack, D.A., Tie, X.X., Bofinger, N.D., Wiegand, A.N., Madronich, S., 2004. Seasonal variability of secondary organic aerosol: A global modeling study. J. Geophys. Res. Atmos. 109, n/a-n/a. https://doi.org/10.1029/2003jd003418

Lai, C., Liu, Y., Ma, J., Ma, Q., He, H., 2014. Degradation kinetics of levoglucosan initiated by hydroxyl radical under different environmental conditions. Atmos. Environ. 91, 32–39. https://doi.org/10.1016/j.atmosenv.2014.03.054

REFERENCES

Lam, K.S., Wang, T.J., Wu, C.L., Li, Y.S., 2005. Study on an ozone episode in hot

season in Hong Kong and transboundary air pollution over Pearl River Delta

region of China. Atmos. Environ. 39, 1967–1977.

https://doi.org/10.1016/j.atmosenv.2004.11.023

Lam, S.H.M., Saunders, S.M., Guo, H., Ling, Z.H., Jiang, F., Wang, X.M., Wang,

T.J., 2013. Modelling VOC source impacts on high ozone episode days observed

at a mountain summit in Hong Kong under the influence of mountain-valley

breezes. Atmos. Environ. 81, 166–176.

https://doi.org/10.1016/j.atmosenv.2013.08.060

Lau, A.K.H., Yuan, Z., Yu, J.Z., Louie, P.K.K., 2010. Source apportionment of

ambient volatile organic compounds in Hong Kong. Sci. Total Environ. 408,

4138–4149. https://doi.org/10.1016/j.scitotenv.2010.05.025

Lau, W.L., Chan, L.Y., 2003. Commuter exposure to aromatic VOCs in public

transportation modes in Hong Kong. Sci. Total Environ. 308, 143–155.

https://doi.org/10.1016/S0048-9697(02)00647-2

Lee, A., Goldstein, A.H., Keywood, M.D., Gao, S., Varutbangkul, V., Bahreini, R.,

Ng, N.L., Flagan, R.C., Seinfeld, J.H., 2006. Gas-phase products and secondary

aerosol yields from the ozonolysis of ten different terpenes. J. Geophys. Res.

Atmos. 111. https://doi.org/10.1029/2005JD006437

REFERENCES

Lee, B.H., Lopez-Hilfiker, F.D., Mohr, C., Kurtén, T., Worsnop, D.R., Thornton, J.A.,
2014. An iodide-adduct high-resolution time-of-flight chemical-ionization mass
spectrometer: Application to atmospheric inorganic and organic compounds.
Environ. Sci. Technol. 48, 6309–6317. https://doi.org/10.1021/es500362a

Lee, S., Jang, M., Kamens, R.M., 2004. SOA formation from the photooxidation of α-
pinene in the presence of freshly emitted diesel soot exhaust. Atmos. Environ.
38, 2597–2605. https://doi.org/10.1016/j.atmosenv.2003.12.041

Lee, S.C., Chiu, M.Y., Ho, K.F., Zou, S.C., Wang, X., 2002. Volatile organic
compounds (VOCs) in urban atmosphere of Hong Kong. Chemosphere 48, 375–
382. https://doi.org/10.1016/S0045-6535(02)00040-1

Lee, S.C., Lam, S., Kin Fai, H., 2001a. Characterization of VOCs, ozone, and PM10
emissions from office equipment in an environmental chamber. Build. Environ.
36, 837–842. https://doi.org/10.1016/S0360-1323(01)00009-9

Lee, S.C., Li, W.M., Yin Chan, L., 2001b. Indoor air quality at restaurants with
different styles of cooking in metropolitan Hong Kong. Sci. Total Environ. 279,
181–193. https://doi.org/10.1016/S0048-9697(01)00765-3

Lee, S.C., Wang, B., 2006. Characteristics of emissions of air pollutants from
mosquito coils and candles burning in a large environmental chamber. Atmos.

Environ. 40, 2128–2138. https://doi.org/10.1016/j.atmosenv.2005.11.047

Legreid, G., Lööv, J.B., Staehelin, J., Hueglin, C., Hill, M., Buchmann, B., Prevot,

A.S.H., Reimann, S., 2007. Oxygenated volatile organic compounds (OVOCs) at

an urban background site in Zürich (Europe): Seasonal variation and source

allocation. Atmos. Environ. 41, 8409–8423.

https://doi.org/10.1016/j.atmosenv.2007.07.026

Lei, W., Zhang, D., Zhang, R., Molina, L.T., Molina, M.J., 2002a. Rate constants and

isometric branching of the Cl-isoprene reaction. Chem. Phys. Lett. 357, 45–50.

https://doi.org/10.1016/S0009-2614(02)00437-2

Lei, W., Zhang, R., Molina, L.T., Molina, M.J., 2002b. Theoretical study of

chloroalkenylperoxy radicals. J. Phys. Chem. A 106, 6415–6420.

https://doi.org/10.1021/jp025799a

Leone, J.A., Seinfeld, J.H., 1985. Comparative analysis of chemical reaction

mechanisms for photochemical smog. Atmos. Environ. 19, 437–464.

https://doi.org/10.1016/0004-6981(85)90166-0

Leskinen, A., Yli-Pirilä, P., Kuuspalo, K., Sippula, O., Jalava, P., Hirvonen, M.R.,

Jokiniemi, J., Virtanen, A., Komppula, M., Lehtinen, K.E.J., 2015.

Characterization and testing of a new environmental chamber. Atmos. Meas.

REFERENCES

Tech. 8, 2267–2278. https://doi.org/10.5194/amt-8-2267-2015

Lewandowski, M., Jaoui, M., Offenberg, J.H., Krug, J.D., Kleindienst, T.E., 2015.
Atmospheric oxidation of isoprene and 1,3-butadiene: Influence of aerosol
acidity and relative humidity on secondary organic aerosol. Atmos. Chem. Phys.
15, 3773–3783. https://doi.org/10.5194/acp-15-3773-2015

Li, K., Chen, L., Han, K., Lv, B., Bao, K., Wu, X., Gao, X., Cen, K., 2017. Smog
chamber study on aging of combustion soot in isoprene/SO2/NOx system:
Changes of mass, size, effective density, morphology and mixing state. Atmos.
Res. 184, 139–148. https://doi.org/10.1016/j.atmosres.2016.10.011

Li, K., Li, J., Tong, S., Wang, W., Huang, R.J., Ge, M., 2019. Characteristics of
wintertime VOCs in suburban and urban Beijing: Concentrations, emission
ratios, and festival effects. Atmos. Chem. Phys. 19, 8021–8036.
https://doi.org/10.5194/acp-19-8021-2019

Li, K., Wang, W., Ge, M., Li, J., Wang, D., 2014. Optical properties of secondary
organic aerosols generated by photooxidation of aromatic hydrocarbons. Sci.
Rep. 4. https://doi.org/10.1038/srep04922

Li, L., Chen, Y., Zeng, L., Shao, M., Xie, S., Chen, W., Lu, S., Wu, Y., Cao, W.,
2014. Biomass burning contribution to ambient volatile organic compounds

(VOCs) in the chengdu-chongqing region (CCR), China. Atmos. Environ. 99, 403–410. https://doi.org/10.1016/j.atmosenv.2014.09.067

Liakakou, E., Vrekoussis, M., Bonsang, B., Donousis, C., Kanakidou, M., Mihalopoulos, N., 2007. Isoprene above the Eastern Mediterranean: Seasonal variation and contribution to the oxidation capacity of the atmosphere. Atmos. Environ. 41, 1002–1010. https://doi.org/10.1016/j.atmosenv.2006.09.034

Ling, Z.H., Guo, H., 2014. Contribution of VOC sources to photochemical ozone formation and its control policy implication in Hong Kong. Environ. Sci. Policy 38, 180–191. https://doi.org/10.1016/j.envsci.2013.12.004

Liu, T., Wang, X., Deng, W., Zhang, Y., Chu, B., Ding, X., Hu, Q., He, H., Hao, J., 2015. Role of ammonia in forming secondary aerosols from gasoline vehicle exhaust. Sci. China Chem. 58, 1377–1384. https://doi.org/10.1007/s11426-015-5414-x

Liu, Y., Brito, J., Dorris, M.R., Rivera-Rios, J.C., Seco, R., Bates, K.H., Artaxo, P., Duvoisin, S., Keutsch, F.N., Kim, S., Goldstein, A.H., Guenther, A.B., Manzi, A.O., Souza, R.A.F., Springston, S.R., Watson, T.B., McKinney, K.A., Martin, S.T., 2016a. Isoprene photochemistry over the Amazon rainforest. Proc. Natl. Acad. Sci. U. S. A. 113, 6125–6130. https://doi.org/10.1073/pnas.1524136113

Liu, Y., Kuwata, M., McKinney, K.A., Martin, S.T., 2016b. Uptake and release of gaseous species accompanying the reactions of isoprene photo-oxidation products with sulfate particles. Phys. Chem. Chem. Phys. 18, 1595–1600. https://doi.org/10.1039/c5cp04551g

Liu, Y., Shao, M., Fu, L., Lu, S., Zeng, L., Tang, D., 2008. Source profiles of volatile organic compounds (VOCs) measured in China: Part I. Atmos. Environ. 42, 6247–6260. https://doi.org/10.1016/j.atmosenv.2008.01.070

Liu, Y.J., Herdlinger-Blatt, I., McKinney, K.A., Martin, S.T., 2013. Production of methyl vinyl ketone and methacrolein via the hydroperoxyl pathway of isoprene oxidation. Atmos. Chem. Phys. 13, 5715–5730. https://doi.org/10.5194/acp-13-5715-2013

Loh, M.M., Levy, J.I., Spengler, J.D., Houseman, E.A., Bennett, D.H., 2007. Ranking cancer risks of organic hazardous air pollutants in the United States. Environ. Health Perspect. 115, 1160–1168. https://doi.org/10.1289/ehp.9884

Louie, P.K.K., Ho, J.W.K., Tsang, R.C.W., Blake, D.R., Lau, A.K.H., Yu, J.Z., Yuan, Z., Wang, X., Shao, M., Zhong, L., 2013. VOCs and OVOCs distribution and control policy implications in Pearl River Delta region, China. Atmos. Environ. 76, 125–135. https://doi.org/10.1016/j.atmosenv.2012.08.058

REFERENCES

Lu, K., Zhang, Y., Su, H., Brauers, T., Chou, C.C., Hofzumahaus, A., Liu, S.C., Kita, K., Kondo, Y., Shao, M., Wahner, A., Wang, J., Wang, X., Zhu, T., 2010. Oxidant (O3 + NO2) production processes and formation regimes in Beijing. J. Geophys. Res. Atmos. 115, D07303. https://doi.org/10.1029/2009JD012714

Lui, K.H., Ho, S.S.H., Louie, P.K.K., Chan, C.S., Lee, S.C., Hu, D., Chan, P.W., Lee, J.C.W., Ho, K.F., 2017. Seasonal behavior of carbonyls and source characterization of formaldehyde (HCHO) in ambient air. Atmos. Environ. 152, 51–60. https://doi.org/10.1016/j.atmosenv.2016.12.004

Luo, W., Wang, B., Liu, S., He, J., Jishu, C.W.-H.K. yu, 2011, U., 2011. VOC ozone formation potential and emission sources in the atmosphere of Guangzhou. Environ. Sci. Technol. (in Chinese) 24, 80–86.

Lyu, X., Guo, H., Yao, D., Lu, H., Huo, Y., Xu, W., Kreisberg, N., Goldstein, A.H., Jayne, J., Worsnop, D., Tan, Y., Lee, S.C., Wang, T., 2020. In Situ Measurements of Molecular Markers Facilitate Understanding of Dynamic Sources of Atmospheric Organic Aerosols. Environ. Sci. Technol. 54, 11058–11069. https://doi.org/10.1021/acs.est.0c02277

Mcdonald, J.D., Zielinska, B., Fujita, E.M., Sagebiel, J.C., Chow, J.C., Watson, J.G., 2000. Fine particle and gaseous emission rates from residential wood combustion. Environ. Sci. Technol. 34, 2080–2091.

REFERENCES

https://doi.org/10.1021/es9909632

McMurry, P.H., Grosjean, D., 1985. Gas and Aerosol Wall Losses in Teflon Film

Smog Chambers. Environ. Sci. Technol. 19, 1176–1182.

https://doi.org/10.1021/es00142a006

Mentel, T.F., Springer, M., Ehn, M., Kleist, E., Pullinen, I., Kurtén, T., Rissanen, M.,

Wahner, A., Wildt, J., 2015. Formation of highly oxidized multifunctional

compounds: Autoxidation of peroxy radicals formed in the ozonolysis of alkenes

- Deduced from structure-product relationships. Atmos. Chem. Phys. 15, 6745–

6765. https://doi.org/10.5194/acp-15-6745-2015

Middleton, P., 1995. Sources of air pollutants. United States.

Miller, M.S., Friedlander, S.K., Hidy, G.M., 1972. A chemical element balance for

the Pasadena aerosol. J. Colloid Interface Sci. 39, 165–176.

https://doi.org/10.1016/0021-9797(72)90152-X

Miyoshi, A., Hatakeyama, S., Washida, N., 1994. OH radical- initiated

photooxidation of isoprene: An estimate of global CO production. J. Geophys.

Res. 99, 18779. https://doi.org/10.1029/94jd01334

Mo, Z., Shao, M., Lu, S., 2016. Compilation of a source profile database for

hydrocarbon and OVOC emissions in China. Atmos. Environ. 143, 209–217.

https://doi.org/10.1016/j.atmosenv.2016.08.025

Möhler, O., Stetzer, O., Schaefers, S., Linke, C., Schnaiter, M., Tiede, R., Saathoff,

H., Krämer, M., Mangold, A., Budz, P., Zink, P., Schreiner, J., Mauersberger, K.,

Haag, W., Kärcher, B., Schurath, U., 2003. Experimental investigation of

homogeneous freezing of sulphuric acid particles in the aerosol chamber AIDA.

Atmos. Chem. Phys. 3, 211–223. https://doi.org/10.5194/acp-3-211-2003

Mølhave, L., 2003. Organic compounds as indicators of air pollution, in: Indoor Air.

John Wiley & Sons, Ltd, pp. 12–19. https://doi.org/10.1034/j.1600-

0668.13.s.6.2.x

Monks, P.S., 2005. NucleobasesGas-phase radical chemistry in the troposphere.

Chem. Soc. Rev. 34, 376–395. https://doi.org/10.1039/b307982c

Mugica, V., Vega, E., Arriaga, J.L., Ruiz, M.E., 1998. Determination of motor vehicle

profiles for non-methane organic compounds in the mexico city metropolitan

area. J. Air Waste Manag. Assoc. 48, 1060–1068.

https://doi.org/10.1080/10473289.1998.10463770

Mugica, V., Vega, E., Chow, J., Reyes, E., Sánchez, G., Arriaga, J., Egami, R.,

Watson, J., 2001. Speciated non-methane organic compounds emissions from

food cooking in Mexico. Atmos. Environ. 35, 1729–1734.

REFERENCES

https://doi.org/10.1016/S1352-2310(00)00538-0

Mutzel, A., Poulain, L., Berndt, T., Iinuma, Y., Rodigast, M., Böge, O., Richters, S., Spindler, G., Sipilä, M., Jokinen, T., Kulmala, M., Herrmann, H., 2015. Highly Oxidized Multifunctional Organic Compounds Observed in Tropospheric Particles: A Field and Laboratory Study. Environ. Sci. Technol. 49, 7754–7761. https://doi.org/10.1021/acs.est.5b00885

Na, K., Moon, K.C., Yong, P.K., 2005. Source contribution to aromatic VOC concentration and ozone formation potential in the atmosphere of Seoul. Atmos. Environ. 39, 5517–5524. https://doi.org/10.1016/j.atmosenv.2005.06.005

Nelson, P.F., Quigley, S.M., 1984. The hydrocarbon composition of exhaust emitted from gasoline fuelled vehicles. Atmos. Environ. 18, 79–87. https://doi.org/10.1016/0004-6981(84)90230-0

Ng, N.L., Kwan, A.J., Surratt, J.D., Chan, A.W.H., Chhabra, P.S., Sorooshian, A., Pye, H.O.T., Crounse, J.D., Wennberg, P.O., Flagan, R.C., Seinfeld, J.H., 2008. Secondary organic aerosol (SOA) formation from reaction of isoprene with nitrate radicals (NO3). Atmos. Chem. Phys. 8, 4117–4140. https://doi.org/10.5194/acp-8-4117-2008

Nguyen, T.B., Bateman, A.P., Bones, D.L., Nizkorodov, S.A., Laskin, J., Laskin, A.,

2010. High-resolution mass spectrometry analysis of secondary organic aerosol

generated by ozonolysis of isoprene. Atmos. Environ. 44, 1032–1042.

https://doi.org/10.1016/j.atmosenv.2009.12.019

Nguyen, T.B., Tyndall, G.S., Crounse, J.D., Teng, A.P., Bates, K.H., Schwantes,

R.H., Coggon, M.M., Zhang, L., Feiner, P., Milller, D.O., Skog, K.M., Rivera-

Rios, J.C., Dorris, M., Olson, K.F., Koss, A., Wild, R.J., Brown, S.S., Goldstein,

A.H., De Gouw, J.A., Brune, W.H., Keutsch, F.N., Seinfeld, J.H., Wennberg,

P.O., 2016. Atmospheric fates of Criegee intermediates in the ozonolysis of

isoprene. Phys. Chem. Chem. Phys. 18, 10241–10254.

https://doi.org/10.1039/c6cp00053c

Ou, J., Zheng, J., Li, R., Huang, X., Zhong, Z., Zhong, L., Lin, H., 2015. Speciated

OVOC and VOC emission inventories and their implications for reactivity-based

ozone control strategy in the pearl river delta region, China. Sci. Total Environ.

530–531, 393–402. https://doi.org/10.1016/j.scitotenv.2015.05.062

Paatero, P., 1997. Least squares formulation of robust non-negative factor analysis, in:

Chemometrics and Intelligent Laboratory Systems. pp. 23–35.

https://doi.org/10.1016/S0169-7439(96)00044-5

Pacifico, F., Harrison, S.P., Jones, C.D., Sitch, S., 2009. Isoprene emissions and

climate. Atmos. Environ. https://doi.org/10.1016/j.atmosenv.2009.09.002

REFERENCES

Pandis, S.N., Harley, R.A., Cass, G.R., Seinfeld, J.H., 1992. Secondary organic aerosol formation and transport. Atmos. Environ. Part A, Gen. Top. 26, 2269–2282. https://doi.org/10.1016/0960-1686(92)90358-R

Pankow, J.F., Chang, E.I., 2008. Variation in the sensitivity of predicted levels of atmospheric organic particulate matter (OPM). Environ. Sci. Technol. 42, 7321–7329. https://doi.org/10.1021/es8003377

Park, J., Jongsma, C.G., Zhang, R., North, S.W., 2004. OH/OD initiated oxidation of isoprene in the presence of O2 and NO. J. Phys. Chem. A 108, 10688–10697. https://doi.org/10.1021/jp040421t

Paulot, F, Crounse, J.D., Kjaergaard, H.G., Kroll, J.H., Seinfeld, J.H., Wennberg, P.O., 2009. Isoprene photooxidation: New insights into the production of acids and organic nitrates. Atmos. Chem. Phys. 9, 1479–1501. https://doi.org/10.5194/acp-9-1479-2009

Paulot, Fabien, Crounse, J.D., Kjaergaard, H.G., Kürten, A., Clair, J.M.S., Seinfeld, J.H., Wennberg, P.O., 2009. Unexpected epoxide formation in the gas-phase photooxidation of isoprene. Science (80-.). 325, 730–733. https://doi.org/10.1126/science.1172910

Paulot, F., Henze, D.K., Wennberg, P.O., 2012. Impact of the isoprene photochemical

cascade on tropical ozone. Atmos. Chem. Phys. 12, 1307–1325.

https://doi.org/10.5194/acp-12-1307-2012

Paulson, S.E., Seinfeld, J.H., 1992. Development and evaluation of a photooxidation

mechanism for isoprene. J. Geophys. Res. 97, 10779–10790.

https://doi.org/10.1029/92jd01914

Peeters, J., Müller, J.F., Stavrakou, T., Nguyen, V.S., 2014. Hydroxyl radical

recycling in isoprene oxidation driven by hydrogen bonding and hydrogen

tunneling: The upgraded LIM1 mechanism. J. Phys. Chem. A 118, 8625–8643.

https://doi.org/10.1021/jp5033146

Peeters, J., Nguyen, T.L., Vereecken, L., 2009. HOx radical regeneration in the

oxidation of isoprene. Phys. Chem. Chem. Phys. 11, 5935–5939.

https://doi.org/10.1039/b908511d

Pétron, G., Harley, P., Greenberg, J., Guenther, A., 2001. Seasonal temperature

variations influence isoprene emission. Geophys. Res. Lett. 28, 1707–1710.

https://doi.org/10.1029/2000GL011583

Phillips, M., Gleeson, K., Hughes, J.M.B., Greenberg, J., Cataneo, R.N., Baker, L.,

McVay, W.P., 1999. Volatile organic compounds in breath as markers of lung

cancer: A cross-sectional study. Lancet 353, 1930–1933.

https://doi.org/10.1016/S0140-6736(98)07552-7

Pitten, F.A., Bremer, J., Kramer, A., 2000. Air contamination with volatile organic compounds (VOC's) and health complaints. Dtsch. Medizinische Wochenschrift 125, 545–550. https://doi.org/10.1055/s-2007-1024338

Platt, U., Heintz, F., 1994. Nitrate Radicals in Tropospheric Chemistry. Isr. J. Chem. 34, 289–300. https://doi.org/10.1002/ijch.199400033

Poirot, R.L., Wishinski, P.R., Hopke, P.K., Polissar, A. V., 2001. Comparative application of multiple receptor methods to identify aerosol sources in northern Vermont. Environ. Sci. Technol. 35, 4622–4636. https://doi.org/10.1021/es010588p

Polissar, A. V., Hopke, P.K., Paatero, P., Malm, W.C., Sisler, J.F., 1998. Atmospheric aerosol over Alaska 2. Elemental composition and sources. J. Geophys. Res. Atmos. 103, 19045–19057. https://doi.org/10.1029/98JD01212

Presto, A.A., Miracolo, M.A., Donahue, N.M., Robinson, A.L., 2010. Secondary organic aerosol formation from high-NOx Photo-oxidation of low volatility precursors: N-alkanes. Environ. Sci. Technol. 44, 2029–2034. https://doi.org/10.1021/es903712r

Pusede, S.E., Cohen, R.C., 2012. On the observed response of ozone to NOx and

VOC reactivity reductions in San Joaquin Valley California 1995-present.
Atmos. Chem. Phys. 12, 8323–8339. https://doi.org/10.5194/acp-12-8323-2012

Read, K.A., Carpenter, L.J., Arnold, S.R., Beale, R., Nightingale, P.D., Hopkins, J.R.,
Lewis, A.C., Lee, J.D., Mendes, L., Pickering, S.J., 2012. Multiannual
observations of acetone, methanol, and acetaldehyde in remote tropical Atlantic
air: Implications for atmospheric OVOC budgets and oxidative capacity.
Environ. Sci. Technol. 46, 11028–11039. https://doi.org/10.1021/es302082p

Reimann, S., Calanca, P., Hofer, P., 2000. The anthropogenic contribution to isoprene
concentrations in a rural atmosphere. Atmos. Environ. 34, 109–115.
https://doi.org/10.1016/S1352-2310(99)00285-X

Rissanen, M.P., Kurtén, T., Sipilä, M., Thornton, J.A., Kangasluoma, J., Sarnela, N.,
Junninen, H., Jørgensen, S., Schallhart, S., Kajos, M.K., Taipale, R., Springer,
M., Mentel, T.F., Ruuskanen, T., Petäjä, T., Worsnop, D.R., Kjaergaard, H.G.,
Ehn, M., 2014. The formation of highly oxidized multifunctional products in the
ozonolysis of cyclohexene. J. Am. Chem. Soc. 136, 15596–15606.
https://doi.org/10.1021/ja507146s

Rohrer, F., Bohn, B., Brauers, T., Brüning, D., Johnen, F.J., Wahner, A., Kleffmann,
J., 2005. Characterisation of the photolytic HONO-source in the atmosphere
simulation chamber SAPHIR. Atmos. Chem. Phys. 5, 2189–2201.

REFERENCES

https://doi.org/10.5194/acp-5-2189-2005

Rollins, A.W., Kiendler-Scharr, A., Fry, J.L., Brauers, T., Brown, S.S., Dorn, H.P., Dubé, W.P., Fuchs, H., Mensah, A., Mentel, T.F., Rohrer, F., Tillmann, R., Wegener, R., Wooldridge, P.J., Cohen, R.C., 2009. Isoprene oxidation by nitrate radical: Alkyl nitrate and secondary organic aerosol yields. Atmos. Chem. Phys. 9, 6685–6703. https://doi.org/10.5194/acp-9-6685-2009

Rudolph., Koppmann, R., Plass-Dülmer, C., 1996. The budgets of ethane and tetrachloroethene:... - Google Scholar. Atmos. Environ. 30, 1887–1894.

Rumchev, K.B., Spickett, J.T., Bulsara, M.K., Phillips, M.R., Stick, S.M., 2002. Domestic exposure to formaldehyde significantly increases the risk of asthma in young children. Eur. Respir. J. 20, 403–408. https://doi.org/10.1183/09031936.02.00245002

Ruppert, L., Heinz Becker, K., 2000. A product study of the OH radical-initiated oxidation of isoprene: Formation of C5-unsaturated diols. Atmos. Environ. 34, 1529–1542. https://doi.org/10.1016/S1352-2310(99)00408-2

Sahu, L.K., Pal, D., Yadav, R., Munkhtur, J., 2016. Aromatic VOCs at Major Road Junctions of a Metropolis in India: Measurements Using TD-GC-FID and PTR-TOF-MS Instruments. Aerosol Air Qual. Res. 16, 2405–2420.

REFERENCES

https://doi.org/10.4209/aaqr.2015.11.0643

Sahu, L.K., Yadav, R., Tripathi, N., 2020. Aromatic compounds in a semi-urban site

of western India: Seasonal variability and emission ratios. Atmos. Res. 246.

https://doi.org/10.1016/j.atmosres.2020.105114

Sander, S.P., Friedl, R.R., Golden, D.M., Kurylo, M.J., Moortgat, G.K., Wine, P.H.,

Ravishankara, A.R., Kolb, C.E., Molina, M.J., Diego, S., Jolla, L., Huie, R.E.,

Orkin, V.L., 2006. Chemical Kinetics and Photochemical Data for Use in

Atmospheric Studies Evaluation Number 15. Cross Sect. California, 1–153.

Santos, F., Longo, K., Guenther, A., Kim, S., Gu, D., Oram, D., Forster, G., Lee, J.,

Hopkins, J., Brito, J., Freitas, S., 2018. Biomass burning emission disturbances

of isoprene oxidation in a tropical forest. Atmos. Chem. Phys. 18, 12715–12734.

https://doi.org/10.5194/acp-18-12715-2018

Schade, G.W., Custer, T.G., 2004. OVOC emissions from agricultural soil in northern

Germany during the 2003 European heat wave. Atmos. Environ. 38, 6105–6114.

https://doi.org/10.1016/j.atmosenv.2004.08.017

Schade, G.W., Solomon, S.J., Dellwik, E., Pilegaard, K., Ladstätter-Weissenmayer,

A., 2011. Methanol and other VOC fluxes from a Danish beech forest during late

springtime. Biogeochemistry 106, 337–355. https://doi.org/10.1007/s10533-010-

REFERENCES

9515-5

Schauer, J.J., Kleeman, M.J., Cass, G.R., Simoneit, B.R.T., 2001. Measurement of

emissions from air pollution sources. 3. C1-C29 organic compounds from

fireplace combustion of wood. Environ. Sci. Technol. 35, 1716–1728.

https://doi.org/10.1021/es001331e

Schiffman, S.S., 1998. Livestock Odors: Implications for Human Health and Well-

Being. J. Anim. Sci. 76, 1343–1355. https://doi.org/10.2527/1998.7651343x

Schwantes, R.H., Teng, A.P., Nguyen, T.B., Coggon, M.M., Crounse, J.D., St. Clair,

J.M., Zhang, X., Schilling, K.A., Seinfeld, J.H., Wennberg, P.O., 2015. Isoprene

NO3 Oxidation Products from the RO2 + HO2 Pathway. J. Phys. Chem. A 119,

10158–10171. https://doi.org/10.1021/acs.jpca.5b06355

Seinfeld, J.H., Pandis, S.N., Noone, K., 2016. Atmospheric Chemistry and Physics:

From Air Pollution to Climate Change, John Wiley & Sons.

https://doi.org/10.1063/1.882420

Seinfeld, J.H., Pandis, S.N., Noone, K., 1998. Atmospheric Chemistry and Physics:

From Air Pollution to Climate Change. Phys. Today 51, 88–90.

https://doi.org/10.1063/1.882420

Sharkey, T.D., Singsaas, E.L., Vanderveer, P.J., Geron, C., 1996. Field measurements

of isoprene emission from trees in response to temperature and light. Tree Physiol. 16, 649–654. https://doi.org/10.1093/treephys/16.7.649

Sharkey, T.D., Yeh, S., 2001. Isoprene emission from plants. Annu. Rev. Plant Biol. 52, 407–436. https://doi.org/10.1146/annurev.arplant.52.1.407

Shaw, S.L., Gantt, B., Meskhidze, N., 2010. Production and Emissions of Marine Isoprene and Monoterpenes: A Review. Adv. Meteorol. 2010, 1–24. https://doi.org/10.1155/2010/408696

Sillman, S., He, D., 2002. Some theoretical results concerning O3-NOx-VOC chemistry and NOx-VOC indicators. J. Geophys. Res. Atmos. 107, 4659. https://doi.org/10.1029/2001JD001123

Singh, H.B., Gregory, G.L., Anderson, B., Browell, E., Sachse, G.W., Davis, D.D., Crawford, J., Bradshaw, J.D., Talbot, R., Blake, D.R., Thornton, D., Newell, R., Merrill, J., 1996. Low ozone in the marine boundary layer of the tropical Pacific Ocean: Photochemical loss, chlorine atoms, and entrainment. J. Geophys. Res. Atmos. 101, 1907–1917. https://doi.org/10.1029/95JD01028

Singh, H.B., Kanakidou, M., Crutzen, P.J., Jacob, D.J., 1995. High concentrations and photochemical fate of oxygenated hydrocarbons in the global troposphere. Nature 378, 50–54. https://doi.org/10.1038/378050a0

REFERENCES

Singh, H.B., O'Hara, D., Herlth, D., Sachse, W., Blake, D.R., Bradshaw, J.D.,

Kanakidou, M., Crutzen, P.J., 1994. Acetone in the atmosphere: Distribution,

sources, and sinks. J. Geophys. Res. 99, 1805. https://doi.org/10.1029/93jd00764

Singh, H.B., Salas, L.J., Chatfield, R.B., Czech, E., Fried, A., Walega, J., Evans, M.J.,

Field, B.D., Jacob, D.J., Blake, D., Heikes, B., Talbot, R., Sachse, G., Crawford,

J.H., Avery, M.A., Sandholm, S., Fuelberg, H., 2004. Analysis of the

atmospheric distribution, sources, and sinks of oxygenated volatile organic

chemicals based on measurements over the Pacific during TRACE-P. J.

Geophys. Res. D Atmos. 109, D15S07. https://doi.org/10.1029/2003JD003883

So, K.L., Wang, T., 2004. C3-C12 non-methane hydrocarbons in subtropical Hong

Kong: Spatial-temporal variations, source-receptor relationships and

photochemical reactivity. Sci. Total Environ. 328, 161–174.

https://doi.org/10.1016/j.scitotenv.2004.01.029

So, K.L., Wang, T., 2003. On the local and regional influence on ground-level ozone

concentrations in Hong Kong. Environ. Pollut. 123, 307–317.

https://doi.org/10.1016/S0269-7491(02)00370-6

Sprengnether, M., Demerjian, K.L., Donahue, N.M., Anderson, J.G., 2002. Product

analysis of the OH oxidation of isoprene and 1,3-butadiene in the presence of

NO. J. Geophys. Res. Atmos. 107, ACH 8-1-ACH 8-13.

https://doi.org/10.1029/2001JD000716

Srivastava, A., Sengupta, B., Dutta, S.A., 2005. Source apportionment of ambient VOCs in Delhi City. Sci. Total Environ. 343, 207–220. https://doi.org/10.1016/j.scitotenv.2004.10.008

St Clair, J.M., Rivera-Rios, J.C., Crounse, J.D., Knap, H.C., Bates, K.H., Teng, A.P., Jørgensen, S., Kjaergaard, H.G., Keutsch, F.N., Wennberg, P.O., 2016. Kinetics and Products of the Reaction of the First-Generation Isoprene Hydroxy Hydroperoxide (ISOPOOH) with OH. J. Phys. Chem. A 120, 1441–1451. https://doi.org/10.1021/acs.jpca.5b06532

Starn, T.K., Shepson, P.B., Bertman, S.B., Riemer, D.D., Zika, R.G., Olszyna, K., 1998. Nighttime isoprene chemistry at an urban-impacted forest site. J. Geophys. Res. Atmos. 103, 22437–22447. https://doi.org/10.1029/98JD01201

Stern, J.E., Flagan, R.C., Grosjean, D., Selnfeld, J.H., 1987. Aerosol Formation and Growth in Atmospheric Aromatic Hydrocarbon Photooxidation. Environ. Sci. Technol. 21, 1224–1231. https://doi.org/10.1021/es00165a011

Stevens, J.F., Maier, C.S., 2008. Acrolein: Sources, metabolism, and biomolecular interactions relevant to human health and disease. Mol. Nutr. Food Res. https://doi.org/10.1002/mnfr.200700412

REFERENCES

Stevens, P., L'Esperance, D., Chuong, B., Martin, G., 1999. Measurements of the

kinetics of the OH-initiated oxidation of isoprene: Radical propagation in the OH

+ isoprene + O2 + NO reaction system. Int. J. Chem. Kinet. 31, 637–643.

https://doi.org/10.1002/(SICI)1097-4601(1999)31:9<637::AID-KIN5>3.0.CO;2-

O

Stolwijk, J.A.J., 1990. Assessment of Population Exposure and Carcinogenic Risk

Posed by Volatile Organic Compounds in Indoor Air. Risk Anal. 10, 49–57.

https://doi.org/10.1111/j.1539-6924.1990.tb01019.x

Sun, J., Shen, Z., Huang, Y., Cao, J., Ho, S.S.H., Niu, X., Wang, T., Zhang, Q., Lei,

Y., Xu, H., Liu, H., 2018. VOCs emission profiles from rural cooking and

heating in Guanzhong Plain, China and its potential effect on regional

O<sub>3</sub> and SOA formation. Atmos. Chem. Phys. Discuss.

1–20. https://doi.org/10.5194/acp-2018-36

Szende, B., Tyihák, E., 2010. Effect of formaldehyde on cell proliferation and death.

Cell Biol. Int. 34, 1273–1282. https://doi.org/10.1042/cbi20100532

Taiwo, A.M., Harrison, R.M., Shi, Z., 2014. A review of receptor modelling of

industrially emitted particulate matter. Atmos. Environ.

https://doi.org/10.1016/j.atmosenv.2014.07.051

REFERENCES

Takekawa, H., Minoura, H., Yamazaki, S., 2003. Temperature dependence of

    secondary organic aerosol formation by photo-oxidation of hydrocarbons.

    Atmos. Environ. 37, 3413–3424. https://doi.org/10.1016/S1352-2310(03)00359-

    5

Talbot, R., Mao, H., Sive, B., 2005. Diurnal characteristics of surface level O3 and

    other important trace gases in New England. J. Geophys. Res. D Atmos. 110, 1–

    16. https://doi.org/10.1029/2004JD005449

Tam, B.N., Neumann, C.M., 2004. A human health assessment of hazardous air

    pollutants in Portland, OR. J. Environ. Manage. 73, 131–145.

    https://doi.org/10.1016/j.jenvman.2004.06.012

Tanaka, T., Wada, K., Hisamoto, J., … H.S.-U.P., 2003, U., 2003. Chamber material

    made of Al alloy and heater block. US Pat. 6521046.

Tang, J.H., Chan, L.Y., Chan, C.Y., Li, Y.S., Chang, C.C., Liu, S.C., Wu, D., Li,

    Y.D., 2007. Characteristics and diurnal variations of NMHCs at urban, suburban,

    and rural sites in the Pearl River Delta and a remote site in South China. Atmos.

    Environ. 41, 8620–8632. https://doi.org/10.1016/j.atmosenv.2007.07.029

Teng, A.P., Crounse, J.D., Wennberg, P.O., 2017. Isoprene Peroxy Radical Dynamics.

    J. Am. Chem. Soc. 139, 5367–5377. https://doi.org/10.1021/jacs.6b12838

REFERENCES

Tham, Y.J., Wang, Z., Li, Q., Yun, H., Wang, W., Wang, X., Xue, L., Lu, K., Ma, N., Bohn, B., Li, X., Kecorius, S., Größ, J., Shao, M., Wiedensohler, A., Zhang, Y., Wang, T., 2016. Significant concentrations of nitryl chloride sustained in the morning: Investigations of the causes and impacts on ozone production in a polluted region of northern China. Atmos. Chem. Phys. 16, 14959–14977. https://doi.org/10.5194/acp-16-14959-2016

Tiwari, V., Hanai, Y., Masunaga, S., 2010. Ambient levels of volatile organic compounds in the vicinity of petrochemical industrial area of Yokohama, Japan. Air Qual. Atmos. Heal. 3, 65–75. https://doi.org/10.1007/s11869-009-0052-0

Tran, S., Bonsang, B., Gros, V., Peeken, I., Sarda-Esteve, R., Bernhardt, A., Belviso, S., 2013. A survey of carbon monoxide and non-methane hydrocarbons in the Arctic Ocean during summer 2010. Biogeosciences 10, 1909–1935. https://doi.org/10.5194/bg-10-1909-2013

Tröstl, J., Chuang, W.K., Gordon, H., Heinritzi, M., Yan, C., Molteni, U., Ahlm, L., Frege, C., Bianchi, F., Wagner, R., Simon, M., Lehtipalo, K., Williamson, C., Craven, J.S., Duplissy, J., Adamov, A., Almeida, J., Bernhammer, A.K., Breitenlechner, M., Brilke, S., Dias, A., Ehrhart, S., Flagan, R.C., Franchin, A., Fuchs, C., Guida, R., Gysel, M., Hansel, A., Hoyle, C.R., Jokinen, T., Junninen, H., Kangasluoma, J., Keskinen, H., Kim, J., Krapf, M., Kürten, A., Laaksonen,

REFERENCES

A., Lawler, M., Leiminger, M., Mathot, S., Möhler, O., Nieminen, T., Onnela,

A., Petäjä, T., Piel, F.M., Miettinen, P., Rissanen, M.P., Rondo, L., Sarnela, N.,

Schobesberger, S., Sengupta, K., Sipilä, M., Smith, J.N., Steiner, G., Tomè, A.,

Virtanen, A., Wagner, A.C., Weingartner, E., Wimmer, D., Winkler, P.M., Ye,

P., Carslaw, K.S., Curtius, J., Dommen, J., Kirkby, J., Kulmala, M., Riipinen, I.,

Worsnop, D.R., Donahue, N.M., Baltensperger, U., 2016. The role of low-

volatility organic compounds in initial particle growth in the atmosphere. Nature

533, 527–531. https://doi.org/10.1038/nature18271

Tsigaridis, K., Kanakidou, M., 2003. Global modelling of secondary organic aerosol

in the troposphere: A sensitivity analysis. Atmos. Chem. Phys. 3, 1849–1869.

https://doi.org/10.5194/acp-3-1849-2003

Tuazon, E.C., Atkinson, R., 1990. A product study of the gas-phase reaction of

Methacrolein with the OH radical in the presence of NOx. Int. J. Chem. Kinet.

22, 591–602. https://doi.org/10.1002/kin.550220604

Valente, R.J., Thornton, F.C., Williams, E.J., 1995. Field comparison of static and

flow-through chamber techniques for measurement of soil NO emission. J.

Geophys. Res. 100, 147–168. https://doi.org/10.1029/95jd01875

Vlasenko, A., MacDonald, A.M., Sjostedt, S.J., Abbatt, J.P.D., 2010. Formaldehyde

measurements by Proton transfer reaction - Mass spectrometry (PTR-MS):

Correction for humidity effects. Atmos. Meas. Tech. 3, 1055–1062.

https://doi.org/10.5194/amt-3-1055-2010

Volkamer, R., Ziemann, P.J., Molina, M.J., 2009. Secondary Organic Aerosol

Formation from Acetylene (C2H 2): Seed effect on SOA yields due to organic

photochemistry in the aerosol aqueous phase. Atmos. Chem. Phys. 9, 1907–

1928. https://doi.org/10.5194/acp-9-1907-2009

Wang, B., Liu, Y., Shao, M., Lu, S.H., Wang, M., Yuan, B., Gong, Z.H., He, L.Y.,

Zeng, L.M., Hu, M., Zhang, Y.H., 2016. The contributions of biomass burning to

primary and secondary organics: A case study in Pearl River Delta (PRD),

China. Sci. Total Environ. 569–570, 548–556.

https://doi.org/10.1016/j.scitotenv.2016.06.153

Wang, J., Doussin, J.F., Perrier, S., Perraudin, E., Katrib, Y., Pangui, E., Picquet-

Varrault, B., 2011. Design of a new multi-phase experimental simulation

chamber for atmospheric photosmog, aerosol and cloud chemistry research.

Atmos. Meas. Tech. 4, 2465–2494. https://doi.org/10.5194/amt-4-2465-2011

Wang, L., Milford, J.B., 2001. Reliability of optimal control strategies for

photochemical air pollution. Environ. Sci. Technol. 35, 1173–1180.

https://doi.org/10.1021/es001358y

REFERENCES

Wang, T., Dai, J., Lam, K.S., Nan Poon, C., Brasseur, G.P., 2019. Twenty-Five Years

of Lower Tropospheric Ozone Observations in Tropical East Asia: The Influence

of Emissions and Weather Patterns. Geophys. Res. Lett. 46, 11463–11470.

https://doi.org/10.1029/2019GL084459

Wang, T., Tham, Y.J., Xue, L., Li, Q., Zha, Q., Wang, Z., Poon, S.C.N., Dubé, W.P.,

Blake, D.R., Louie, P.K.K., Luk, C.W.Y., Tsui, W., Brown, S.S., 2016.

Observations of nitryl chloride and modeling its source and effect on ozone in

the planetary boundary layer of southern China. J. Geophys. Res. 121, 2476–

2489. https://doi.org/10.1002/2015JD024556

Wang, T., Wei, X.L., Ding, A.J., Poon, C.N., Lam, K.S., Li, Y.S., Chan, L.Y., Anson,

M., 2009. Increasing surface ozone concentrations in the background atmosphere

of Southern China, 1994-2007. Atmos. Chem. Phys. 9, 6217–6227.

https://doi.org/10.5194/acp-9-6217-2009

Wang, T., Xue, L., Brimblecombe, P., Lam, Y.F., Li, L., Zhang, L., 2017. Ozone

pollution in China: A review of concentrations, meteorological influences,

chemical precursors, and effects. Sci. Total Environ. 575, 1582–1596.

https://doi.org/10.1016/j.scitotenv.2016.10.081

Wang, W.G., Li, K., Zhou, L., Ge, M.F., Hou, S.Q., Tong, S.R., Mu, Y.J., Jia, L.,

2015. Evaluation and application of dual-reactor chamber for studying

atmospheric oxidation processes and mechanisms. Wuli Huaxue Xuebao/ Acta

Phys. - Chim. Sin. 31, 1251–1259.

https://doi.org/10.3866/PKU.WHXB201504161

Wang, X., Liu, T., Bernard, F., Ding, X., Wen, S., Zhang, Y., Zhang, Z., He, Q., Lü,

S., Chen, J., Saunders, S., Yu, J., 2014. Design and characterization of a smog

chamber for studying gas-phase chemical mechanisms and aerosol formation.

Atmos. Meas. Tech. 7, 301–313. https://doi.org/10.5194/amt-7-301-2014

Warneck, P., 1999. Chemistry of the Natural Atmosphere, Elsevier. ed.

Warneke, C., Holzinger, R., Hansel, A., Jordan, A., Lindinger, W., Pöschl, U.,

Williams, J., Hoor, P., Fischer, H., Crutzen, P.J., Scheeren, H.A., Lelieveld, J.,

2001a. Isoprene and its oxidation products methyl vinyl ketone, methacrolein,

and isoprene related peroxides measured online over the tropical rain forest of

Surinam in March 1998. J. Atmos. Chem. 38, 167–185.

https://doi.org/10.1023/A:1006326802432

Warneke, C., Karl, T., Judmaier, H., Hansel, A., Jordan, A., Lindinger, W., Crutzen,

P.J., 1999. Acetone, methanol, and other partially oxidized volatile organic

emissions from dead plant matter by abiological processes: Significance for

atmospheric HO(X) chemistry. Global Biogeochem. Cycles 13, 9–17.

https://doi.org/10.1029/98GB02428

REFERENCES

Warneke, C., Van Der Veen, C., Luxembourg, S., De Gouw, J.A., Kok, A., 2001b. Measurements of benzene and toluene in ambient air using proton-transfer-reaction mass spectrometry: Calibration, humidity dependence, and field intercomparison. Int. J. Mass Spectrom. 207, 167–182. https://doi.org/10.1016/S1387-3806(01)00366-9

Watson, J.G., Chow, J.C., Fujita, E.M., 2001. Review of volatile organic compound source apportionment by chemical mass balance. Atmos. Environ. https://doi.org/10.1016/S1352-2310(00)00461-1

Wennberg, P.O., Bates, K.H., Crounse, J.D., Dodson, L.G., McVay, R.C., Mertens, L.A., Nguyen, T.B., Praske, E., Schwantes, R.H., Smarte, M.D., St Clair, J.M., Teng, A.P., Zhang, X., Seinfeld, J.H., 2018. Gas-Phase Reactions of Isoprene and Its Major Oxidation Products. Chem. Rev. https://doi.org/10.1021/acs.chemrev.7b00439

Wenxing, W., Ying, X., Ziyu, L., Science, W.H.-C.E., 1995, U., 1995. Study on reaction rate constants of CH4 and its life-time. China Environ. Sci. 4.

Wolfe, A.H., Patz, J.A., 2002. Reactive nitrogen and human health: Acute and long-term implications, in: Ambio. Royal Swedish Academy of Sciences, pp. 120–125. https://doi.org/10.1579/0044-7447-31.2.120

REFERENCES

Wu, R., Li, J., Hao, Y., Li, Y., Zeng, L., Xie, S., 2016. Evolution process and sources of ambient volatile organic compounds during a severe haze event in Beijing, China. Sci. Total Environ. 560–561, 62–72. https://doi.org/10.1016/j.scitotenv.2016.04.030

Wu, S., Lü, Z., Hao, J., Zhao, Z., Li, J., Takekawa, H., Minoura, H., Yasuda, A., 2007. Construction and characterization of an atmospheric simulation smog chamber. Adv. Atmos. Sci. 24, 250–258. https://doi.org/10.1007/s00376-007-0250-3

Xie, X., Shao, M., Liu, Y., Lu, S., Chang, C.C., Chen, Z.M., 2008. Estimate of initial isoprene contribution to ozone formation potential in Beijing, China. Atmos. Environ. 42, 6000–6010. https://doi.org/10.1016/j.atmosenv.2008.03.035

Xu, Y., Jia, L., Ge, M., Du, L., Wang, G., Wang, D., 2006. A kinetic study of the reaction of ozone with ethylene in a smog chamber under atmospheric conditions. Chinese Sci. Bull. 51, 2839–2843. https://doi.org/10.1007/s11434-006-2180-3

Yen, C.H., Horng, J.J., 2009. Volatile organic compounds (VOCs) emission characteristics and control strategies for a petrochemical industrial area in middle Taiwan. J. Environ. Sci. Heal. - Part A Toxic/Hazardous Subst. Environ. Eng. 44, 1424–1429. https://doi.org/10.1080/10934520903217393

REFERENCES

Yuan, B., Hu, W.W., Shao, M., Wang, M., Chen, W.T., Lu, S.H., Zeng, L.M., Hu, M., 2013. VOC emissions, evolutions and contributions to SOA formation at a receptor site in eastern China. Atmos. Chem. Phys. 13, 8815–8832. https://doi.org/10.5194/acp-13-8815-2013

Yuan, B, Hu, W.W., Shao, M., Wang, M., Chen, W.T., Lu, S.H., Zeng, L.M., Hu, M., 2013. VOC emissions, evolutions and contributions to SOA formation at a receptor site in Eastern China. Atmos. Chem. Phys. Discuss. 13, 6631–6679. https://doi.org/10.5194/acpd-13-6631-2013

Yuan, B., Liu, Y., Shao, M., Lu, S., Streets, D.G., 2010. Biomass burning contributions to ambient VOCs species at a receptor site in the Pearl River delta (PRD), China. Environ. Sci. Technol. 44, 4577–4582. https://doi.org/10.1021/es1003389

Yuan, B., Shao, M., de Gouw, J., Parrish, D.D., Lu, S., Wang, M., Zeng, L., Zhang, Q., Song, Y., Zhang, J., Hu, M., 2012. Volatile organic compounds (VOCs) in urban air: How chemistry affects the interpretation of positive matrix factorization (PMF) analysis. J. Geophys. Res. Atmos. 117, n/a-n/a. https://doi.org/10.1029/2012JD018236

Zhang, D., Zhang, R., North, S.W., 2003. Experimental Study of NO Reaction with Isoprene Hydroxyalkyl Peroxy Radicals. J. Phys. Chem. A 107, 11013–11019.

REFERENCES

https://doi.org/10.1021/jp0360016

Zhang, F., Shang, X., Chen, H., Xie, G., Fu, Y., Wu, D., Sun, W., Liu, P., Zhang, C.,
Mu, Y., Zeng, L., Wan, M., Wang, Y., Xiao, H., Wang, G., Chen, J., 2020.
Significant impact of coal combustion on VOCs emissions in winter in a North
China rural site. Sci. Total Environ. 720, 137617.
https://doi.org/10.1016/j.scitotenv.2020.137617

Zhang, Haofei, Rattanavaraha, W., Zhou, Y., Bapat, J., Rosen, E.P., Sexton, K.G.,
Kamens, R.M., 2011. A new gas-phase condensed mechanism of isoprene-NOx
photooxidation. Atmos. Environ. 45, 4507–4521.
https://doi.org/10.1016/j.atmosenv.2011.04.011

Zhang, H, Surratt, J.D., Lin, Y.H., Bapat, J., Kamens, R.M., 2011. Effect of relative
humidity on SOA formation from isoprene/NO photooxidation: Enhancement of
2-methylglyceric acid and its corresponding oligoesters under dry conditions.
Atmos. Chem. Phys. 11, 6411–6424. https://doi.org/10.5194/acp-11-6411-2011

Zhang, H., Ye, X., Cheng, T., Chen, J., Yang, X., Wang, L., Zhang, R., 2008. A
laboratory study of agricultural crop residue combustion in China: Emission
factors and emission inventory. Atmos. Environ. 42, 8432–8441.
https://doi.org/10.1016/j.atmosenv.2008.08.015

REFERENCES

Zhang, Q., Streets, D.G., Carmichael, G.R., He, K.B., Huo, H., Kannari, A., Klimont,

Z., Park, I.S., Reddy, S., Fu, J.S., Chen, D., Duan, L., Lei, Y., Wang, L.T., Yao,

Z.L., 2009. Asian emissions in 2006 for the NASA INTEX-B mission. Atmos.

Chem. Phys. 9, 5131–5153. https://doi.org/10.5194/acp-9-5131-2009

Zhang, Y., Wang, X., Barletta, B., Simpson, I.J., Blake, D.R., Fu, X., Zhang, Z., He,

Q., Liu, T., Zhao, X., Ding, X., 2013. Source attributions of hazardous aromatic

hydrocarbons in urban, suburban and rural areas in the Pearl River Delta (PRD)

region. J. Hazard. Mater. 250–251, 403–411.

https://doi.org/10.1016/j.jhazmat.2013.02.023

Zhao, Y., Chan, J.K., Lopez-Hilfiker, F.D., McKeown, M.A., D'Ambro, E.L., Slowik,

J.G., Riffel, J.A., Thornton, J.A., 2017. An electrospray chemical ionization

source for real-time measurement of atmospheric organic and inorganic vapors.

Atmos. Meas. Tech. 10, 3609–3625. https://doi.org/10.5194/amt-10-3609-2017

Zheng, J., Shao, M., Che, W., Zhang, L., Zhong, L., Zhang, Y., Streets, D., 2009.

Speciated VOC emission inventory and spatial patterns of ozone formation

potential in the Pearl River Delta, China. Environ. Sci. Technol. 43, 8580–8586.

https://doi.org/10.1021/es901688e

Zhu, H., Wang, H., Jing, S., Wang, Y., Cheng, T., Tao, S., Lou, S., Qiao, L., Li, L.,

Chen, J., 2018. Characteristics and sources of atmospheric volatile organic

REFERENCES

compounds (VOCs) along the mid-lower Yangtze River in China. Atmos.

Environ. 190, 232–240. https://doi.org/10.1016/j.atmosenv.2018.07.026

Zou, Y., Deng, X.J., Zhu, D., Gong, D.C., Wang, H., Li, F., Tan, H.B., Deng, T., Mai,

B.R., Liu, X.T., Wang, B.G., 2015. Characteristics of 1 year of observational

data of VOCs, NOx and O3 at a suburban site in Guangzhou, China. Atmos.

Chem. Phys. 15, 6625–6636. https://doi.org/10.5194/acp-15-6625-2015